# MONTHLY WEATHER REVIEW

VOLUME 83 NUMBER 1

JANUARY 1955

CONTENTS



U. S. DEPARTMENT OF COMMERCE • WEATHER BUREAU

# PUBLICATIONS OF THE U. S. WEATHER BUREAU

As the national meteorological service for the United States, the Weather Bureau issues several periodicals, serials, and miscellaneous publications on weather, climate, and meteorological science as required to carry out its public service functions. The principal periodicals and serials are described on this page and on the inside of the back cover. A more complete listing of Weather Bureau publications is available upon request to Chief, U. S. Weather Bureau, Washington 25, D. C.

Orders for publications should be addressed to the Superintendent of Documents, Government Printing Office, Washington 25, D. C.

## MONTHLY WEATHER REVIEW

First published in 1872, the Monthly Weather Review serves as a medium of publication for technical contributions in the field of meteorology, principally in the branches of synoptic and applied meteorology. In addition each issue contains an article descriptive of the atmospheric circulation during the month over the Northern Hemisphere with particular reference to the effect on weather in the United States. A second article deals with some noteworthy feature of the month's weather. Illustrated. Annual subscription: Domestic, $3.00; Foreign, $4.00; 30¢ per copy. Subscription to the *Review* does not include the *Supplements* which have been issued irregularly and are for sale separately.

## WEEKLY WEATHER AND CROP BULLETIN

Issued on Wednesday of each week, the bulletin covers the weather of the week and its effects on crops and farm activities. Short reports from individual States are supplemented by maps of average temperature and total precipitation. In the winter months a chart of snow depth is included. Subscription: Annual, Domestic $3, Foreign $4; 10¢ per copy. For period December through March: Domestic $1.00, Foreign $1.50.

## CLIMATOLOGICAL DATA—NATIONAL SUMMARY

This monthly publication contains climatological data such as pressure, temperature, winds, rainfall, snowfall, severe storms, floods, etc., for the United States as a whole. A short article describing the weather of the month over the United States, tables of the observational data, and a description of flood conditions are supplemented by 15 charts. An annual issue summarizes weather conditions in the United States for the year. More detailed local data are provided in the Climatological Data (by sections) for 45 sections representing each State or a group of States and Hawaii, Alaska, and the West Indies. Subscription price for either the National Summary or for a Section: $4.00 per year (including annual issue) domestic, $5.50, foreign; 30¢ per monthly issue; 50¢ for annual issue alone.

(Continued on inside back cover)

The Weather Bureau desires that the *Monthly Weather Review* serve as a medium of publication for original contributions within its field, but the publication of a contribution is not to be construed as official approval of the views expressed.

The issue for each month is published as promptly as monthly data can be assembled for preparation of the review of the weather of the month. In order to maintain the schedule with the Public Printer, no proofs will be sent to authors outside of Washington, D. C.

---

The printing of this publication has been approved by the Director of the Bureau of the Budget, February 9, 1955

DEPARTMENT OF COMMERCE
SINCLAIR WEEKS, Secretary

WEATHER BUREAU
F. W. REICHELDERFER, Chief

# MONTHLY WEATHER REVIEW

JAMES E. CASKEY, JR., Editor

Volume 83
Number 1

JANUARY 1955

Closed March 15, 1955
Issued April 15, 1955

## A MECHANISM FOR ASSISTING IN THE RELEASE OF CONVECTIVE INSTABILITY

ROBERT G. BEEBE AND FERDINAND C. BATES

Severe Local Storms Center, Weather Bureau Airport Station, Kansas City, Mo.

[Manuscript received June 14, 1954; revised February 9, 1955]

### ABSTRACT

A model is proposed as one means whereby an air mass characterized by the "typical" tornado sounding is converted to one described by the type of sounding observed in the vicinity of a tornado. By considering certain indications of the vorticity equation, it is possible to analyze configurations of jet axes and jet maxima such that low-level (850 mb.) convergence is surmounted by higher-level (500 mb.) divergence. Thus a model of jet structures is described which assists in, or possibly in some cases effects, the release of convective instability through vertical stretching or lifting. An example is presented to illustrate the use of this model in tornado forecasting and methods of application are outlined.

### 1. INTRODUCTION

Typical pre-tornado soundings which have been described by various investigators usually have in common the characteristic of pronounced convective instability. At the same time, these soundings also share the property of marked parcel stability for the lower moist layer. It is therefore necessary that the air column, particularly the lower moist layer, be subjected to considerable lifting before the convective instability can be realized. The manner in which the convective instability is released, or set up for release, is perhaps the least understood of the various aspects of severe local storm forecasting. The objective of this study is to describe one means, a model of jet structures, which can assist in the release of convective instability and in some cases possibly effect this release.

The mechanism to be described consists of a pattern of horizontal convergence at low levels surmounted by horizontal divergence at some higher level. The resulting vertical motion thus contributes to the conversion, usually gradual, of the vertical structure of the environment from one of marked convective instability with dry air aloft and an inversion-capped moist layer to one of marked parcel instability in which moisture penetrates to greater heights and the capping inversion is eliminated. The area considered here is much larger than that of an individual thunderstorm or tornado and it is emphasized that the microstructure of the tornado itself is not speculated upon here. This study deals with the environment during the intermediate processes of the realization of convective instability. It will be shown that this model may be delineated synoptically by certain combinations of low and high level jet structures. "Jet" as used here shall refer to a horizontal wind speed maximum.

### 2. RELATED INVESTIGATIONS

The model postulated agrees with empirical findings of the pioneers in the field of tornado forecasting. Varney [1] in 1926, was one of the first to point out the existence of a temperature inversion with relatively dry air over a layer of about 6,000 feet of moist, warm air as a precedent

333845—55——1

condition for tornado development. A little later that same year, Humphreys [2] stated:

> Mid-air temperature inversions appear to be quite common and the lapse rates next above these inversions [increase] very rapid[ly], often nearly or quite of adiabatic value. In short, so far as one can infer from these few observations [26 observations by sounding balloon or kite], the atmosphere in the neighborhood of a tornado appears to be unusually stratified, and tending to become unstable at one or more levels.

In 1942, Lloyd [3] presented several precedent soundings and was perhaps the first to point out that the soundings were convectively unstable. Like previous investigators, he attributed the release of the great instability to the movement from the west of cold air aloft over a warm, moist layer at the surface.

The importance of convective instability in the development of tornadoes was first illustrated by Showalter [4] in a proposed typical sounding which was based upon many soundings taken prior to tornado development and within the same air mass. He proposed that the convective instability could be released through free convection if mechanical lifting occurred, and the mechanical lifting could be produced by horizontal convergence or frontal lifting. Fawbush, Miller, and Starrett [5, 6] proposed six criteria necessary for tornado development which agreed with earlier investigations. It should be noted here that Fawbush, Miller, and Starrett, Tepper [7, 8, 9], and others suggest that this lifting occurs rather suddenly.

More recently Beebe [10], in an analysis of tornado proximity soundings (tornado occurred within 50 miles of a RAOB station and within the hour following release time), showed that the air mass in which tornadoes develop is no longer characterized by the "typical" sounding. None of these proximity soundings showed the low-level inversion while moisture was noted to great heights. Thus, these proximity soundings more nearly resembled the mean thunderstorm sounding shown by Byers [11]. Further study of these data suggests that the transformation of the "typical" sounding is a gradual process occurring over a period of several hours rather than as a sudden conversion.

## 3. DEVELOPMENT OF THE MODEL

The hypothesis presented is that the environment preceding tornado activity is acted upon by a dynamic mechanism consisting of horizontal convergence at low levels and horizontal divergence at a height sufficient to produce the modifications noted. This low-level convergence causes vertical stretching of the lower atmospheric layers and, in the environs of tornado inception, produces parcel instability and causes moisture to be carried upward into the middle troposphere.

A valid relationship of observable parameters which will delineate such a structure is the vorticity equation which may be stated:*

$$\frac{d\eta}{dt}=-\eta\,\mathrm{div}_2\,V+S+F \tag{1}$$

where $\eta$ = vertical component of absolute vorticity
$\frac{d\eta}{dt}$ = time rate of change of vertical component of absolute vorticity on a particle in motion
$V$ = horizontal velocity
$\mathrm{div}_2\,V$ = horizontal divergence
$S$ = torque of horizontal solenoid field
$F$ = horizontal torque of frictional forces

Since this equation may be considered either as scalar, or, to the same effect, as consisting of coaxial vectors, it may be restated:

$$\mathrm{div}_2\,V=-\frac{1}{\eta}\frac{d\eta}{dt}+\frac{S}{\eta}+\frac{F}{\eta} \tag{2}$$

A measure of the horizontal divergence may thus be obtained by considering some area at the height desired and noting:

a) the time rate of change of absolute vorticity of particles moving horizontally through the area,
b) the horizontal solenoid field within the area, and
c) the magnitude of the frictional torque within the area.

For an order of magnitude estimate of the values of horizontal divergence required to significantly modify an environment, an approximate computation may be made. Insofar as the atmosphere may be approximated by an incompressible fluid, the equation of continuity may be stated:

$$\frac{\partial w}{\partial z}=-\mathrm{div}_2\,V \tag{3}$$

where $w$ is the vertical component of velocity. Assuming a distribution of horizontal divergence with height such as that shown in figure 1, it may be stated:

$$\mathrm{div}_2\,V=\mathrm{div}_2\,V_0\cos\frac{\pi z}{6000},\ (z\text{ in meters}) \tag{4}$$

where subscript 0 refers to surface $z=0$. Combining (3) and (4) and integrating with from $z=0$ to arbitrary height $z$,

$$w_z=-\frac{6000}{\pi}\,\mathrm{div}_2\,V_0\sin\frac{\pi z}{6000},\ (\mathrm{m/sec.}) \tag{5}$$

A value for $\mathrm{div}_2\,V_0$ may now be inserted in (5). This value is computed from the value for $\mathrm{div}_2\,V_z$ at a height of about 1500 meters, or 850 mb., near the Flint, Mich. tornado as obtained by Cressman [12], viz: $-10^{-5}$ sec.$^{-1}$

$$\mathrm{div}_2\,V_0=\mathrm{div}_2\,V_z\sec\frac{\pi z}{6000}=-10^{-5}\,1.4\ \mathrm{sec.}^{-1} \tag{6}$$

---

*The term representing the interchange of vorticity between the horizontal and vertical is omitted. A qualitative evaluation of this neglected term indicates that it acts to modify the distribution of the vertical motion within the regions identified by the other terms, but that it does not act to reduce the maximum vertical motion or to shift this point or area of vertical motion from the significant regions.

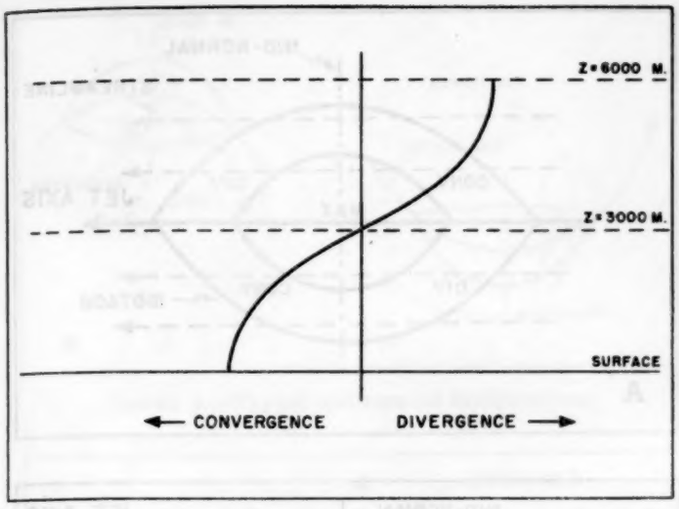


FIGURE 1.—Distribution of horizontal divergence with height assumed for computational purposes.

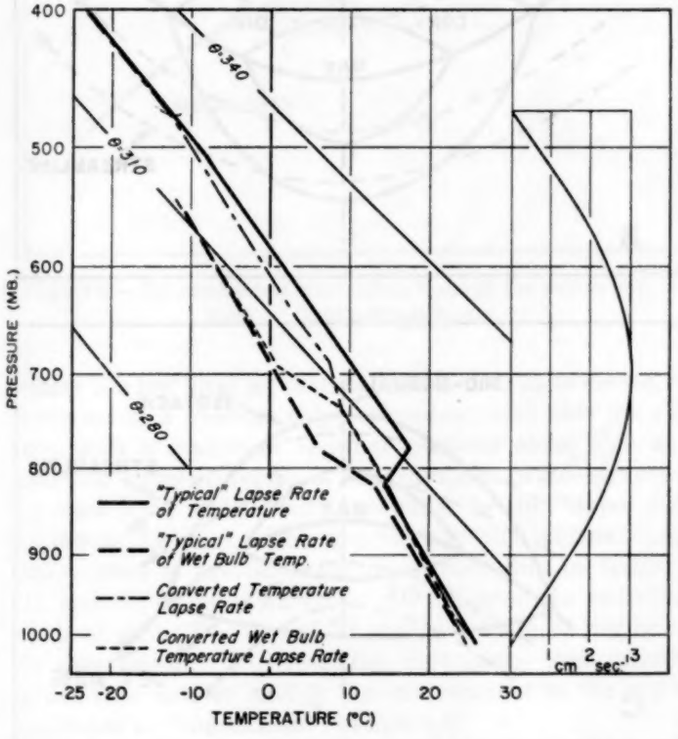


FIGURE 2.—A "typical" sounding shown before and after modification by lifting. The vertical motion field acting is shown at right.

Inserting this value in (5), a pattern of vertical motion is obtained:

$$w_s \simeq 3 \sin \frac{\pi z}{6000}, \text{ (cm sec.}^{-1}\text{)} \tag{7}$$

This distribution of $w$ is shown on the right side of figure 2. Permitting this pattern to act on the Fawbush-Miller typical tornado sounding [13] for a period of 10 hours yields the result shown in figure 2.

This time period of action was frequently observed in cases of modifications of environment studied, but it is probably near the maximum significant time interval. It may be that modification by such means is effected occasionally in as short a time interval as one hour ($10^{-4}$ sec$^{-1}$). Since Cressman's data were based upon a relatively large grid, such an order of magnitude is not excessive for small areas. This sets the following limit:

$$|\text{div}_2 V_0| \geq 10^{-5} \text{ sec.}^{-1} \tag{8}$$

Since, except in some unusual circumstances, particularly at low levels, $\left|\frac{S}{\eta}\right| \ll 10^{-5}$ sec.$^{-1}$, it is necessary that the first and third terms on the right in (2) make the contributions of the proper magnitude. This can be the case usually only in the vicinity of marked wind maxima, or jets. It is necessary, then, to determine which configurations of such features will delineate the mechanism sought. Restating (2)

$$\text{div}_2 V = -\frac{1}{\eta}\frac{\partial \eta}{\partial t} - \frac{V}{\eta}\frac{\partial \eta}{\partial s} + \frac{S}{\eta} + \frac{F}{\eta} \tag{9}$$

where $s$ is distance and $V$ is speed along the trajectory.

In order to utilize (9) in a practical manner, the following assumptions are made:

a) the condition is steady state, i. e. $\frac{\partial \eta}{\partial t} = 0$

b) the trajectory of a particle moving through the field may be approximated by a streamline, and

c) $\eta$ is always positive.

Equation (9) may then be expanded in finite difference form as follows:

$$\text{div}_2 V = \underbrace{-\frac{VK}{\eta}\frac{\Delta V}{\Delta s}}_{\text{(I)}} \underbrace{-\frac{V^2}{\eta}\frac{\Delta K}{\Delta s}}_{\text{(II)}} \underbrace{+\frac{V}{\eta}\frac{\Delta}{\Delta s}\left(\frac{\Delta V}{\Delta n}\right)}_{\text{(III)}} \underbrace{-\frac{\beta v}{\eta}}_{\text{(IV)}} + \underbrace{\frac{S}{\eta}}_{\text{(V)}} + \underbrace{\frac{F}{\eta}}_{\text{(VI)}} \tag{10}$$

where $V$=speed of particle along the streamline
$K$=streamline curvature
$s$=distance along streamline
$n$=distance along normal to streamline—positive to left of flow
$v$=north-south component of velocity—positive for south wind
$\beta$=Rossby parameter=rate of change of coriolis parameter northward=$\frac{2\,\Omega \cos \phi}{a}$ where $\Omega$ is angular velocity of the earth and $a$ is radius of the earth.

Utilizing (10), it is possible to analyze various geometrical and geographical configurations of jet axes and jet maxima for regions of action of the dynamic mechanism. Directing attention to the first three terms on the right, consider:

a) A jet axis with curvature but without maxima. Here only term II is significant since $\Delta V = 0$. Figure 3 shows the characteristic divergence

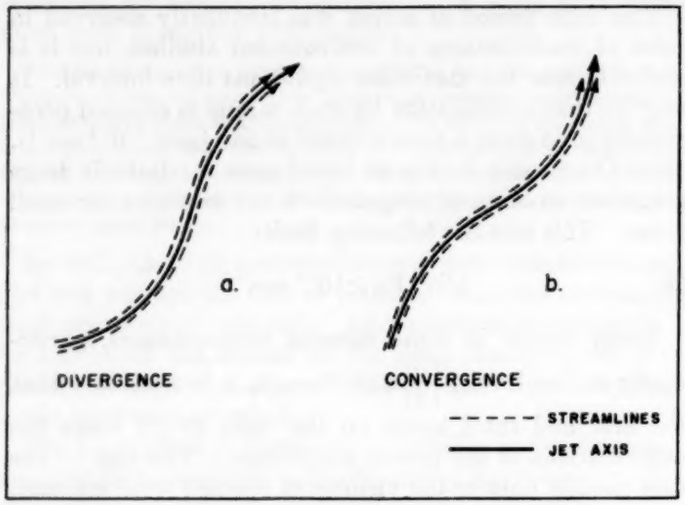


FIGURE 3.—Horizontal divergence patterns related to jet axes due to curvature alone.

patterns. (The azimuthal orientation is not significant, since term IV is not considered here.)

b) A jet maximum without curvature. Here, since $K$ and $\Delta K=0$, only term III is significant. Characteristic related divergence patterns are shown in figure 4A.

c) A jet maximum with cyclonic curvature maximum coincident. Terms I, II, and III are significant and divergence patterns are shown in figure 4B.

d) A jet maximum with anticyclonic curvature maximum coincident. Again terms I, II, and III are significant (fig. 4C.)

Many combinations of the foregoing divergence patterns are possible and two optimum patterns of divergence over convergence are shown in figure 5. The foregoing has been treated at length by Riehl et al. [14]. It should be noted that the area dealt with here is in the magnitude range of cyclogenesis, so that similar conditions should apply. There is no inconsistency with other procedures, e. g. the work of Sutcliffe [15].

It may be further noted that term IV contributes to convergence with southerly flow, and vice versa; term V contributes to convergence with warm air advection, and vice versa; and term VI contributes to convergence with positive relative vorticity and vice versa. The proper function of term VI is difficult to state, but it is not unreasonable to consider it of significant magnitude at low levels, permitting considerable convergence with less intense jet structures than those required at higher levels.

A low level southerly jet from a warm, moist source region acts in two ways to create an environment similar to that noted in the majority of tornado occurrences. First, through the advection of moisture at low levels such a jet acts to create convective instability in the region it undercuts. Secondly, it acts to create a means for effecting the release of this convective instability in the following manner. To the left of the axis of this jet,

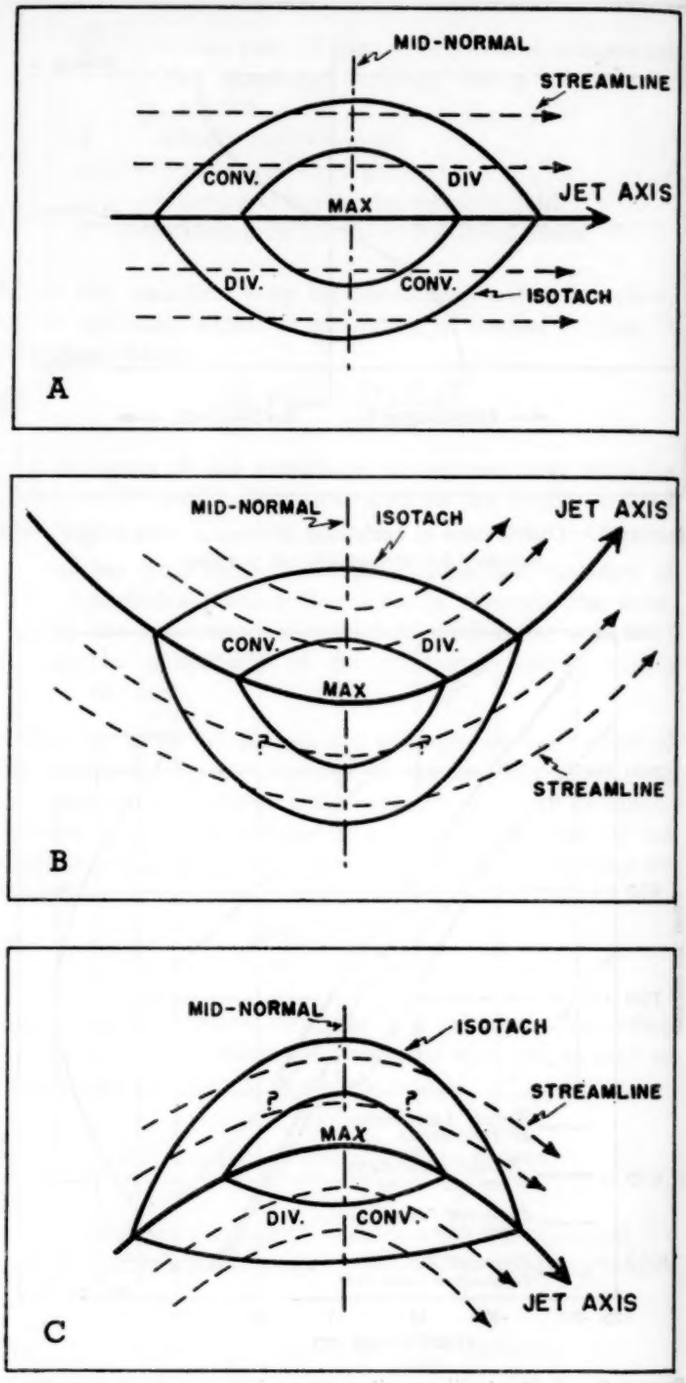


FIGURE 4.—Horizontal divergence patterns related to a jet maximum. (A) Without curvature due to inertial terms only. (B) At maximum cyclonic curvature point due to inertial terms only. (C) At maximum anticyclonic curvature point due to inertial terms only.

terms IV, V, and VI of (10) contribute to convergence, while to the right of the axis, term VI opposes the other terms and the region is indeterminate for qualitative evaluation. Thus, a region of convergence is delineated to the left of the axis (to the west and strongest in the northern end where warm advection is greatest). The deformation of the mean isotherms through the layer in

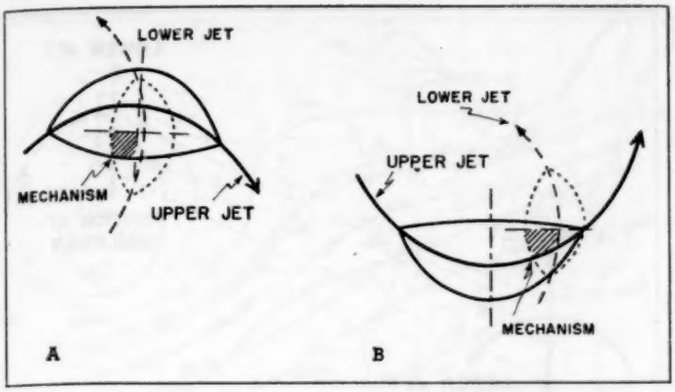


FIGURE 5.—Typical optimum jet configurations.

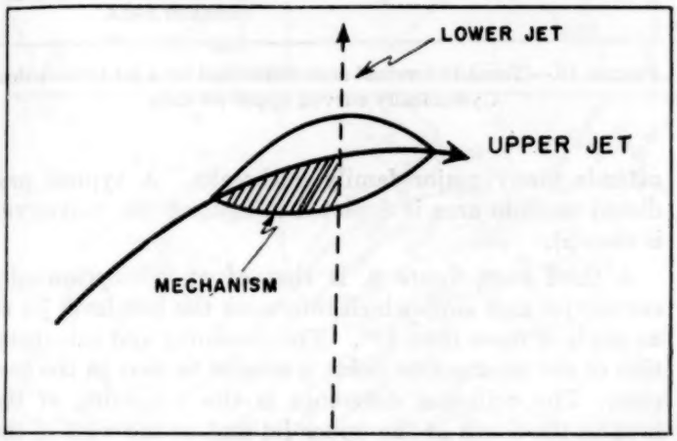


FIGURE 6.—Jet mechanism established through the action of a low level jet from a warm source.

which the low level jet is embedded is such as to create, or accentuate, a thermal ridge coincident with this jet axis and with a maximum thermal gradient along this axis near its difluent region. The resultant wind structure at some level aloft should be similar to the "upper jet" shown in figure 6. The quadrant of the jet maximum aloft noted is favorable for divergence due to terms I, II, and III of equation (10). At this level the contributions of terms IV, V, and VI should usually be negligible in comparison. The resulting divergence over convergence thus acts to modify the environment in the region indicated as "mechanism" in figure 6.

## 4. APPLICATION

The use of this model in tornado forecasting is based primarily upon a careful analysis of jet, or wind maxima, axes at the 850- and 500-mb. levels The prognosis of these jet axes may be accomplished through the application of contour prognoses, extrapolation, and anticipated reactions of appropriate thickness fields. The low level jet is also closely related to surface developments and displacements so that variations in intensity must be weighted accordingly.

In general, the jet axis or wind maxima at the 500-mb.

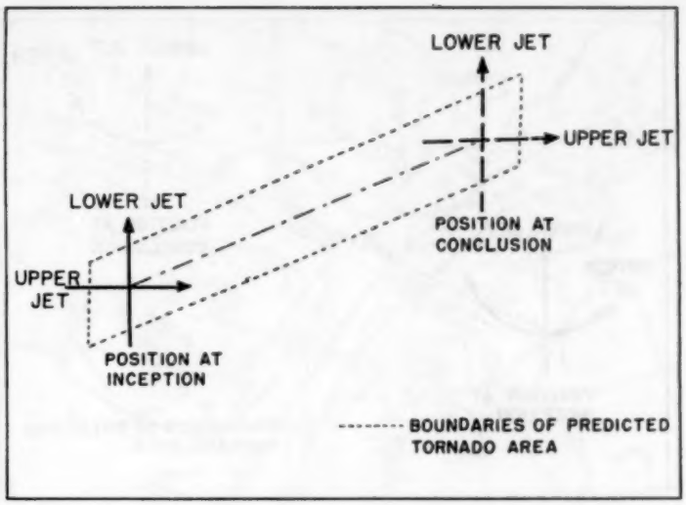


FIGURE 7.—Tornado forecast area delineated by a jet intersection. No curvature and angle of intersection >45°.

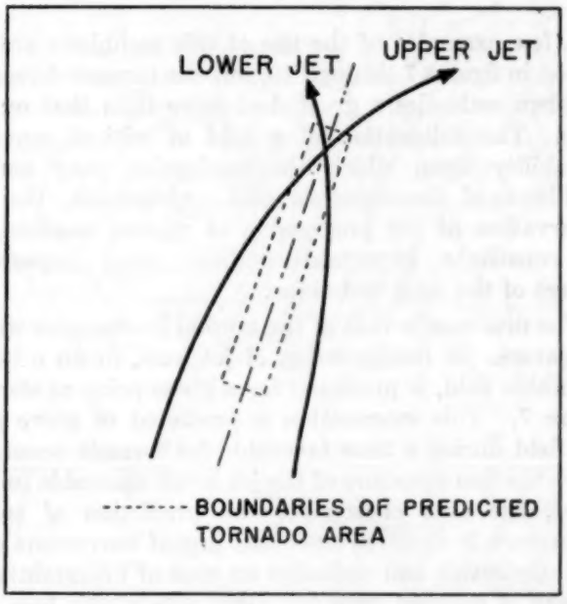


FIGURE 8.—Tornado forecast area delineated by a jet intersection. Anticyclonically curved upper jet axis and angle of intersection ≤45°.

level that is of concern here is that which lies to the southeast of the major jet axis. These secondary jets may often constitute little more than the southern or southeastern boundary of a plateau of high wind speed extending to the right (usually southeast) of the major jet axis. (An exception to this generalized case exists in the situation illustrated in fig. 10 where the 500-mb. jet of interest is usually the major jet at that level.) The intensification of this secondary jet is frequently noted on 500-mb. charts prior to tornado occurrence and the wind maximum at the time and site of occurrence is generally quite apparent. It is stressed that the interest here is that divergence and wind shear at the 500-mb. level may often be used to delineate a vertical motion field.

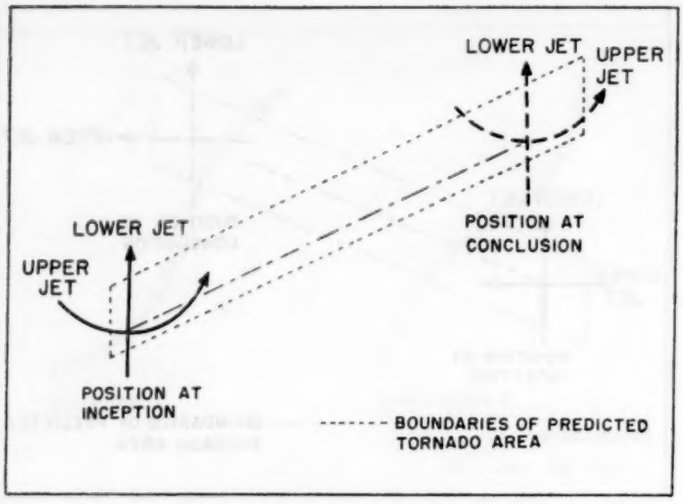


FIGURE 9.—Tornado forecast area delineated by a jet intersection. Anticyclonically curved upper jet axis and angle of intersection >45°.

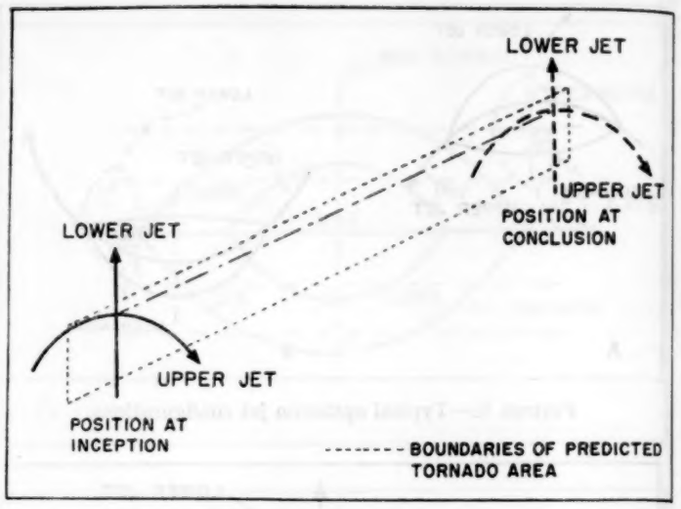


FIGURE 10.—Tornado forecast area delineated by a jet intersection. Cyclonically curved upper jet axis.

A few examples of the use of this technique are illustrated in figures 7 through 10, but the tornado forecasting problem embodies a great deal more than that outlined here. The delineation of a field of critical convective instability upon which the mechanism may act, the problems of frontogenesis and cyclogenesis, the close observation of the progression of related weather, etc., all constitute important—perhaps more important—phases of the total technique.

The first case is that of the normal intersection without curvature. A configuration of jet axes, in an otherwise favorable field, is predicted for a given point as shown in figure 7. This intersection is predicted to move across the field during a time favorable for tornado occurrence. Since the fine structure of the jet is not amenable to treatment, the area chosen for the prediction of tornado occurrence is centered upon the line of movement of the jet intersection and embodies an area of uncertainty, due to lack of detailed data, on either side of this line. The occurrences will usually be found very close to the intersection and seldom consist of more than one or two tornadoes.

The second case, figure 8, is that of the anticyclonically curved upper jet axis oriented at an angle of 45° or less with respect to the lower jet axis. With this structure, the significant area is related to a line from the point of intersection (or the extended intersection point if the jets do not actually intersect) southwestward, bisecting the angle between the two jets as shown in figure 8. The reasoning here is that undelineable fine structures branch from the main jet axes and interact very nearly along the bisecting line. The probability of such interaction is a function of the spatial separation of the jets and, thus, of the angle between them. Occurrences usually break out first in the south and move northward along the line bisector. This pattern is frequently quasi-stationary and attends many major family outbreaks. A typical predicted tornado area is depicted in figure 8 (no movement is shown).

A third case, figure 9, is that of an anticyclonically curved jet axis aloft which intersects the low level jet at an angle of more than 45°. The reasoning and extrapolation of the intersection point is similar to that in the first case. The principal difference is the weighting of the area to the south of the upper jet and to the west of the lower jet axis for probability of occurrence. The limits of error in positioning the jet axes require inclusion of the intersection point and some area to the north and east. A typical area for tornadoes with such a configuration is shown in figure 9.

A fourth case, figure 10, is that of the intersection of a cyclonically curved jet aloft with a low level jet. This situation is also similar to the first case but weight is given to the area to the north and west of the upper jet, as shown in figure 10. This type is representative of the elusive "cold" type occurrences, such as the Hartford, Conn., storm of May 10, 1954. In these situations the low level jet is not necessarily well defined but surface indices place the occurrence in a region of pronounced low-level convergence. Occurrences with this type of jet structure are usually less intense, rarely attended by more than one or two tornadoes, and frequently associated with "funnel clouds aloft."

## 5. EXAMPLE

The magnitude of horizontal convergence or divergence is not amenable to either easy or exact calculation. However, a qualitative evaluation of the validity and use of this model may be illustrated through an example of the severe tornado outbreak of March 21–22, 1952.

A rather complete picture of the synoptic situation and thermodynamic properties of this air mass has been given

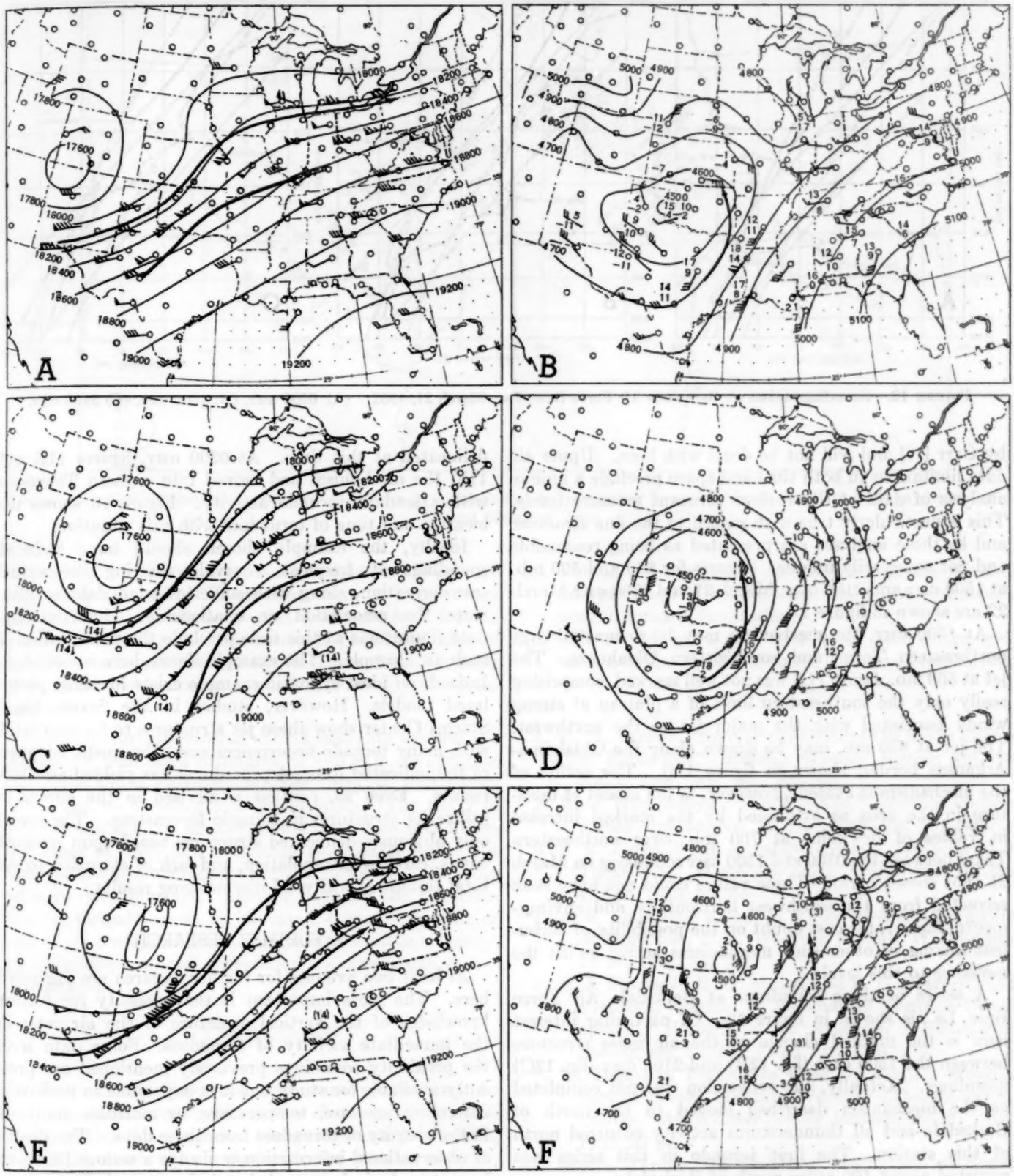


FIGURE 11.—Sectional 500- and 850-mb. charts. Solid lines are contours at 100-ft. intervals. Wind barbs show speed in knots (half barb = 5 knots, full barb = 10 knots, pennant = 50 knots). (A) 500 mb., 1500 GMT, March 21, 1952. (B) 850 mb., 1500 GMT, March 21, 1952. (C) 500 mb., 2100 GMT, March 21, 1952. (D) 850 mb., 2100 GMT, March 21, 1952. (E) 500 mb., 0300 GMT, March 22, 1952. (F) 850 mb., 0300 GMT, March 22, 1952.

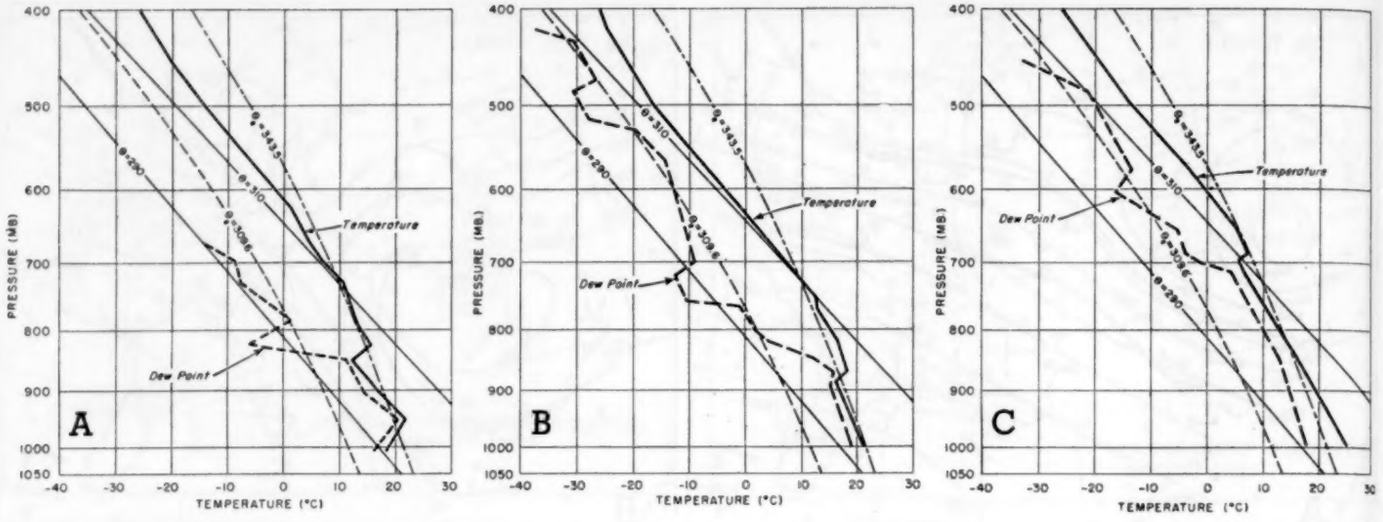


FIGURE 12.—Soundings taken at Barksdale Air Force Base, La., March 21, 1952. (A) 0900 GMT, (B) 1500 GMT, (C) 2100 GMT.

by Carr [16] and will not be dealt with here. Upper air data limitations in both time and space preclude a unique analysis of data at the various constant pressure levels. This is particularly true with regard to the fine structure and so these analyses are presented as being reasonable and not necessarily unique. Charts for 850 and 500 mb. at 1500 GMT and 2100 GMT, March 21 and 0300 GMT March 22 are shown in figure 11.

At 1500 GMT, the mechanism may be delineated over northeastern Texas and southeastern Oklahoma. The jet at 500 mb., figure 11A was not well marked, comprising really only the southeastern limit of a plateau of strong winds associated with the major jet to the northwest. The jet at 850 mb. may be drawn along the Oklahoma-Arkansas border, shown in figure 11B. The action of the mechanism is evident, however, in the ascent of moisture in the area as evidenced by the marked increase in values of dewpoint at 700 mb. over northeastern Texas between the 0300 and 1500 GMT soundings on March 21 (not shown here). These values could not have been advected from the southwest horizontally and environmental lapse rates cast doubt on the possibility of turbulent mixing or other such mechanisms acting to lift the moisture to this level.

A series of three soundings at Barksdale Air Force Base, La., is shown in figure 12. Of particular interest here is the marked change in the air mass structure between the 1500 GMT (fig. 12B) and 2100 GMT (fig. 12C) soundings. Actually, the conversion was not completed as the mechanism described moved to the north of Barksdale and all thunderstorm activity occurred north of this station. The first tornado in this series was reported about 100 miles north of Barksdale.

At 2100 GMT, figures 11C and 11D, the mechanism had moved into southwestern Arkansas and marks rather well the area of the first occurrence, which was nearly synoptic. The two jet patterns were somewhat better delineated at this time. At 0300 GMT, figures 11E and 11F, the mechanism had moved into western Tennessee with attendant tornado activity. Figure 13 shows the location and time of tornadoes with this situation.

Ideally, the example chosen should have included soundings at frequent intervals showing the actual transformation, along with sufficient wind data to illustrate the association or relationship. Unfortunately, data limitations at this time preclude the presentation of such an example. The example shown here is not ideal. Indeed, no ideal synoptic example exists for most postulated models. However, studies in the Severe Local Storms Center show these jet structures to be associated with many tornado occurrences and subsequent adoption of the indicated forecast procedures has yielded excellent results. Even so, caution is advised in the efforts to utilize jet structures in tornado forecasting. The use of only obviously delineated structures based upon reported winds, careless extrapolation, and lack of attention to the total technique will yield discouraging results.

## 6. FURTHER RESEARCH

At least two avenues for further research are suggested here. The more important is the necessity for further knowledge of the vertical structure of the air mass in the immediate vicinity of tornadoes. Some data from the proximity soundings previously mentioned are presently available for study but it is impossible to positively determine pressure, temperature, or moisture gradients in the vicinity of tornadoes from these data. The dearth of observational information is always a serious handicap in meteorological research but it is particularly acute in the field of severe local storms. The aerological nature of such information is stressed since it has been the experience of severe weather forecasters that surface data alone are too frequently inconclusive, and sometimes

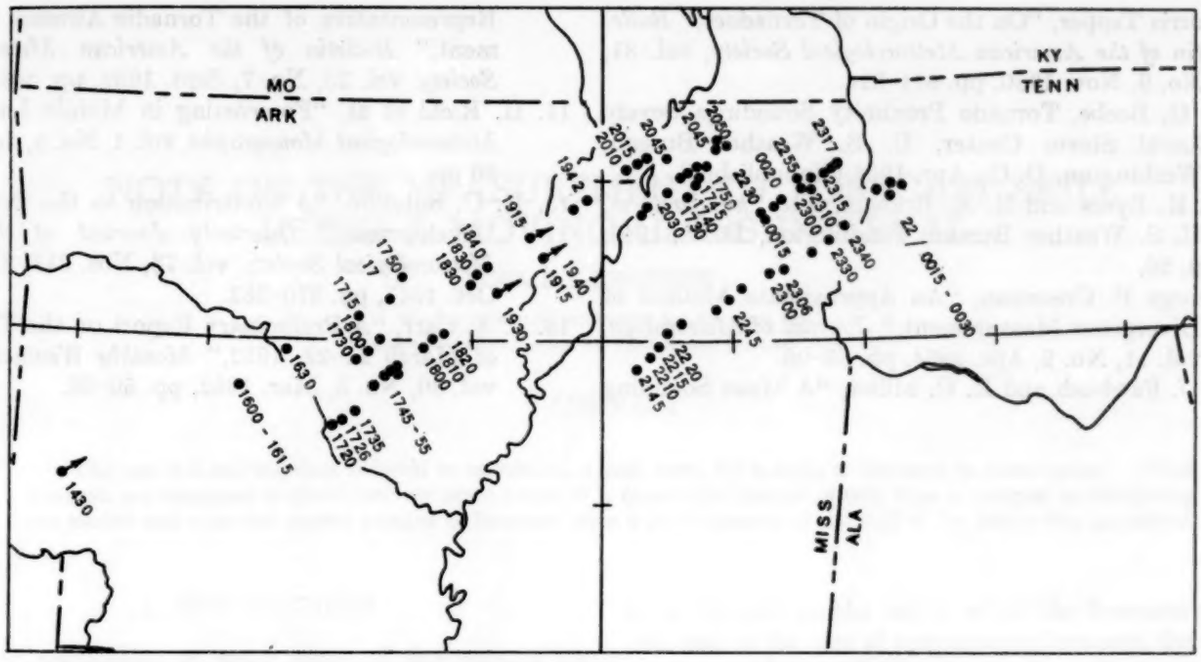


FIGURE 13.—Plot of tornado occurrences on March 21 through the early morning hours of March 22, 1952. Times shown are in Central Standard Time.

misleading. It will therefore become necessary to procure additional aerological information from a more dense network than is presently available, at least for a limited period for study, before our meteorological knowledge of tornado development can justify forecasts of much smaller areas than those now attempted (10,000–20,000 square miles).

Secondly, further research should take into account the differences in air mass structures, as well as in the synoptic situations which evidently produce them, so that occurrences can be classified into broad types. The study of proximity soundings already points to at least four different types of precedent soundings (soundings within the airmass in which tornadoes occurred, but some 6–12 hours prior to development). Another basis for the classification of tornado types is indicated through the use of related jet configurations, and indices to relative intensity, areal distribution, and probability are inherent in such a classification.

## 7. CONCLUSIONS

(a) Patterns of divergence over convergence may be delineated on synoptic weather charts by appropriate jet structures which are observable and predictable, within reasonable limits, with the present observational network.

(b) The model of jet structures proposed here acts upon convectively unstable air to create, or help create, limited areas of optimum parcel instability wherein maximum thunderstorm activity and tornadoes occur.

(c) This model constitutes an extension of the physical interpretation of several empirical rules successfully used in tornado forecasting.

(d) This model, when used with other parameters, provides a method which is useful in tornado forecasting.

## REFERENCES

1. B. M. Varney, "Aerological Evidence as to the Causes of Tornadoes," *Monthly Weather Review*, vol. 54, No. 4, Apr. 1926, pp. 163–165.
2. W. J. Humphreys, "The Tornado," *Monthly Weather Review*, vol. 54, No. 12, Dec. 1926, pp. 501–503.
3. J. R. Lloyd, "The Development and Trajectories of Tornadoes," *Monthly Weather Review*, vol. 70, No. 4, Apr. 1942, pp. 65–75.
4. A. K. Showalter and J. R. Fulks, *Preliminary Report on Tornadoes*, U. S. Weather Bureau, Washington, D. C., 1943, 162 pp.
5. E. J. Fawbush, R. C. Miller, and L. G. Starrett, "An Empirical Method of Forecasting Tornado Development," *Bulletin of the American Meteorological Society*, vol. 32, No. 1 Jan. 1951, pp. 1–9.
6. "A Digest of Procedures Used by the Air Weather Service Severe Weather Warning (Thunderstorm) Center," *Air Weather Service Manual*, 105–37, Nov. 1952, 63 pp.
7. Morris Tepper, "A Proposed Mechanism of Squall Lines: The Pressure Jump Line," *Journal of Meteorology*, vol. 7, No. 1, Feb. 1950, pp. 21–29.
8. Morris Tepper, "Radar and Synoptic Analysis of a Tornado Situation," *Monthly Weather Review*, vol. 78, No. 9, Sept. 1950, pp. 170–176.

333845—55——2

9. Morris Tepper, "On the Origin of Tornadoes," *Bulletin of the American Meteorological Society*, vol. 31, No. 9, Nov. 1950, pp. 311–314.
10. R. G. Beebe, Tornado Proximity Soundings, Severe Local Storm Center, U. S. Weather Bureau, Washington, D. C., Apr. 1954 (Unpublished).
11. H. R. Byers and R. R. Braham, *The Thunderstorm*, U. S. Weather Bureau, Washington, D. C., 1949, p. 20.
12. George P. Cressman, "An Approximate Method of Divergence Measurement," *Journal of Meteorology*, vol. 11, No. 2, Apr. 1954, pp. 83–90.
13. E. J. Fawbush and R. C. Miller, "A Mean Sounding Representative of the Tornadic Airmass Environment," *Bulletin of the American Meteorological Society*, vol. 33, No. 7, Sept. 1952, pp. 303–307.
14. H. Riehl et al, "Forecasting in Middle Latitudes," *Meteorological Monographs*, vol. 1, No. 5, June 1952, 80 pp.
15. R. C. Sutcliffe, "A Contribution to the Problem of Development," *Quarterly Journal of the Royal Meteorological Society*, vol. 73, Nos. 317, 318, July-Oct. 1947, pp. 370–383.
16. J. A. Carr, "A Preliminary Report on the Tornadoes of March 21–22, 1952," *Monthly Weather Review*, vol. 80, No. 3, Mar. 1952, pp. 50–58.

# NOTE ON THE MEASUREMENT OF FORECAST SKILL USING A MOVING CLASS INTERVAL

DONALD L. JORGENSEN

Weather Bureau Airport Station, San Francisco, Calif.

[Manuscript received October 13, 1952; revised February 14, 1955]

## ABSTRACT

The use of a moving class interval in calculating a skill score for a series of forecasts is investigated. When forecasts are expressed in quantitatively exact terms, it is found that the use of this type of interval in calculating the correct and expected correct number of forecasts gives a good measure of the skill of the forecasting procedure.

## 1. INTRODUCTION

In the verification of many types of forecasts, it has become common practice to express the data in the form of a contingency table and from this to derive a skill score [1]. The most common type of table consists of two categories, but as many categories as desired can be used. As pointed out by Vernon [2], the conventional skill score gives the same weight to each incorrect forecast regardless of the size of the error. In the same way, each correct forecast is given the same weight regardless of the size of the error, where the size of the greatest possible error which can be verified as correct is a function of the size of the class interval. This latter characteristic becomes of significance when forecasts are issued in quantitative terms, such as temperature forecasts to the exact degree, and then verified by classes. For example, a class interval of 7° would allow a temperature forecast falling at one end of the class interval to be verified by an observed value falling at the other end, even though exhibiting an error of 6°. At the other extreme, a forecast may be evaluated as incorrect with an error as small as 1° for those rather frequent occasions when the forecast value falls in one class interval and the observed value falls just across the class boundary into an adjoining class. In order to compensate for these recognized deficiencies, Vernon has proposed two types of scores to evaluate forecasts in terms of the magnitude of the error (see [2]).

In this paper, a modification of the conventional skill score is proposed which corrects some of the deficiencies resulting from rigid class intervals, while at the same time maintaining the general characteristics of the conventional score.

## 2. CONCEPT OF A MOVING CLASS INTERVAL

For verification purposes, the usefulness of a series of forecasts may be considered as dependent on the degree to which the verifying observations come within a specified allowable error of the forecast values. The allowable error depends on the use to which the forecasts are to be put, and in the case of temperature forecasts, for example, might vary from 2° for frost protection when temperatures are near or below freezing to much larger values for general public use. Thus, a verification scheme which evaluates as correct only those forecasts which come within a given plus or minus amount of the observed value has a usefulness well founded in practice. If we assume that a temperature forecast must come within 3° to be of full use to a particular recipient, then the verifying range in which the observed value must fall is within $\pm 3°$ of the forecast value. We see at once that we have what corresponds to a moving class interval with the forecast value at the center and the interval covering a 7° range. A system which uses a moving class interval for forecast verification would verify as correct many forecasts in common with a system using comparable fixed class intervals. However, certain forecasts would verify as correct in one system but not in the other.

## 3. CONVENTIONAL SKILL SCORE

The conventional skill score $S$ is usually expressed by the relationship:

$$S=\frac{C-E_c}{T-E_c} \tag{1}$$

where

$C$=number of correct forecasts based on a specified criterion.

$T$=total number of forecasts.

$E_c$=number of forecasts which could be expected to be correct on a chance basis with a random distribution of the forecasts over the period for which the score is calculated.

In order to evaluate (1) in terms of a moving class interval, certain of the quantities involved in the expression for the score, i. e., the value for $C$ and $E_c$, need to be derived in a somewhat different manner, since they are not obtainable from the usual contingency table. The

number of correct forecasts, $C$, may be obtained by counting the forecasts which fulfill the verifying criterion set forth. In determining the value of $E_c$, it may be assumed that the probability of an individual forecast to succeed on chance is equal to the ratio of the number of ways it can succeed to the number of ways it can both succeed and fail. Thus, the expression for obtaining the total number of expected correct forecasts for a particular temperature, $t$, may be written:

$$(E_c)_t = N_t \frac{f_{t\pm 3}}{T} \tag{2}$$

where

$N_t$=number of times the forecast of the given temperature, $t$, is made.

$f_{t\pm 3}$=number of occurrences in array of data of the observed temperatures which fall within $\pm 3°$ of the forecast temperature.

$T$=total number of cases.

Summing over all forecast temperatures, we may write:

$$E_c = \sum_{t=t'}^{t''} N_t \frac{f_{t\pm 3}}{T} \tag{3}$$

where

$t'$=lowest forecast temperature.

$t''$=highest forecast temperature.

Substituting the quantities $C$, $T$, and $E_c$, thus obtained, into (1) gives the skill score.

## 4. EXAMPLE OF SKILL SCORE BASED ON MOVING CLASS INTERVAL

Harman [3], in a paper on forecasting maximum temperatures for Sacramento, Calif., verified his forecasts on the basis of a $\pm 3°$ allowable error. Data taken from his study are used to illustrate the calculation of a skill score based on a moving class interval in the following example. In his paper, maximum temperature forecasts for the afternoon are made on data available at 7:15 a. m., local time, and cover a period for July and August for the years 1946 through 1952, with the years of 1951 and 1952 used as test data. Combined dependent and independent data will be used in the example that follows.

The pertinent data for the calculation of a skill score based on a moving class interval appear in table 1. Columns 1 through 4 pertain to observed data, and include the frequency of occurrence of given temperatures, the number of occurrences within $\pm 3°$ of the given temperature, and the ratio of the number of occurrences within $\pm 3°$ to the total number of cases. This latter value is the probability that a forecast of the given temperature will be correct on chance. (These probability values may be calculated on a climatological basis, and once this is done for a particular forecast problem, the calculation of the skill score is simplified.) Column 5 gives the number of forecasts for each temperature, and column 6 the product of the probability ratio in column 4 and the number of forecasts issued in column 5, which furnishes the number of expected correct forecasts for each temperature. The sum of column 6 gives $E_c$, the number of forecasts expected to be correct on a chance basis.

TABLE 1.—*Data used in calculating skill score based on a moving class interval of ±3°F., Sacramento, Calif., July and August 1946–52*

| (1) Maximum temperature (°F.) | (2) Frequency of occurrence of given temp. | (3) Number of occurrences within ±3° of given temp. | (4) Ratio of number in col. 3 to total number forecasts | (5) Number forecasts of given temp. | (6) Product of cols. 4 and 5 |
|---|---|---|---|---|---|
| | $f_t$ | $f_{t\pm 3}$ | $f_{t\pm 3}/T$ | $N_t$ | $(E_c)_t$ |
| 69 | 1 | 3 | 0.007 | | |
| 70 | 1 | 3 | .007 | | |
| 71 | 0 | 5 | .012 | | |
| 72 | 1 | 8 | .019 | | |
| 73 | 0 | 8 | .019 | 1 | 0.02 |
| 74 | 2 | 14 | .034 | | |
| 75 | 3 | 18 | .043 | 2 | .09 |
| 76 | 1 | 25 | .060 | 2 | .12 |
| 77 | 7 | 31 | .075 | 2 | .15 |
| 78 | 4 | 43 | .104 | 2 | .21 |
| 79 | 8 | 49 | .118 | 3 | .35 |
| 80 | 6 | 58 | .140 | 5 | .70 |
| 81 | 14 | 59 | .143 | 3 | .43 |
| 82 | 9 | 68 | .164 | 15 | 2.46 |
| 83 | 10 | 83 | .200 | 8 | 1.60 |
| 84 | 8 | 100 | .242 | 11 | 2.66 |
| 85 | 13 | 113 | .273 | 18 | 4.91 |
| 86 | 23 | 119 | .287 | 20 | 5.74 |
| 87 | 23 | 130 | .314 | 27 | 8.48 |
| 88 | 27 | 138 | .333 | 22 | 7.33 |
| 89 | 15 | 157 | .379 | 20 | 7.58 |
| 90 | 21 | 153 | .370 | 25 | 9.25 |
| 91 | 16 | 150 | .362 | 21 | 7.60 |
| 92 | 32 | 150 | .362 | 35 | 12.67 |
| 93 | 19 | 161 | .389 | 33 | 12.84 |
| 94 | 20 | 154 | .372 | 19 | 7.07 |
| 95 | 27 | 152 | .367 | 21 | 7.71 |
| 96 | 26 | 126 | .304 | 19 | 5.78 |
| 97 | 14 | 122 | .295 | 15 | 4.42 |
| 98 | 14 | 106 | .256 | 21 | 5.38 |
| 99 | 6 | 87 | .210 | 8 | 1.68 |
| 100 | 15 | 65 | .157 | 6 | .94 |
| 101 | 4 | 55 | .133 | 4 | .53 |
| 102 | 8 | 43 | .104 | 10 | 1.04 |
| 103 | 4 | 38 | .092 | 3 | .28 |
| 104 | 4 | 26 | .063 | 3 | .19 |
| 105 | 2 | 23 | .056 | 3 | .17 |
| 106 | 1 | 16 | .039 | 4 | .16 |
| 107 | 3 | 12 | .029 | 2 | .06 |
| 108 | 1 | 8 | .019 | 1 | .02 |
| 109 | 1 | 6 | .014 | | |
| Total | | | | 414 | 120.62 |

The number of correct forecasts $C$, i. e., the number for which the observed temperature fell within $\pm 3°$ of the forecast value, is 310. The total number of forecasts $T$ is 414, and the expected correct, $E_c$, as given at the bottom of column 6 is 120.6. Substituting these data into (1) gives a skill score of .65, the skill measured by the moving class interval technique.

## 5. COMPARISON OF SKILL SCORES

The magnitude of the skill score exhibited by a series of forecasts depends upon the particular procedure for calculating the skill. Each method of calculating skill will produce a different figure, with each score representing a somewhat different basis for the evaluation of the forecasts. In as much as the conventional type of score has come to represent a standard, it is of interest to compare the score obtained by the moving class interval with the fixed class interval. The skill score for the same data arranged in a contingency table made up of fixed class intervals of 7° is as follows:

$$S=\frac{276-115.5}{414-115.5}=.54$$

On the basis of a uniform $\pm 3°$ allowable error, the forecasts verified by means of the moving class interval are correctly verified in every instance in contrast to the case of fixed intervals where errors of as much as 6° can be evaluated as correct and errors of as little as 1° can be evaluated as incorrect. A comparison of the two types of scores indicates the difference in the apparent skill which is gained or lost when the verification is carried out under the differing criteria. Comparing the data contained in the two scores, it is seen that there is a net gain of 34 forecasts evaluated as correct by the moving class interval.

From the standpoint of the user who receives the forecasts and the forecaster who prepares them, the increase in percentage correct from 67 percent to 75 percent as well as the increase in the skill from .54 to .65 represents a significant improvement in the verifying procedure.

## REFERENCES

1. G. W. Brier and R. A. Allen, "Verification of Weather Forecasts," *Compendium of Meteorology*, American Meteorological Society, Boston, 1951, pp. 841–848.
2. E. M. Vernon, "A New Concept of Skill Score for Rating Quantitative Forecasts," *Monthly Weather Review*, vol. 81, No. 10, October 1953, pp. 326–329.
3. W. E. Harman, "An Objective Method for Forecasting the Maximum Temperature at Sacramento, California," U. S. Weather Bureau Office, Pomona, Calif., September 1952 (unpublished manuscript, revised November 1953, available at U. S. Weather Bureau, Washington, D. C.).

# THE WEATHER AND CIRCULATION OF JANUARY 1955[1]

## A Month with a Mean Wave of Record Length

WILLIAM H. KLEIN

Extended Forecast Section, U. S. Weather Bureau, Washington, D. C.

### 1. MEAN CIRCULATION

The mean circulation at the 700-mb. level during January 1955 was characterized by extremely long wavelengths at middle latitudes of the Northern Hemisphere. Figure 1 shows a hemispheric wave number of only three around 40°–45° N., with principal troughs located in Europe, Japan, and the western Atlantic, and ridges in the eastern Atlantic, eastern Pacific, and central Asia.[2] This long wavelength was sustained by a strong zonal current, in agreement with Rossby's classical wave formula [1]. Figure 2A shows the presence of a well developed mean 700-mb. jet stream in most of the hemisphere at middle latitudes, while figure 2B indicates that mean wind speeds were greater than normal in most of this area. Wind speeds decreased sharply, however, in regions of strong horizontal wind shear both north and south of the principal jet axis. Partly as a result, wavelengths were considerably shorter at both high and low latitudes than they were at middle latitudes. At higher latitudes, for example, there are 4 troughs in figure 1, with several additional troughs at low latitudes, over lower California, Iran, India, and the central Pacific.

Of particular interest is the long half wavelength which existed in the northern United States on the monthly mean chart between the ridge off the west coast and the trough off the east coast.[2] Measured at the 40° latitude circle, the distance between this ridge and trough in figure 1 is 81° longitude, the longest half wavelength ever observed on a 700-mb. monthly mean chart in this area at 40° N. In a previous paper [2] the author has demonstrated that systems with long half wavelengths on monthly mean charts in North America during winter are usually characterized by the following additional properties: Large amplitude in both North America and the Pacific, large difference in speed between strong winds at the trough and weak winds at the ridge, trough deeper and farther east than normal, ridge stronger and farther west than normal, trough with less northeast-southwest tilt than usual, and low value of the hemispheric zonal index.

TABLE 1.—*Comparison between mean winter values of various wave properties on monthly mean 700-mb. charts and January 1955 values (from fig. 1)*

| Property | Winter mean | January 1955 |
|---|---|---|
| Trough location at 40° N | 77° W | 56° W. |
| Ridge location at 40° N | 123° W | 137° W. |
| Ridge location along contour (upstream from trough at 40° N.) | 124° W | 130° W. |
| Half wavelength at 40° N | 46° of long. | 81° of long. |
| Contour half wavelength (upstream from trough at 40° N.). | 47° of long. | 74° of long. |
| Amplitude (upstream along contour from trough at 40° N.). | 12° of lat. | 23° of lat. |
| Geostrophic wind speed at trough at 40° N | 16 m. p. s. | 16 m. p. s. |
| Geostrophic wind speed at ridge (upstream along contour). | 10 m. p. s. | 6 m. p. s. |
| Wind speed difference (trough minus ridge) | 6 m. p. s. | 10 m. p. s. |
| Height at trough at 40° N | 9,650 ft. | 9,320 ft. |
| Height anomaly at trough at 40° N | −113 ft. | −500 ft. |
| Height anomaly at ridge (upstream along contour) | +81 ft. | +120 ft. |
| Horizontal trough tilt (30° N. location–50° N. location) | 14° of long. | 8° of long. |
| Amplitude from ridge upstream to Pacific trough | 15° of lat. | 21° of lat. |
| Zonal index in Western Hemisphere | 11.8 m. p. s. | 10.6 m. p. s. |

Every one of these typical concomitants of long wavelength was present this month, as indicated in table 1 which compares the mean values of these characteristics during all winter months from December 1932 to March 1951 (col. 2), with their values in January 1955 obtained from figure 1 (col. 3). To further illustrate the fact that this month's wave pattern, despite its extreme nature, generally satisfied the interrelationships previously established for monthly mean waves, table 2 was prepared. This table lists six values of wave amplitude for January 1955, estimated from simultaneous values of other wave

TABLE 2.—*Values of double amplitude (in ° lat. measured from trough at 40° N. upstream along contour to ridge in western Canada) obtained by entering graphs of [2] with January 1955 values of various wave properties (measured from fig. 1 and listed in table 1)*

| Figure no. in ref. [2] | Dependent variables | Estimated amplitude January 1955 |
|---|---|---|
| 4 | Contour half wavelength | 26 |
| 5 | Contour half wavelength and windspeed difference (trough minus ridge). | 20 |
| 6 | Height at trough and Pacific amplitude | 20 |
| 14 | Contour half wavelength and height at trough | 26 |
| 15 | Contour half wavelength and Pacific amplitude | 19 |
| 16 | Height anomalies at trough and ridge (upstream along contour). | 22 |
| Mean estimate | | 22 |
| Actual value | | 23 |

[1] See Charts I-XV following p. 31 for analyzed climatological data for the month.

[2] Trough and ridge are defined as points of lowest and highest latitude reached by the contours.

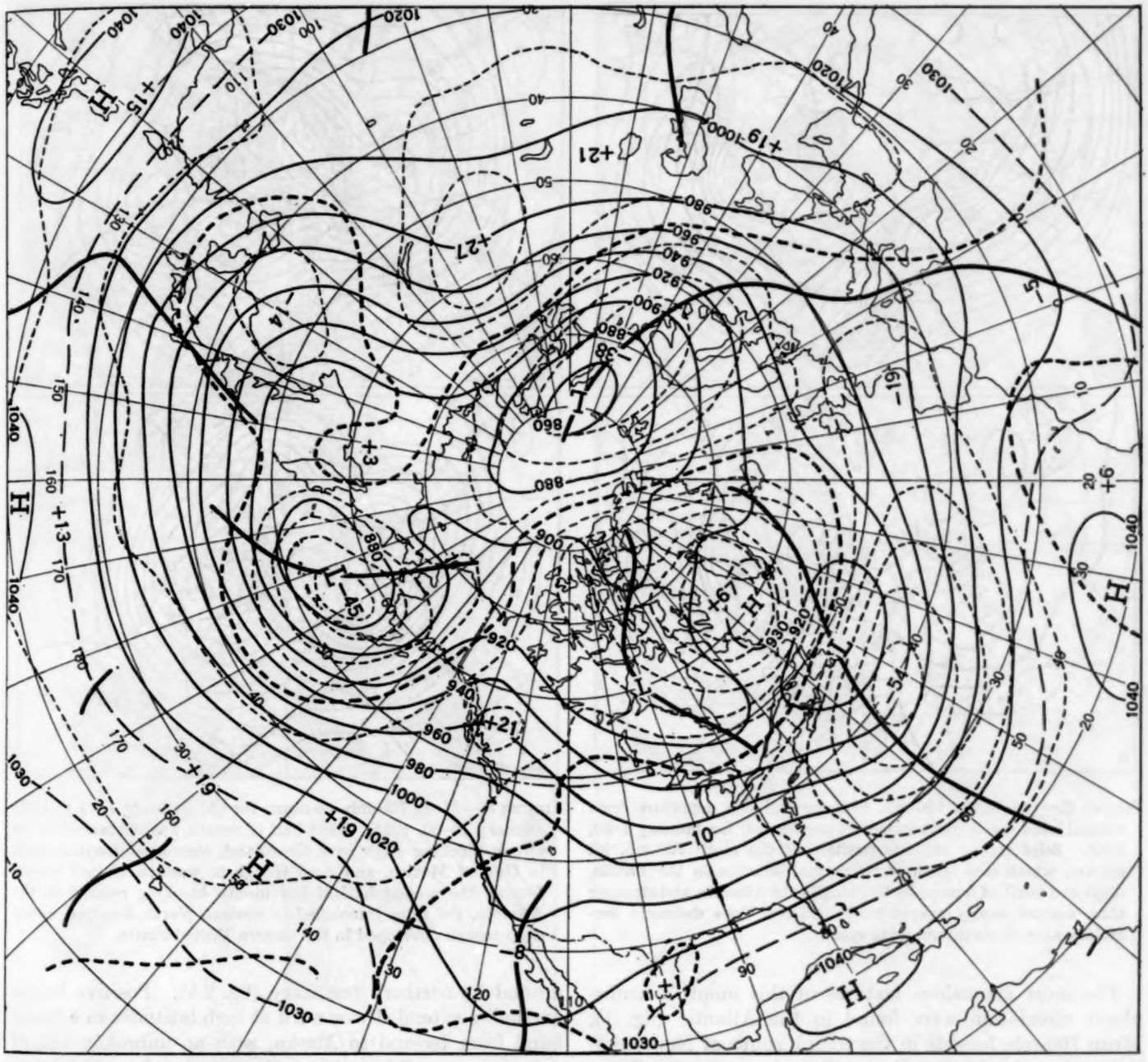

FIGURE 1.—Mean 700-mb. contours and height departure from normal (both in tens of feet) for January 1–30, 1955. Note long half wavelength at 40° N. between stronger than normal ridge in eastern Pacific and deepest mean trough on record in western Atlantic. Other significant features are strong blocking High over Davis Strait and deep Aleutian Low.

characteristics in figure 1 on the basis of graphs presented in 1952 [2]. All of the estimated amplitudes are in good agreement with the value of 23° of latitude actually observed, and the mean estimate differs from the actual by only 1°.

This month's extremely long wavelength in the northern United States can be rationalized in another way. After all, the system of locating a trough at the lowest latitude reached by the contour is an arbitrary one. If, instead, we define a trough as a region of maximum contour curvature, then there is a trough through the Mississippi Valley in figure 1, where a separate center of negative height anomaly also appears. In fact, a minimum-latitude trough was actually present in this area during the second half of the month, as illustrated by the 15-day mean map in figure 3B. During the first half of the month the wavelength slack was taken up by the trough in the southwest United States, which extended to latitude 43° N. on the 15-day mean map in figure 3A, but to only 37° N. on the monthly mean chart (fig. 1). The monthly mean, with its long wavelength, was therefore the average of two different half-month circulations, each with a normal wavelength.

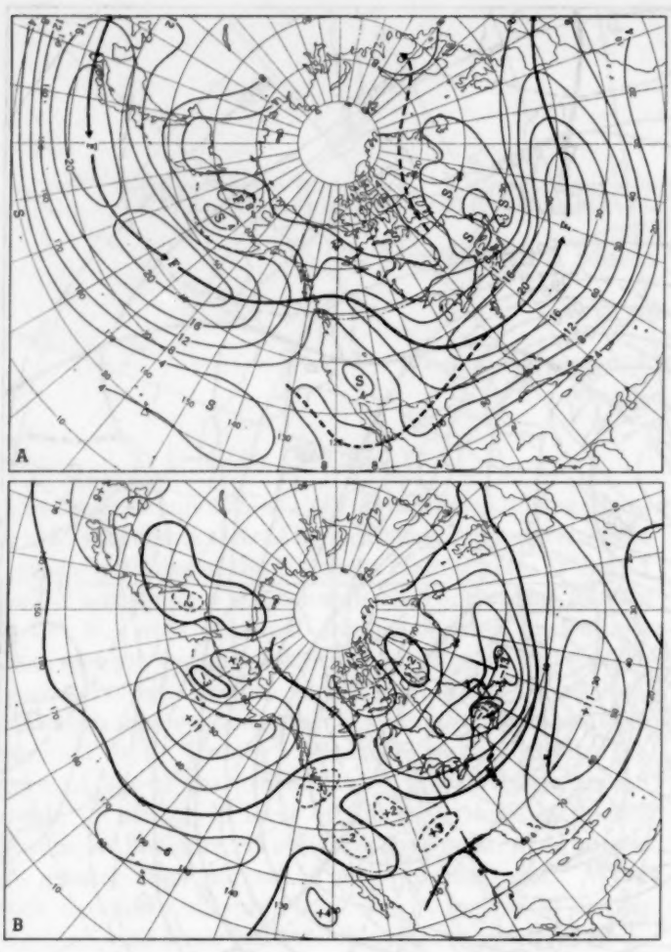


FIGURE 2.—(A) Mean 700-mb. isotachs and (B) departure from normal wind speed (both in meters per second) for January 1–30, 1955. Solid arrows indicate position of the mean 700-mb. jet stream, which was north of its normal location in the Pacific, displaced south of normal by blocking in the Atlantic, and stronger than normal nearly everywhere. Dashed lines delineate secondary axes of maximum wind speed.

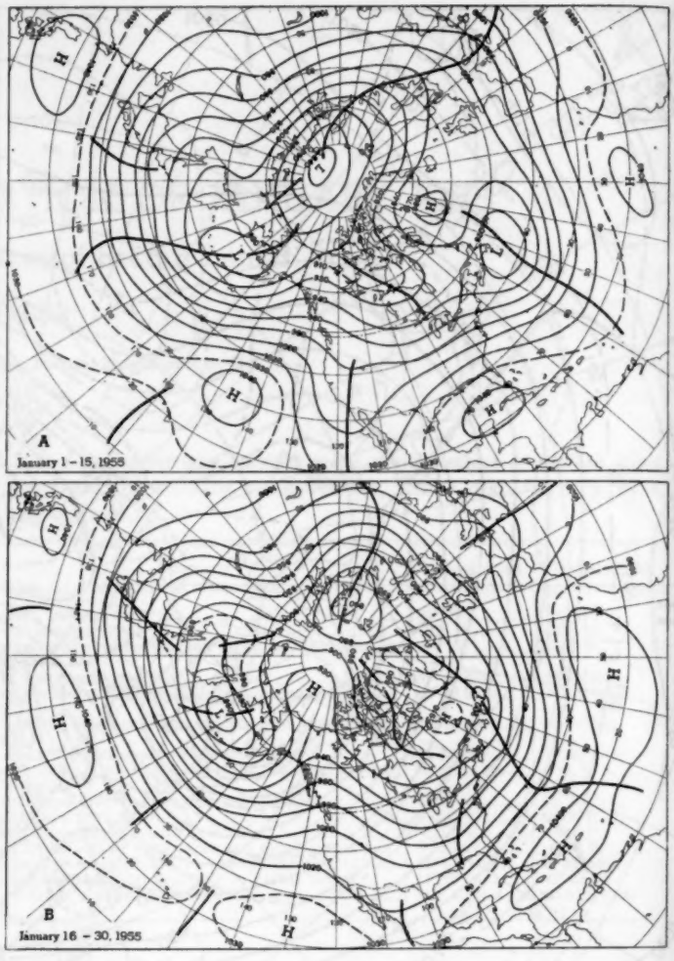


FIGURE 3.—Mean 700-mb. contours for (A) January 1–15 and (B) January 16–30, 1955. First half of month was characterized by strong blocking High over Greenland, strong subtropical High in Gulf of Mexico, and deep trough in western United States. During the second half of the month blocking relaxed in the Atlantic, the ridge intensified in western North America, and a deep trough developed in the eastern United States.

The most anomalous features of this month's hemispheric circulation were found in the Atlantic (fig. 1). Mean 700-mb. heights in the trough south of Newfoundland were the lowest observed during any month on record, beginning October 1932. The extreme negative height anomaly of −540 ft. represented a departure of more than 3 standard deviation units—a rare event. At sea level (Chart XI) pressures in a 992-mb. mean Low southeast of Newfoundland averaged 23 mb. below normal, the largest anomaly in any part of the Atlantic during any January in the 56 years of record dating back to 1899.

The abnormal displacement of the Icelandic Low to Newfoundland was intimately related to the presence of a strong blocking High over the Davis Strait where extreme positive departures were 670 ft. at 700 mb. and 21 mb. at sea level. This block was accompanied in typical fashion by a split jet stream with the principal current passing south of the block and a weak secondary branch diverted around its northern periphery (fig. 2A). Positive height anomalies extended westward at high latitudes in a broad band from Iceland to Alaska, with an unbroken belt of negative anomalies to the south extending from California to the Mediterranean Sea. Development of this block was responsible for displacing the deep polar vortex, which had played a prominent role in the weather and circulation of the previous two months [3, 4], from the Canadian Arctic into Novaya Zemlya. This change came about mainly during the second half of the month, when a closed High developed in the Arctic north of Alaska at the same time that the original block over Greenland and eastern Canada became much weaker (compare figs. 3A and B).

In order to facilitate comparison between this month's circulation pattern and the typical January condition, figure 4 was prepared showing the frequency of troughs and ridges within equal-area 10° boxes from 20° to 70° N. on all monthly mean 700-mb. charts for January from

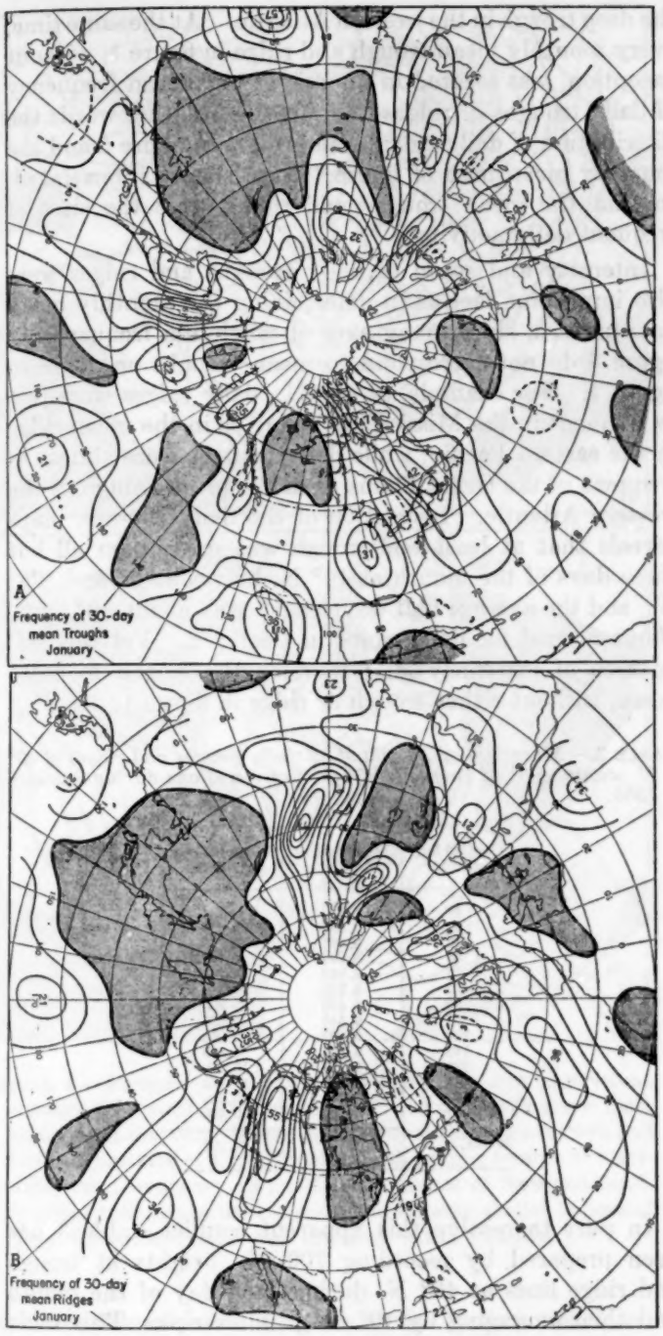


FIGURE 4.—Geographical frequency (%) of monthly mean troughs (A) and ridges (B) within equal-area 10° boxes from 20° to 70° N. on 700-mb. charts for January from 1933 to 1955. The lines of equal frequency are drawn at intervals of 10 percent except for intermediate (5%) lines which are dashed. Areas of zero frequency are stippled. Centers of maximum frequency are labeled in roman type, centers of minimum frequency in italics.

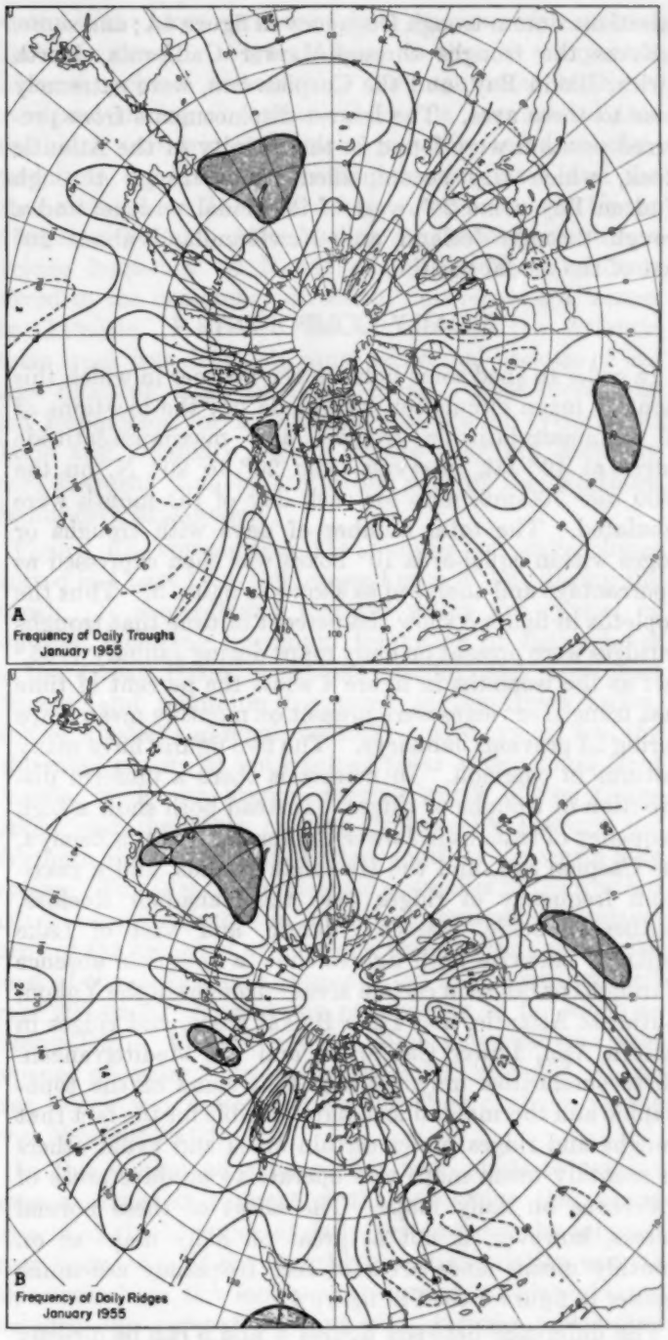


FIGURE 5.—Geographical frequency (%) of daily troughs (A) and ridges (B) from 20° to 80° N. on 1500 GMT 700-mb. charts for January 1955. Analysis is same as in figure 4.

1933 to 1955. Similar studies have been published for the winter season [2] and for daily maps [5]. Comparison with figure 1 reveals that every ridge in the Northern Hemisphere on this month's mean chart was located close to an axis of maximum frequency of ridge occurrence in figure 4B. This was especially true of the ridges in western Canada and central Siberia, both of which were situated in regions where ridges were present in more than half of the Januarys since 1933.

The troughs on this month's 700-mb. map were not located as close as were the ridges to their modal or most frequent January positions. Nevertheless, most troughs in figure 1 were situated within 10° of longitude from an

axis of maximum trough frequency in figure 4A; and some, such as the troughs through Lower California, North Africa, Baffin Bay, and the Caspian Sea, were extremely close to these axes. The largest displacements from preferred position were found in the vicinity of the Atlantic block, which was accompanied by a trough through Hudson Bay some 20° west of its modal position and a trough through Iceland and Newfoundland about 20° east of the modal position.

## 2. DAILY COMPONENTS

In order to shed some light on the manner in which this month's mean circulation was made up, the locations of all minimum-latitude troughs and maximum-latitude ridges at 10° lat. intervals from 20° to 80° N. on the 1500 GMT 700-mb. map for each day of the month were tabulated. The total number of days with troughs or ridges within equal-area 10° boxes was then expressed as a percentage and analyzed as shown in figure 5. Thus the isopleths in figure 5 show the percent of time that troughs or ridges were present on daily maps during January 1955,[3] just as the isopleths in figure 4 show the percent of time that troughs or ridges were present on monthly mean maps during 23 previous Januarys. The two figures have many features in common. In neither is there a uniform distribution of troughs or ridges. Instead both show a high frequency of troughs in Lower California, Novaya Zemlya, the Caspian Sea, and the Hawaiian Islands, and a maximum frequency of ridges over the Canadian Rockies, southeast Pacific, eastern Atlantic, and west of Lake Baikal. Likewise both figures show a complete absence of troughs or ridges in certain areas—troughs in the Yukon, southeast Atlantic, and Lake Baikal areas, and ridges in eastern Asia, Lower California, and the Mediterranean. These similarities may indicate that some of the topographic and thermal influences responsible for the fact that troughs and ridges prefer certain areas and avoid others on monthly mean maps also operate to produce areas of preference on daily maps. The effect of these normal factors, however, is not as great on daily maps as on monthly means since areas of zero frequency are much smaller in figure 5 than in figure 4.

The difference between figures 4 and 5 can be directly related to figure 1. Wherever the monthly mean troughs or ridges of figure 1 were west of the modal positions of figure 4, the axis of maximum frequency in figure 5 was also west of the corresponding axis in figure 4, as in the case of troughs in Hudson Bay, Japan, and the Mediterranean and ridges in Kamchatka and the eastern Pacific. On the other hand, axes of maximum frequency in figure 5 were east of their counterparts in figure 4 when the monthly mean trough or ridge of figure 1 was displaced east of its modal position—most conspicuously in the case of the deep trough in the western Atlantic. At the same time, every monthly mean trough and ridge in figure 1, without exception, was located in an axis of maximum frequency of daily troughs or ridges in figure 5. In other words the distribution of daily troughs and ridges in figure 5 and the monthly mean map of figure 1 were closely interrelated, so that the mean troughs and ridges were the sites of frequent daily activity.

Intensity and speed of daily troughs and ridges were also important factors in determining the monthly mean flow pattern, since many axes of maximum frequency in figure 5 do not correspond to mean troughs or ridges in figure 1. For example, at 40° N., daily ridges were just as frequent in the Mississippi Valley as in the mean ridge in the eastern Pacific; while daily troughs were almost as frequent in the Great Plains as in the mean trough in the western Atlantic. Inspection of the daily 700-mb. maps reveals that at least one trough was present on all but three days of the month at 40° N. between 70° and 120° W., and the average half wavelength was about 30° long., about normal for daily maps in this area. Yet this was an area of extremely long wavelength on the monthly mean, without either trough or ridge in figure 1.

TABLE 3.—*Mean 700-mb. height of all daily troughs and ridges at 40° N. within ±5° of longitude of specified meridians during January 1955.*

| Central longitude | Mean height of troughs | Mean height of ridges |
|---|---|---|
| ° W. | ft. | ft. |
| 30 | 9,500 | 9,920 |
| 40 | 9,670 | 9,830 |
| 50 | 8,940 | 9,970 |
| 60 | 9,080 | 9,730 |
| 70 | 9,350 | 9,810 |
| 80 | 9,460 | 9,880 |
| 90 | 9,340 | 9,950 |
| 100 | 9,660 | 9,950 |
| 110 | 9,880 | 9,900 |
| 120 | 9,710 | 10,270 |
| 130 | 9,580 | 10,330 |
| 140 | 9,780 | 10,290 |
| 150 | 9,600 | 10,250 |
| Mean | 9,504 | 10,006 |

In part to resolve this apparent conflict, table 3 has been prepared by recording 700-mb. heights at trough and ridge lines at 40° N. during each day of the month and then averaging by 10° longitude strips. This table shows that troughs at 40° N. were deeper at 50° W. than at any other meridian from 30° to 150° W. At this longitude, near the monthly mean trough, the average 700-mb. height of daily troughs was only 8940 ft. Conversely, ridges attained maximum intensity (mean 700-mb. height of 10,330 ft.) in the vicinity of 130° W., near the monthly mean ridge. In the United States proper, from 75° to 125° W., both troughs and ridges were of approximately average depth. Thus, although daily troughs and ridges were quite frequent in the northern United States during the month, they were not of sufficient intensity to be reflected as a trough or ridge on the monthly mean map. In the adjacent oceans, on the other hand, daily systems attained maximum intensity;

[3] Figure 5 does not indicate the number of *different* troughs or ridges that traversed each area during the month. Such a statistic is preferable in some ways to the number of days with troughs or ridges, but was not computed because it is more difficult to obtain and is given indirectly, for sea level systems in figure 6.

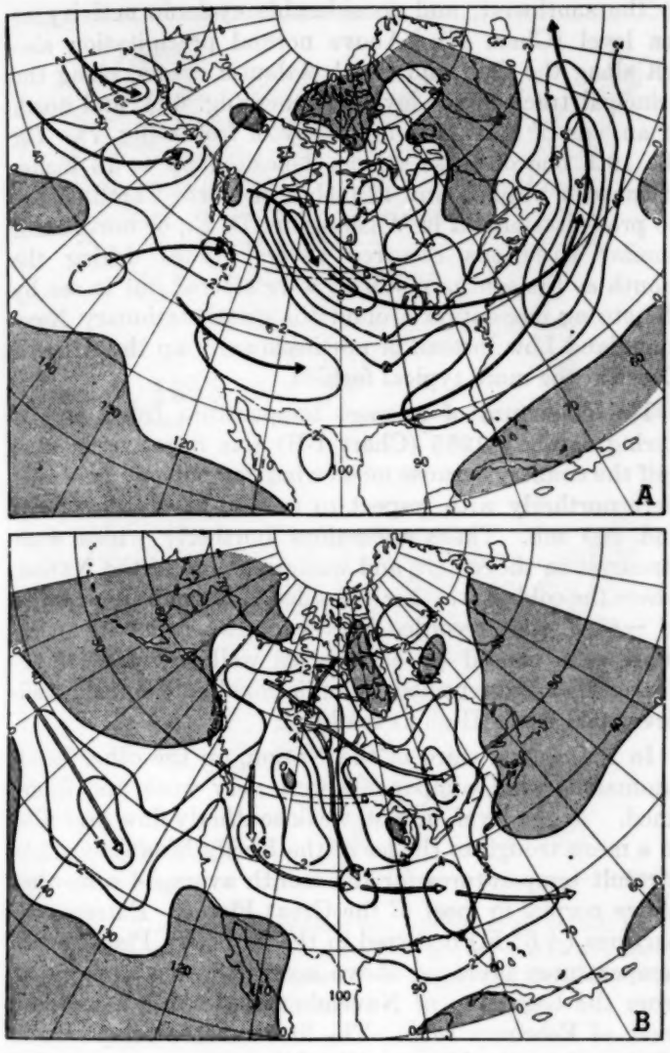


FIGURE 6.—Frequency of cyclone passages (A) and anticyclone passages (B) (within 5° squares at 45° N.) during January 1955. Note principal cyclone tracks (solid arrows) through southern and northern portions of United States, both leading to area of maximum storm frequency (8 per box) southeast of Newfoundland. Principal anticyclone tracks (open arrows) were similar to normal except for marked southward displacement in Atlantic.

and this intensification was one of the factors associated with the appearance of the monthly mean trough and ridge in these areas. This conclusion agrees with the rule used in extended forecasting practice for many years and stated by Namias [6] as "daily troughs undergo their maximum deepening when entering the area of the mean trough."

The rule cited above applies just as well to sea level cyclones as to 700-mb. troughs. This is well illustrated in Chart X by noting the progressive decrease in central pressure of low pressure systems crossing the east coast of the United States. Many of these storms deepened at an average rate of almost 1 mb. per hour as they passed over the warm waters of the Gulf Stream and entered the mean trough south of Newfoundland. Particularly noteworthy is the large number of daily storms which entered this mean trough. Figure 6A shows that as many as 8 different cyclones crossed a 5° box southeast of Newfoundland during the month. Storms approached this area along two principal tracks; one directed northeastward from the Gulf and South Atlantic States, and the other oriented southeastward from Alberta and the Upper Mississippi Valley. After leaving the center of maximum cyclone frequency off Newfoundland, nearly all storms moved in the customary direction, northeastward, across the Atlantic. However, the latitude of the Atlantic storm track was definitely south of normal because of the large blocking High in Davis Strait. This block was also responsible for a complete absence of cyclones in Davis and Denmark Straits, where they are normally more frequent than in any other part of the Northern Hemisphere in January.

Figure 6B summarizes the number of anticyclones plotted in Chart IX which crossed each 5° box during the month. It shows many features which are typical of January, including maximum frequency of anticyclones in the Great Basin, southeast Pacific, and northwest Canada, and minimum frequency in the Great Lakes, Gulf of Alaska, and north Atlantic. Also typical was the bifurcated nature of the track of polar anticyclones from Canada, with one branch curving north of the Great Lakes, and the other curving cyclonically through the Northern Plains and Ohio Valley, south of the warm lake waters. This month's large-scale anomalies in the western Atlantic were reflected in a marked southward displacement of the principal anticyclone track in that area, with most of the daily Highs concentrated in the latitude belt from 20° to 30° N. and one penetrating as far south as Puerto Rico. In fact, not one High traversed the vast expanse of water between latitudes 33° and 60° N., an area which was dominated by the huge cyclonic vortex over Newfoundland.

In this section an attempt has been made to present some evidence in support of the conclusion that many aspects of the behavior of daily systems may be inferred from knowledge of the monthly mean circulation and its departure from the long-period normal. This evidence included the percent of days with troughs and ridges (fig. 5), the number of different Lows and Highs (fig. 6), the intensity of troughs and ridges (table 3), and the intensity of cyclones (Chart X). It is obviously impossible in an article of this type to examine thoroughly all aspects of this problem. This would require much additional data and careful scrutiny of many other factors such as change in speed and amplitude of the waves from day to day.

## 3. THE WEATHER

This month's long half wavelength in the United States on the mean chart was accompanied by prevailing northwesterly flow in most of the country at both 700 mb. (fig. 1) and sea level (Chart XI). As a result little

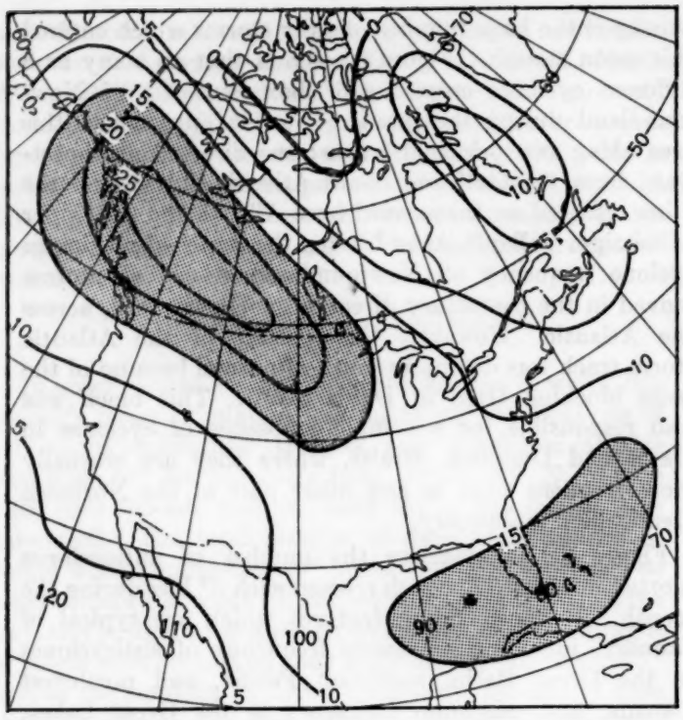


FIGURE 7.—Number of days in January 1955 with surface fronts of any type within squares with sides approximately 500 miles. Data from *Daily Weather Map* at 1:30 p. m. EST. Note maximum frequency of fronts in western Canada and the Gulf of Mexico and small frequency in the United States.

moisture was able to enter the country and generally dry weather prevailed in most sections (Chart III). Less than half the normal precipitation fell in portions of the North and Middle Atlantic States, Ohio Valley, Northern Plains, Northern Plateau, and Rocky Mountain States. Washington, D. C., reported its driest January on record with only .30 in. of precipitation all month. Statewide precipitation in adjoining Maryland and Delaware averaged only 17 percent of normal. At Blue Hill, Mass., this month was not only the driest but also the sunniest January in the 70-year history of the Observatory. In the Great Plains drought conditions were described as the worst since the days of the dust bowl in the 1930's. Statewide precipitation averaged only 35 to 38 percent of normal in Arkansas, Tennessee, Kentucky, and Virginia, but considerably greater amounts fell both north and south of this region. This area of minimum precipitation coincided with an area of minimum cyclonic frequency in figure 6A, between the two principal storm tracks through the Great Lakes and Gulf States.

The only part of the country with excess precipitation over a wide area was the Southwest, with more than twice the normal amount in most of Arizona and southern California, and above normal amounts in Nevada, Utah, and southern parts of New Mexico and Texas. This precipitation was associated with a mean 700-mb. trough through the area, a closed center of negative anomaly to the southwest, and considerable cyclonic activity at sea level (Chart X). Above normal precipitation also fell along the Gulf and South Atlantic coasts, along the principal track of sea level cyclones (fig. 6A), and north of an axis of maximum frequency of fronts (fig. 7). On the 19th one of these storms deposited up to 15 inches of snow in Virginia and 12 inches in North Carolina, but no precipitation fell in Washington, D. C., or northward. Similar situations recurred several times during the month as the southern storms were steered out to sea by the strong circulation around the quasi-stationary Newfoundland Low instead of northeastward up the Atlantic Coast in the more typical fashion.

The departure of average temperature from normal during January 1955 (Chart I-B) was negative in over half the country because mean wind components generally were northerly with respect to normal at both sea level and 700 mb. These anomalous northerly winds were strongest in the eastern and western thirds of the Nation, where the coldest weather prevailed. Extreme departures of −8° F. were recorded in Nevada, where low temperatures were caused by easterly as well as by northerly flow and were intensified by radiational cooling in a well-developed Basin High at sea level.

In the central third of the Nation, on the other hand, anomalous wind components were very weak and ill defined. At sea level, in fact, weak southerly flow prevailed in a mean trough to the lee of the Rocky Mountains. As a result temperatures for the month averaged somewhat above normal in most of the Great Plains. Extreme departures (+6° F.) occurred in the Northern Plains where temperatures averaged above normal during every week from the beginning of November 1954 until the second week of February 1955. The first subzero temperatures of the winter in Minneapolis, Minn., were not recorded until January 16, the latest date on record. The explanation for this extreme warmth is given best by the mean sea level map and its departure from normal (Chart XI), which had all the characteristics demonstrated by Henry [7] and Blair [8] many years ago to be concomitant with mild winters in the northern United States. The Aleutian Low was extremely well developed (16 mb. below normal) and its eastward extension produced a well defined trough in western Canada and below normal sea level pressures throughout Alaska and northwest Canada. At the same time, High pressure cells in the Great Basin and eastern Pacific were stronger than normal. As a result of this pressure distribution mild Pacific air masses dominated the Northern Plains instead of the cold Canadian air normally present. The quasi-stationary frontal zone between these two air masses was north of the United States border most of the month (fig. 7), and cyclonic activity was unusually pronounced in Alberta, Canada (fig. 6A).

Similar factors operated to produce mild Pacific air and above normal temperatures in the Pacific Northwest. Warmth in this region was also associated with above

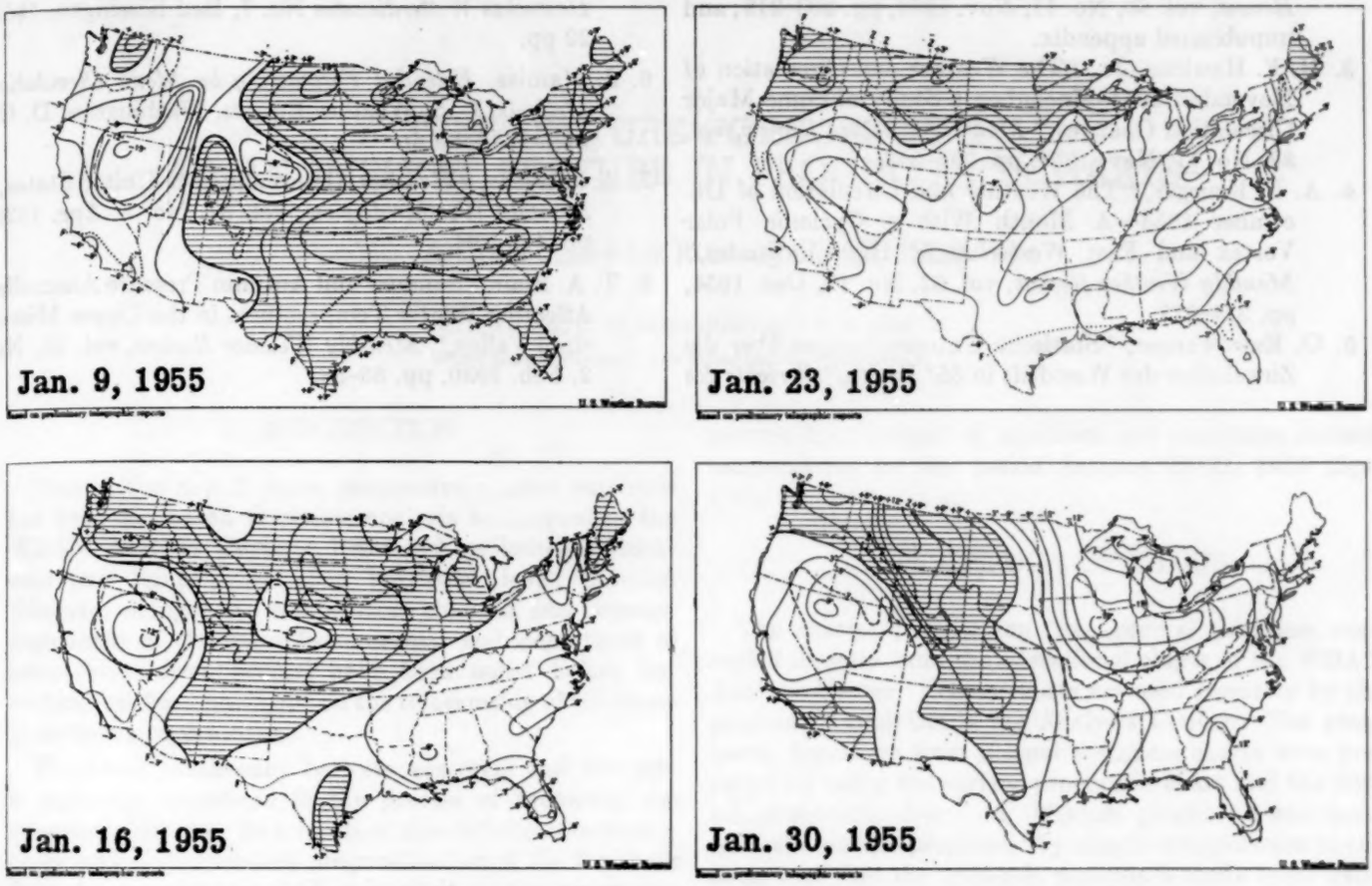


FIGURE 8.—Departure of average temperature from normal for the weeks ending at midnight, local time, on the dates shown. Shading indicates temperatures of normal or above; dotted line shows southern limit of freezing temperatures, dashed line southern limit of zero degrees. Note progressive cooling east of the Continental Divide. (From *Weekly Weather and Crop Bulletin, National Summary*, vol. XLII, Nos. 2, 3, 4, and 5.)

normal heights and ridge conditions at 700 mb. Mild maritime air masses were also responsible for above normal temperatures in northern New England and the Upper Lakes, where stronger than normal northeasterly winds at both sea level and 700 mb. resulted in dominance by air masses originating in the Atlantic instead of in Canada.

Figure 8 reveals an interesting temperature trend which went on during the month. During the first week of January temperatures averaged above normal in practically all parts of the country east of the Rockies—by as much as 15° F. in Illinois. Thereafter progressive cooling occurred, and a major cold wave swept the eastern half of the United States during the final week of January. The coldest weather, averaging 18° F. below normal for the week, occurred in Illinois in almost exactly the same region which had the greatest positive anomaly during the first week of January. This progressive cooling was associated with the westward spread of blocking from Greenland to Alaska during the month, as illustrated by the marked increase in amplitude of the ridge in western North America from the first to the second 15 days of the month (fig. 3).

The outstanding feature of January weather outside the United States was the effect of unusual storminess in Europe. Floods in France and Germany, blizzards in the British Isles and Scandinavia, and shipwrecks in the Mediterranean all resulted from a deeper than normal mean trough in Europe and a southward displacement of the Atlantic storm track by the block in the Greenland area. Other weather highlights included a destructive typhoon in the Philippines, the first January hurricane on record in the Atlantic, and shipwrecks in the deep trough south of Newfoundland.

## REFERENCES

1. C.-G. Rossby and Coll., "Relation Between Variations in the Intensity of the Zonal Circulation of the Atmosphere and the Displacements of the Semipermanent Centers of Action," *Journal of Marine Research*, vol. 2, No. 1, Jan. 1939, pp. 38–55.
2. W. H. Klein, "Some Empirical Characteristics of Long Waves on Monthly Mean Charts," *Monthly Weather*

*Review*, vol. 80, No. 11, Nov. 1952, pp. 203–219; and unpublished appendix.

3. H. F. Hawkins, Jr., "The Weather and Circulation of November 1954—Including a Study of Some Major Circulation Changes," *Monthly Weather Review*, vol. 82, No. 11, Nov. 1954, pp. 335–342.
4. A. F. Krueger, "The Weather and Circulation of December 1954—A Month With a Cyclonic Polar Vortex and Fast Westerlies in High Latitudes," *Monthly Weather Review*, vol. 82, No. 12, Dec. 1954, pp. 374–377.
5. O. Essenwanger, "Statische Untersuchungen über die Zirkulation der Westdrift in 55° Breite," *Berichte des Deutsches Wetterdienstes* No. 7, Bad Kissingen, 1953, 22 pp.
6. J. Namias, *Extended Forecasting by Mean Circulation Methods*, U. S. Weather Bureau, Washington, D. C., Feb. 1947, 89 pp.
7. A. J. Henry, "Weather Abnormalities in United States," *Monthly Weather Review*, vol. 57, No. 5, Apr. 1929, pp. 198–204.
8. T. A. Blair, "Summer and Autumn Pressure Anomalies Affecting Winter Temperatures in the Upper Mississippi Valley," *Monthly Weather Review*, vol. 58, No. 2, Feb. 1930, pp. 53–58.

# TEMPERATURE FORECASTING AS AN IMPLICIT FEATURE IN PROGNOSTIC CHARTS—

## A Case Study for January 23–31, 1955

C. L. KIBLER, C. M. LENNAHAN, AND R. H. MARTIN
WBAN Analysis Center, U. S. Weather Bureau, Washington, D. C.

### 1. INTRODUCTION

During the past 2 years progressively more emphasis has been placed on thickness analysis techniques in the WBAN Analysis Center. Relationships between thickness and temperature at a particular level, between thickness changes and temperature changes, and between departures of thickness from normal and departures of temperature from normal have been noted before but nothing has been published on the relationship of thickness to surface temperatures.

Thickness consistency between sea level and 500 mb. is explicitly considered in the process of preparing the prognostic charts. As a result of this definite consistency check and of independent prognostication of the thickness field the temperature field is implicit in the prognostic chart even though only isobars and contours are shown. On the other hand, thickness must be considered, either directly or indirectly, in any forecast of surface temperature. Furthermore, the correlation between thickness and free air temperatures is indisputedly high because thickness is a direct measure of the air mass temperature. Therefore it remains to determine the degree to which this correlation is applicable in practice to surface temperature forecasting.

It has been observed that a very good computation of the surface minimum temperature can be obtained occasionally by using the departure of 1000–500-mb. thickness from normal. This follows from the hydrostatic relation that a 5.4° F. change [1] in the mean virtual temperature of the layer between 1000 mb. and 500 mb. requires a 200-ft. change in thickness of the layer. A consideration of the converse relationship leads to the plausible conclusion that under favorable conditions every 200-ft. change in thickness requires a 5.4° F. change in surface temperature. The easiest way to apply this type of reasoning seemed to be from the standpoint of temperature and thickness normals. It was therefore considered worthwhile to run a test of a series of synoptic charts rather than a statistical analysis of the data.

In the present article a series of departure from normal thickness charts is presented for comparison with departure from normal of minimum and maximum surface temperatures for the period January 23–31, 1955 (figs. 1–6).

### 2. DESCRIPTION OF CHARTS

The charts of departure from normal thickness were copied directly from the operational charts of the WBAN Analysis Center. These charts are used regularly by the prognostic analysts in the Analysis Center. The prognostic departure from normal thickness charts were prepared by using the surface prognostic chart and the 500-mb. prognostic chart. A 1000-mb. prognostic was made from the surface prognostic by simple interpolation in the same way that the 1000-mb. analysis is made twice daily from the 0330 GMT and the 1530 GMT surface charts. Table 1 gives the conversion values used in the interpolation. A prognostic thickness chart was then prepared by subtracting the prognostic 1000-mb. chart graphically from the prognostic 500-mb. chart.

The departure from normal minimum and maximum temperature charts were prepared from the minimum and maximum temperatures transmitted with the 1230 GMT and 0030 GMT data respectively. A minimum temperature chart and a maximum temperature chart were analyzed for each day and from each of these charts the respective normal chart was subtracted. Thus the departure from normal minimum temperature was obtained by subtract-

TABLE 1.—*Interpolation values for isobars on the mean sea level analysis to obtain the contours on the 1000-mb. analysis [2]*

| 1000-mb. height | Surface temperature of | | | |
|---|---|---|---|---|
| | <0° F. | 0°–35° F. | 35°–70° F. | >70° F. |
| −1000 | 959.0 | 961.5 | 963.5 | 966.0 |
| −800 | 967.0 | 969.0 | 970.5 | 972.5 |
| −600 | 975.0 | 976.5 | 978.0 | 979.5 |
| −400 | 983.0 | 984.0 | 985.0 | 986.0 |
| −200 | 991.5 | 992.0 | 992.5 | 993.0 |
| 0 | 1000.0 | 1000.0 | 1000.0 | 1000.0 |
| +200 | 1008.5 | 1008.0 | 1007.5 | 1007.0 |
| +400 | 1017.0 | 1016.0 | 1015.0 | 1014.0 |
| +600 | 1025.0 | 1024.0 | 1022.5 | 1021.0 |
| +800 | 1033.5 | 1032.0 | 1030.0 | 1028.0 |
| +1000 | 1042.0 | 1040.0 | 1037.5 | 1035.5 |

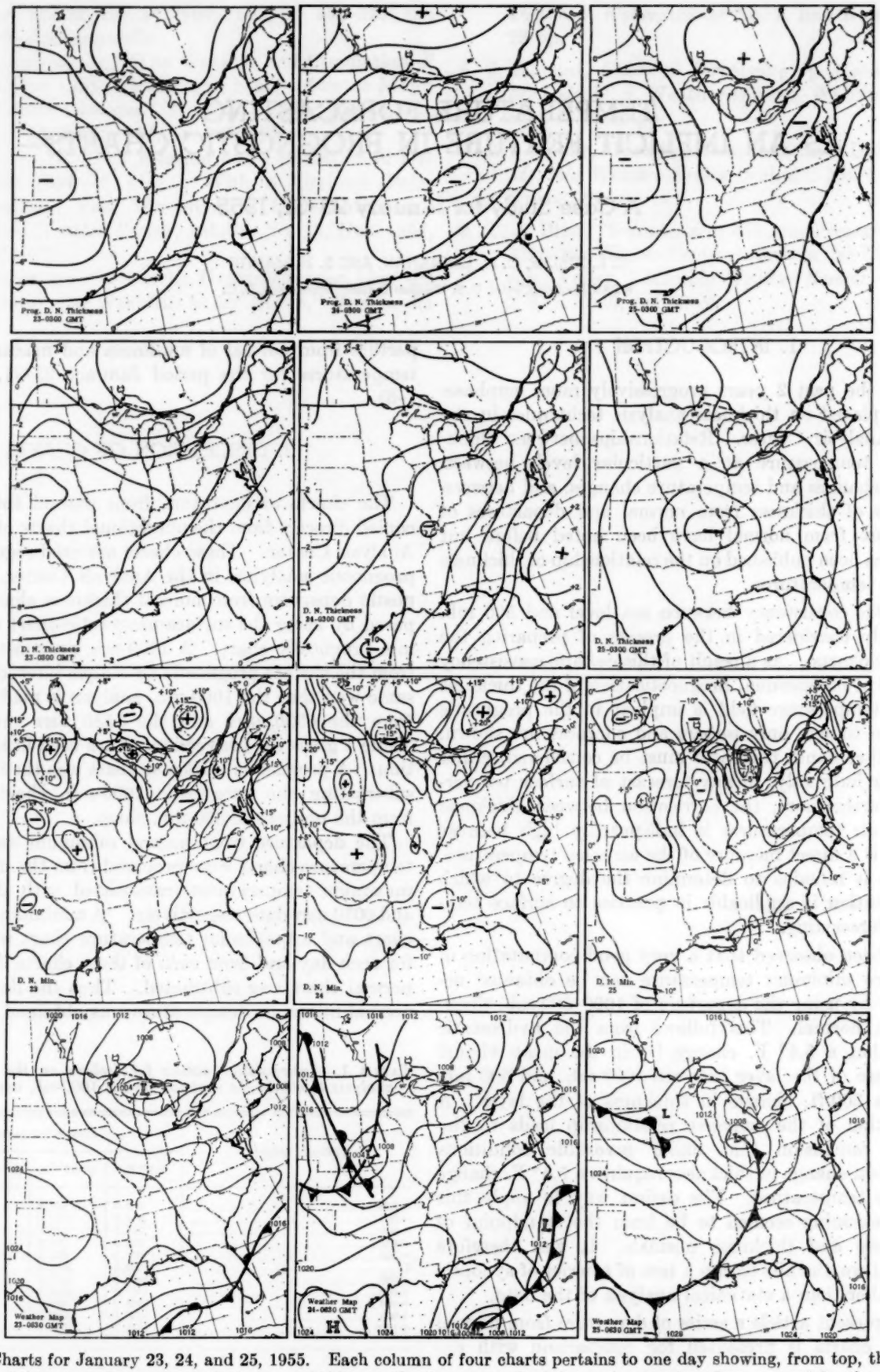


FIGURE 1.—Charts for January 23, 24, and 25, 1955. Each column of four charts pertains to one day showing, from top, the prognostic and observed departure from normal thickness at 0300 GMT, the departure of minimum temperature from normal for the day, and the sea level weather map for 0630 GMT.

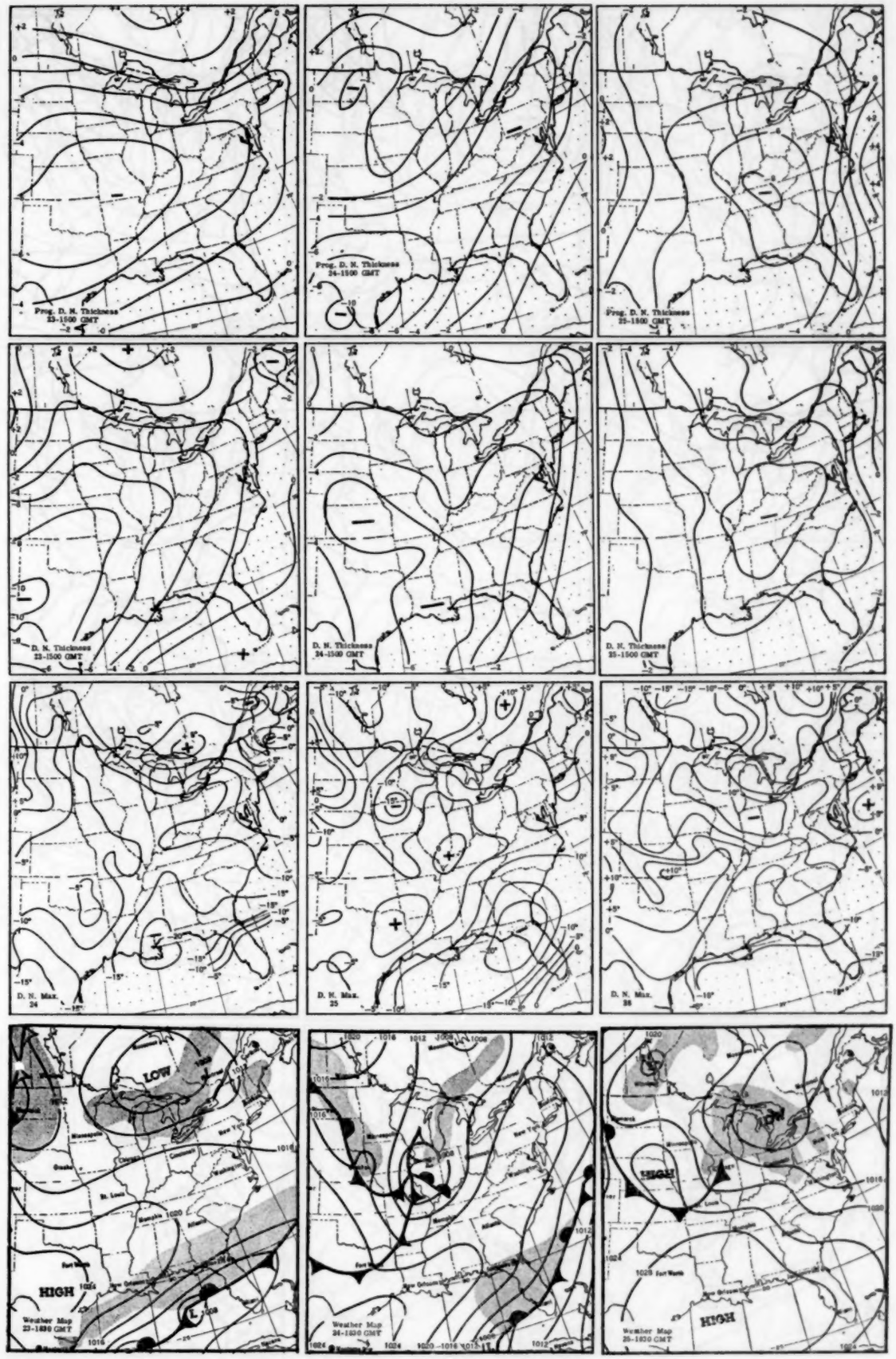


FIGURE 2.—Charts for January 23, 24, and 25, 1955. Each column of four charts pertains to one day showing, from top, the prognostic and observed departure from normal thickness at 1500 GMT, the departure of maximum temperature from normal for the day, and the sea level weather map for 1830 GMT.

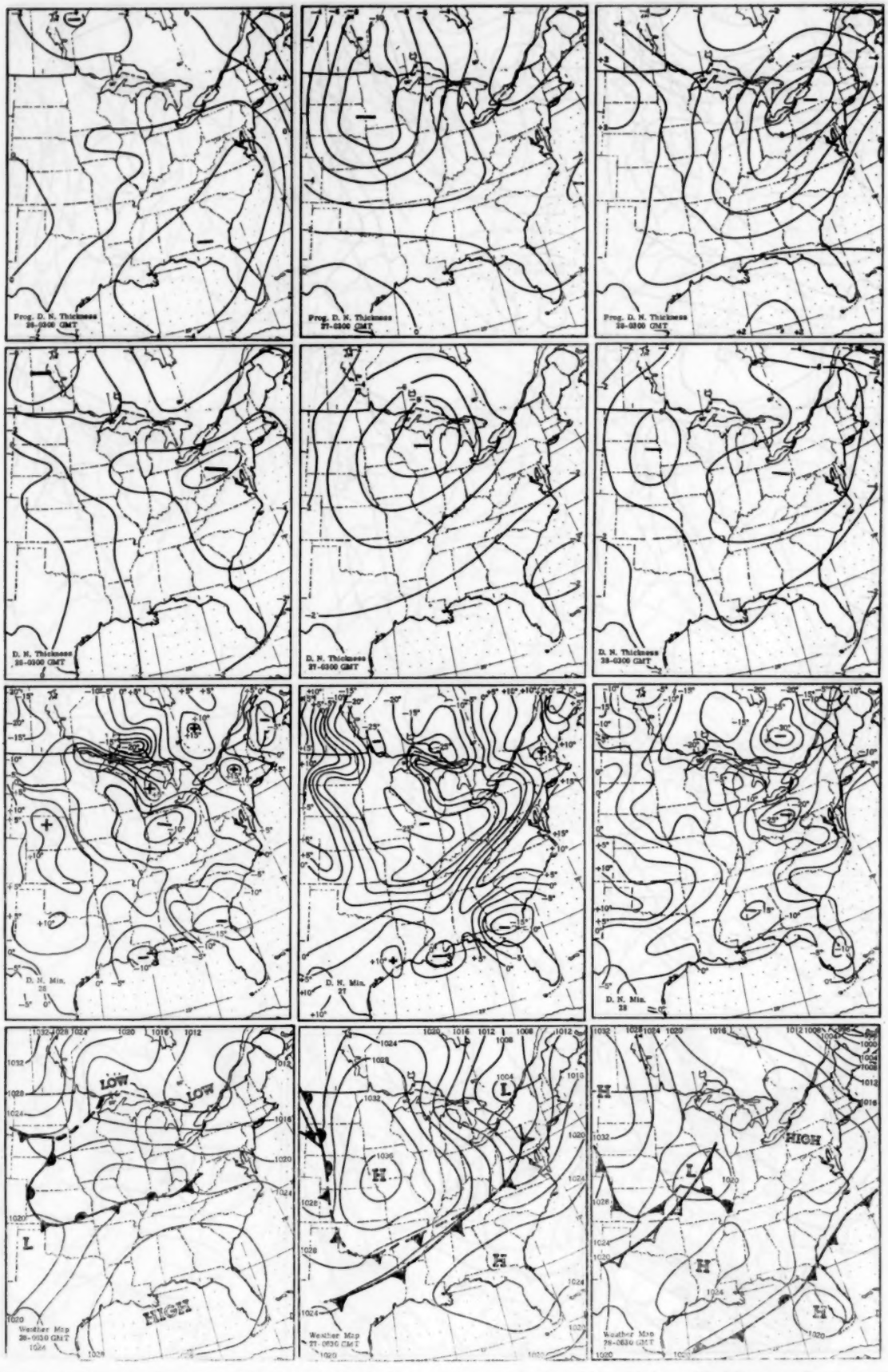


FIGURE 3.—Charts for January 26, 27, and 28, 1955. Each column of four charts pertains to one day showing, from top, the prognostic and observed departure from normal thickness at 0300 GMT, the departure of minimum temperature from normal for the day, and the sea level weather map for 0630 GMT.

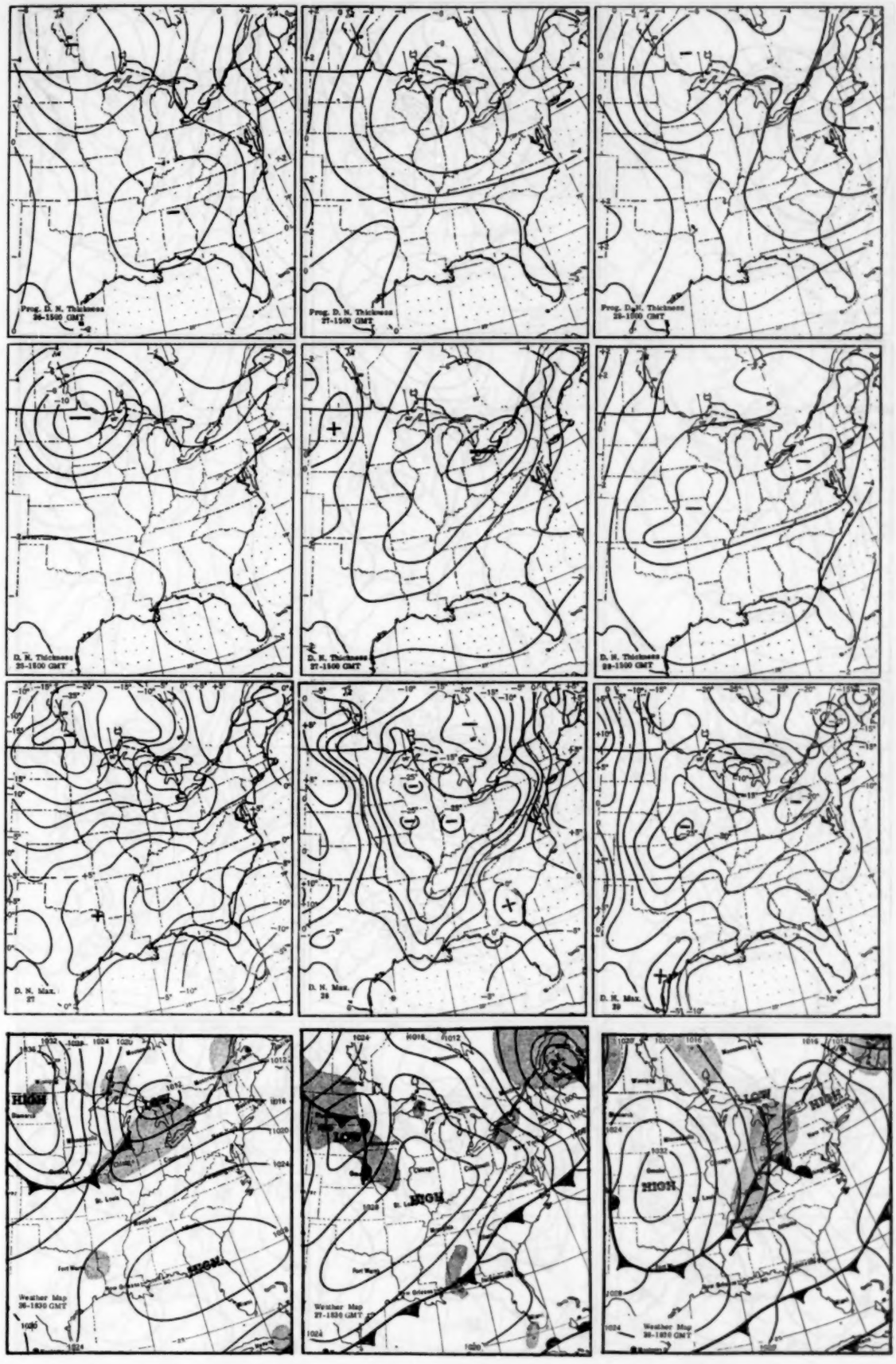

FIGURE 4.—Charts for January 26, 27, and 28, 1955. Each column of four charts pertains to one day showing, from top, the prognostic and observed departure from normal thickness at 1500 GMT, the departure of maximum temperature from normal for the day, and the sea level weather map for 1830 GMT.

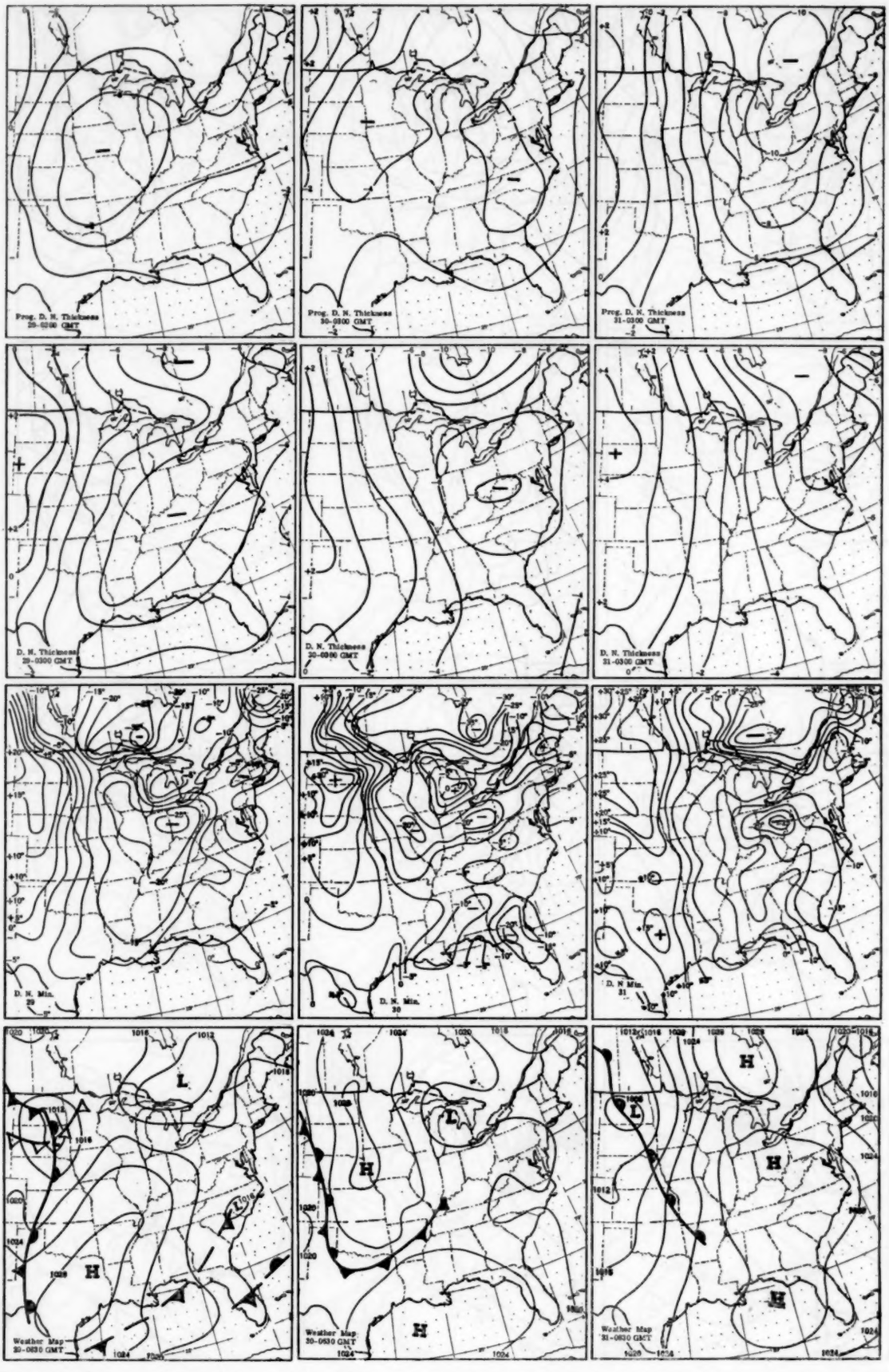

FIGURE 5.—Charts for January 29, 30, and 31, 1955. Each column of four charts pertains to one day showing, from top, the prognostic and observed departure from normal thickness at 0300 GMT, the departure of minimum temperature from normal for the day, and the sea level weather map for 0630 GMT.

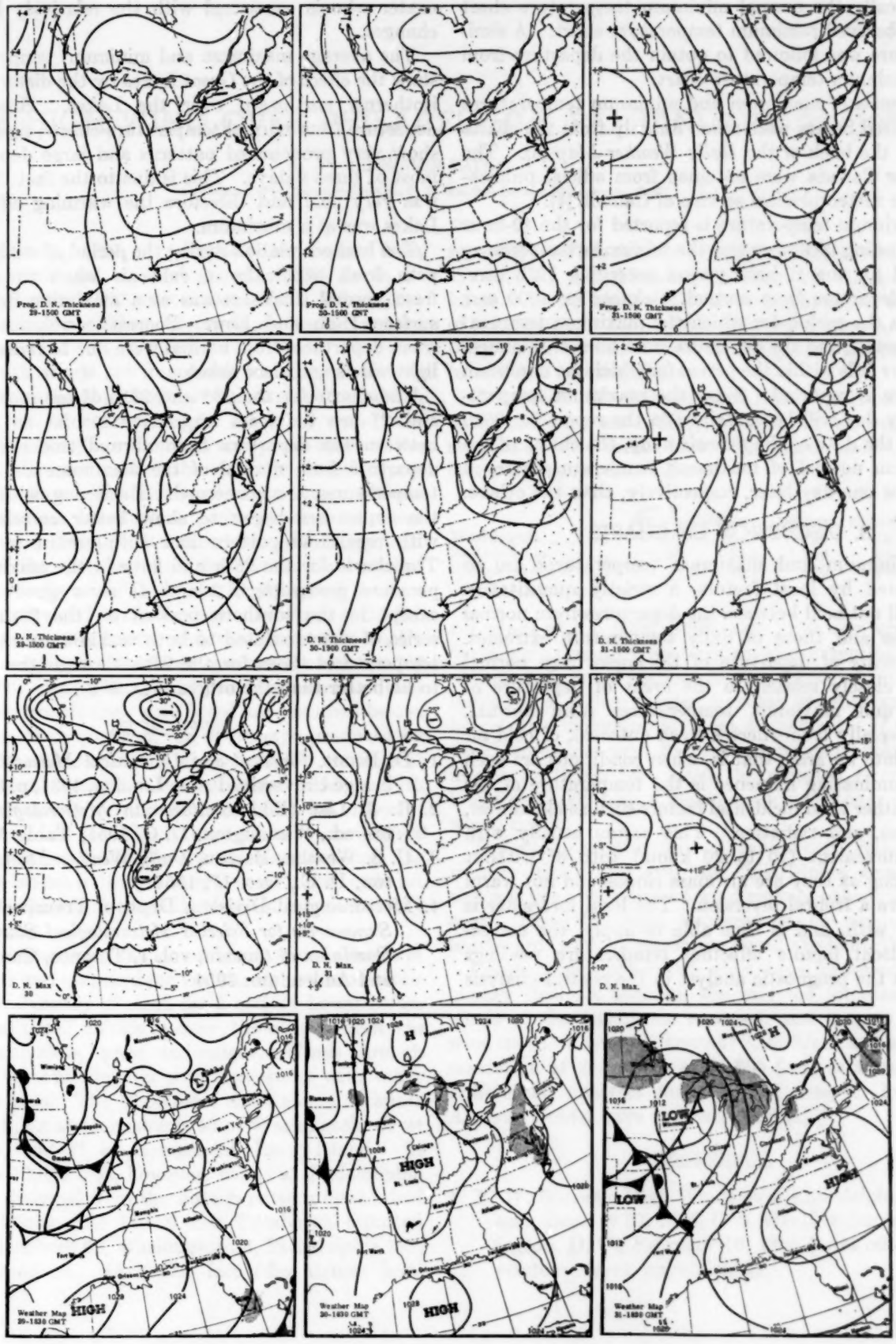


FIGURE 6.—Charts for January 29, 30, and 31, 1955. Each column of four charts pertains to one day showing, from top, the prognostic and observed departure from normal thickness at 1500 GMT, the departure of maximum temperature from normal for the day, and the sea level weather map for 1830 GMT.

ing graphically the normal minimum temperature chart from the observed minimum temperature chart. A similar procedure was followed to obtain the departure from normal maximum temperature chart.

The normals of maximum and minimum temperatures for the United States were taken directly from the charts printed on the back of the *Daily Weather Map* [3]. The normals for Canada were obtained from official publications of the meteorological service of Canada [4].

The maximum temperature is reported for the 12-hour period preceding 0030 GMT and the minimum temperature is reported for the 12-hour period preceding 1230 GMT. Thus the departure from normal thickness for 1500 GMT falls within the period for which the maximum temperature is reported; and the departure from normal thickness for 0300 GMT falls within the period for which the minimum temperature is reported. Since the maximum temperature on any day will be contained in the report for 0030 GMT under the date of the *following day*, the charts of departure from normal of maximum temperature carry a date line for one day later, respectively, than the others.

## 3. DISCUSSION OF CHARTS

Since minimum and maximum temperatures are so often affected by local factors, a strictly quantitative relation will not hold between the departures from normal of thickness and those of daily temperature extremes. However, *areas* of departure of thickness from normal should be closely related to the *areas* of departure of minimum and maximum temperatures from normal. This is especially true where a fresh outbreak of cold air is moving into an area; that is, when conditions are such that the dominating influence is the temperature of the air mass, rather than incidental factors such as cloudiness, precipitation, and radiation. This occurs usually with good air movement (10 to 20 knots) with or without clouds so long as they are air mass clouds and not warm clouds above a frontal inversion. The local forecaster is acquainted with, and is thus able to apply, the corrections for local factors affecting temperature readings better than the prognostic analyst in the central analysis center who is concerned with the relatively large scale changes.

The average maximum and minimum temperatures [3] show the effect of the Great Lakes by the distortion of the isotherms northward over the Lakes. However, the departure from normal temperature charts, figures 1 to 6, show very pronounced patterns and large departures on most of these 9 days. This is due to the fact that the air was very cold and therefore the warming effect of the Lakes was at a maximum.

The best correlation during the period of study occurred with fresh outbreaks of cold air when the departure from normal thickness was at a maximum between the surface High and Low. Poorest correlation occurred when departures from normal were due to radiation (with light winds and clear skies).

The charts for the 23d and 24th of the month (figs. 1 and 2) are the least impressive insofar as agreement between the departure from normal thickness and the departure from normal of the maximum and minimum temperatures are concerned. Beginning with the 25th the departures began to show better correlation both with regard to pattern and with regard to quantity. The charts for the 25th and 26th in the maximum temperature group (figs. 2 and 4) show good agreement except in the southern portion on the 26th. In the series of charts related to both maximum and minimum temperatures those for the 27th through the 31st seem to be better than the others (figs. 3–6).

## REFERENCES

1. D. Brunt, *Physical and Dynamical Meteorology*, Cambridge University Press, London, 1934, p. 3, eq. (16).
2. R. J. List (Ed.) *Smithsonian Meteorological Tables*, 6th ed., Washington, D. C. 1951, Table 57, p. 257.
3. U. S. Weather Bureau, *Daily Weather Map*, Washington, D. C., Dec. 17, 1954.
4. Meteorological Division, Dept. of Transport, *Climatic Summaries for Selected Meteorological Stations in the Dominion of Canada*, vol. 1, Toronto, Canada, 1947, and Addendum, 1954.

# THE HIGH WIND OVER PHILADELPHIA, PA., JANUARY 23, 1955

BENJAMIN RATNER

Climatological Services Division, U. S. Weather Bureau, Washington, D. C.

On January 23, 1955, a teletypewriter report from Philadelphia indicated a wind speed of 396 knots at 23,000 feet, for the 1500 GMT observation. This report has since been the subject of much discussion among meteorologists.

Because high winds are important for many meteorological and operational problems it is desirable to establish whether or not an extreme upper air wind speed was recorded. Accordingly, a thorough study was made of the pertinent wind record and of the synoptic situation prevailing at the time. The findings lead to the conclusion that a mechanical breakdown, probably due to power failure, occurred directly after the 11th minute (approx. 13,000 ft.) of the sounding, and that all data above that point are entirely unreliable. It is estimated from a space-time analysis of available data that winds at 23,000 feet were around 200 knots, and that there was an increase with height to a probable maximum of about 265 knots at 32,000 feet. The general procedures and evidence on which these conclusions were based are discussed below.

For the report in question, the rawin tape produced by the GMD–1A recorder, which was set to give readings at 6-second intervals, contains two successive readings with identical time entry (11.2 minutes), but with different angle readings. It is difficult to determine completely what happened to the equipment at this point, but the presumption is that a disruption of power to the rawin set occurred. At this point the balloon was at approximately 13,000 feet.

To assist in analyzing the synoptic situation, a series of isotach charts was prepared for various transmission levels at 1500 GMT, January 23, and for 6 and 12 hours before and after that time. In this manner, the wind pattern was examined as to time, space, and height. Winds through 12,000 feet for Philadelphia were consistent with other winds in the area. The 12,000-feet chart shows 61 knots at Pittsburgh, 62 at Harrisburg, 46 at Washington, 67 at Philadelphia, and 27 at Hempstead, Long Island. At levels above 12,000 feet, however, winds at Philadelphia increasingly diverged from the isotach pattern established by other stations. At 14,000 feet Pittsburgh reported 66 knots, Harrisburg 62, Washington 83, Philadelphia 183, and Hempstead 60. At 23,000 feet (the highest level reported for Philadelphia), Pittsburgh reported 142 knots, Washington 120, Philadelphia 396, and Hempstead 140 knots. As can be seen, the discord in synoptic continuity of winds occurs somewhere between 12,000 and 14,000 feet, which coincides with the height of the mechanical breakdown mentioned above.

Comparison of winds through time at surrounding stations indicates an orderly progression at each of the stations except Philadelphia. The wind speeds at 23,000 feet were reported as follows:

| | Jan. 23 0300 GMT | 0900 GMT | 1500 GMT | 2100 GMT | Jan. 24 0300 GMT |
|---|---|---|---|---|---|
| Washington | 201 | ------ | 120 | 137 | 122 |
| Philadelphia | 136 | 156 | [1] 396 | 156 | 159 |
| Hempstead | ------ | 128 | 140 | 102 | 130 |

[1] The report in question.

All winds at the 0900, 1500, and 2100 GMT observation times were primarily westerly without exception.

Reports from all stations in the vicinity of Philadelphia indicated a rather regular increase of wind speed with height, to a maximum of about 32,000 feet. If the winds at Philadelphia were to be similarly extrapolated with height to 32,000 feet, from the reported figure of 396 knots at 23,000 feet, a maximum wind of over 600 knots would result.

The synoptic situation on January 23 indicated extremely high winds over the Philadelphia area; in fact, this was one of the highest wind regimes observed over the area. The jet stream appeared to be moving slowly northward, with its maximum speed at about 32,000 feet.

Computations of possible wind shear, based on winds at nearby stations, indicate the extreme improbability of winds of the magnitude reported, and suggest probable wind speeds of near 200 knots at 23,000 feet, and a probable maximum of 265 knots at 32,000 feet, as stated above. Differential analyses made by 10 analysts in WBAN Analysis Center gave similar results [1].

## REFERENCE

1. F. W. Burnett, High Winds over Philadelphia at 1500 GMT, January 23, 1955, U. S. Weather Bureau, Washington, D. C., February 10, 1955 (intra office memorandum report, unpublished).

U. S. GOVERNMENT PRINTING OFFICE: 1955

Chart I. A. Average Temperature (°F.) at Surface, January 1955.

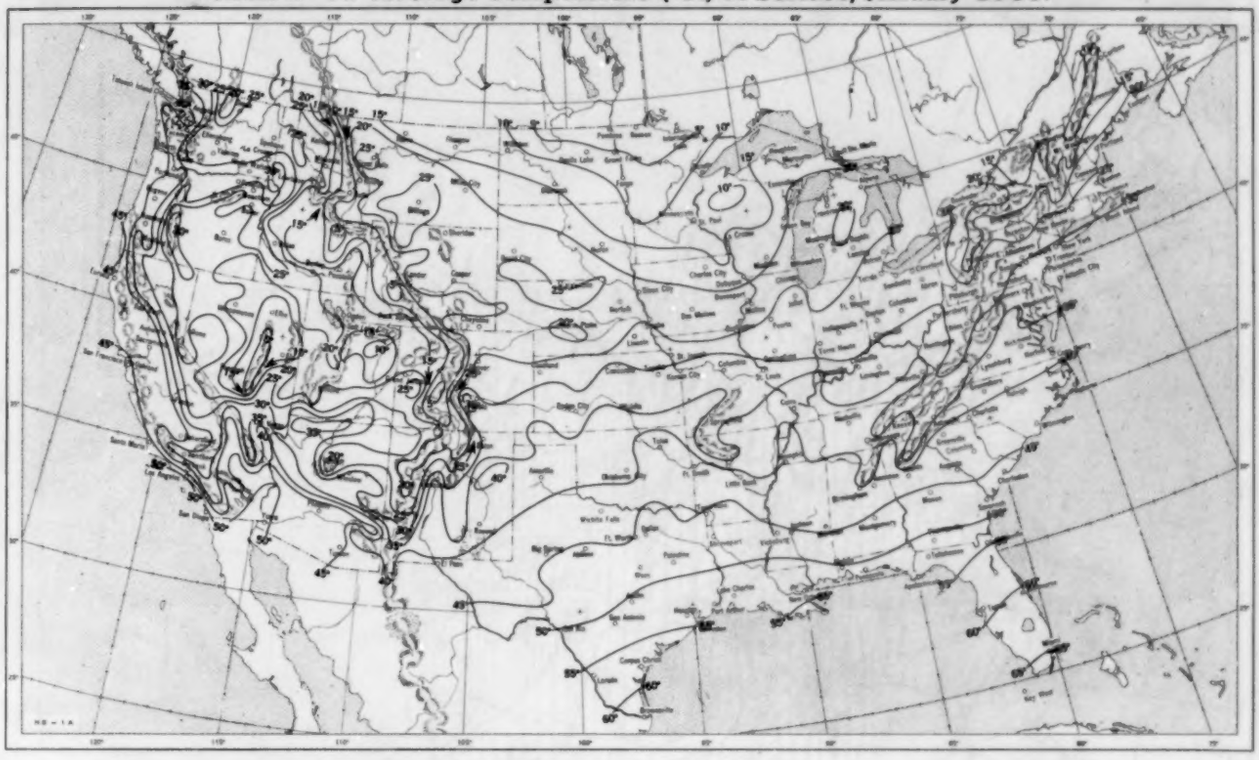

B. Departure of Average Temperature from Normal (°F.), January 1955.

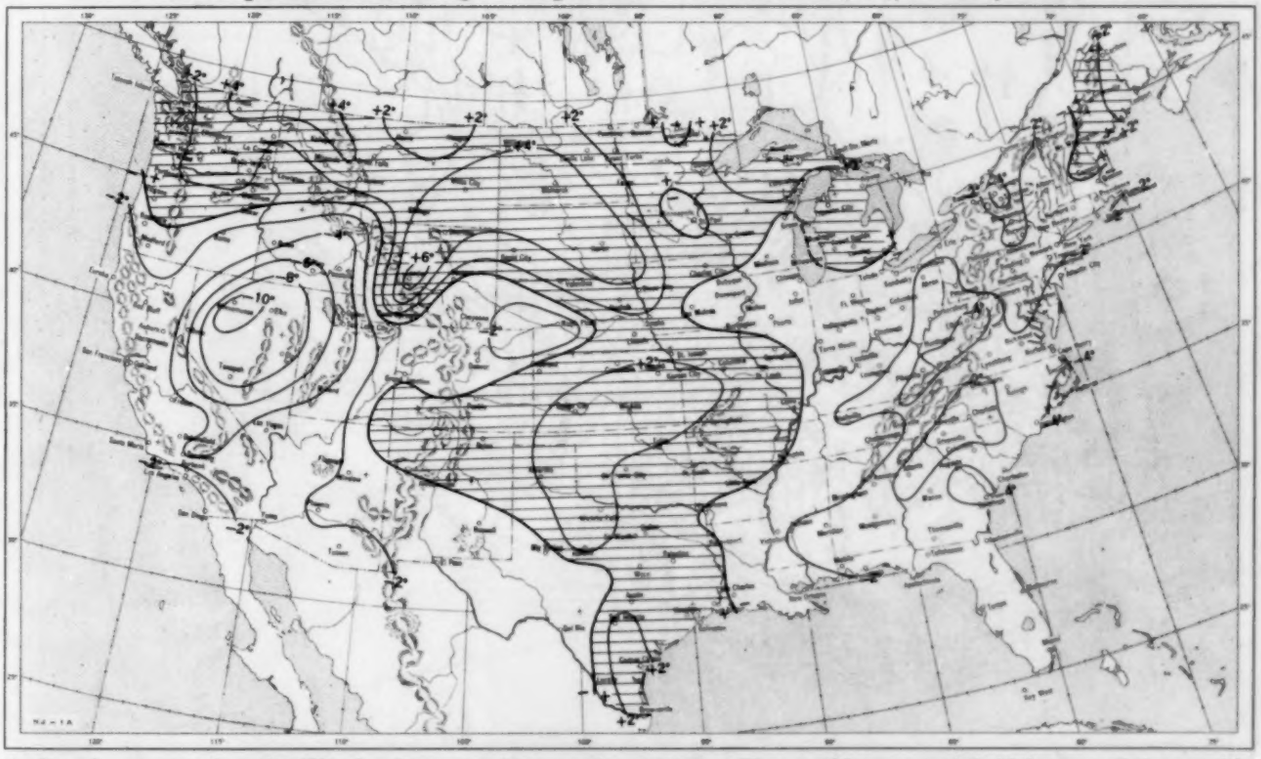

A. Based on reports from 800 Weather Bureau and cooperative stations. The monthly average is half the sum of the monthly average maximum and monthly average minimum, which are the average of the daily maxima and daily minima, respectively.
B. Normal average monthly temperatures are computed for Weather Bureau stations having at least 10 years of record.

Chart II. Total Precipitation (Inches), January 1955.

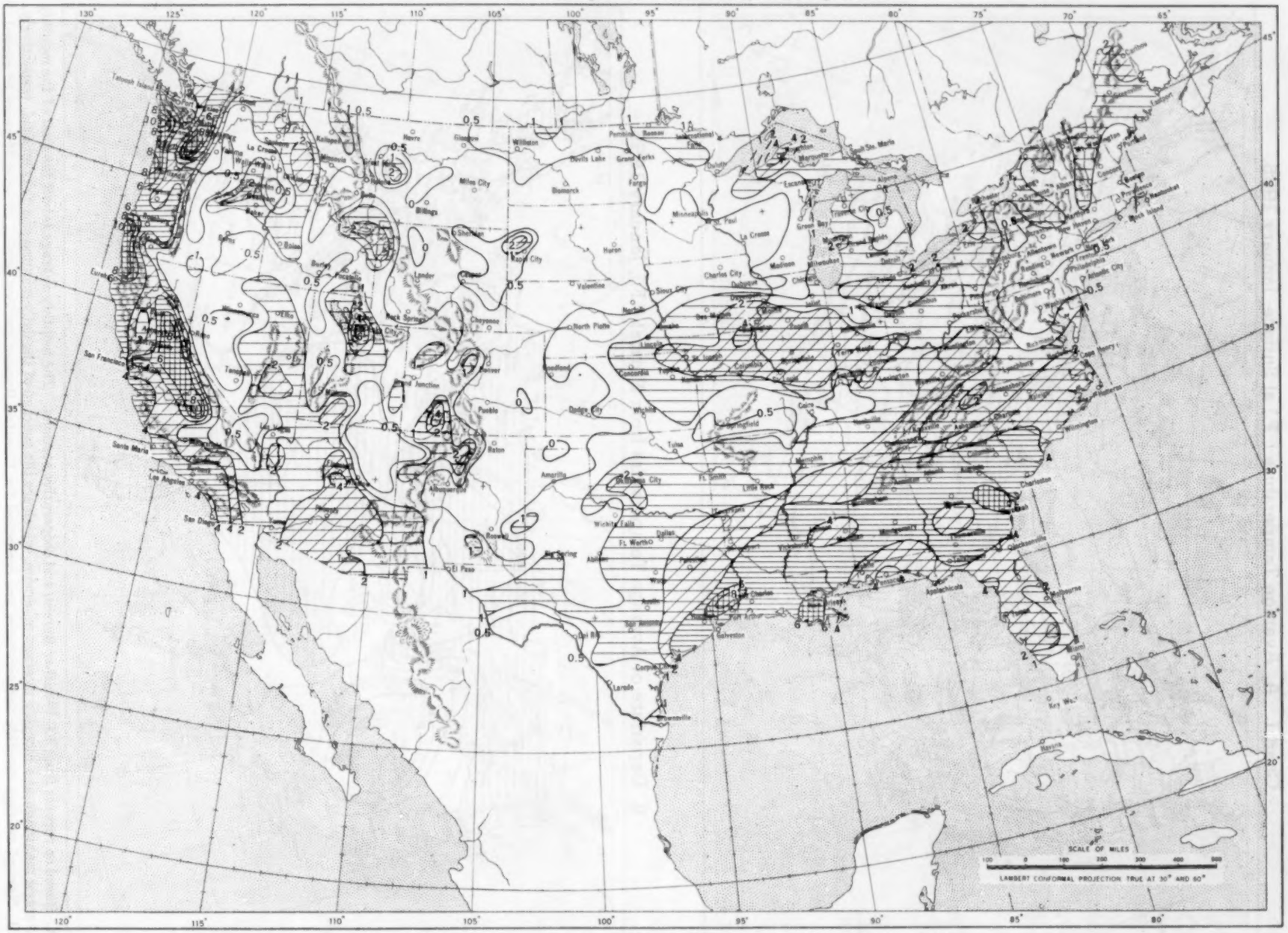


Based on daily precipitation records at 800 Weather Bureau and cooperative stations.

Chart III. A. Departure of Precipitation from Normal (Inches), January 1955.

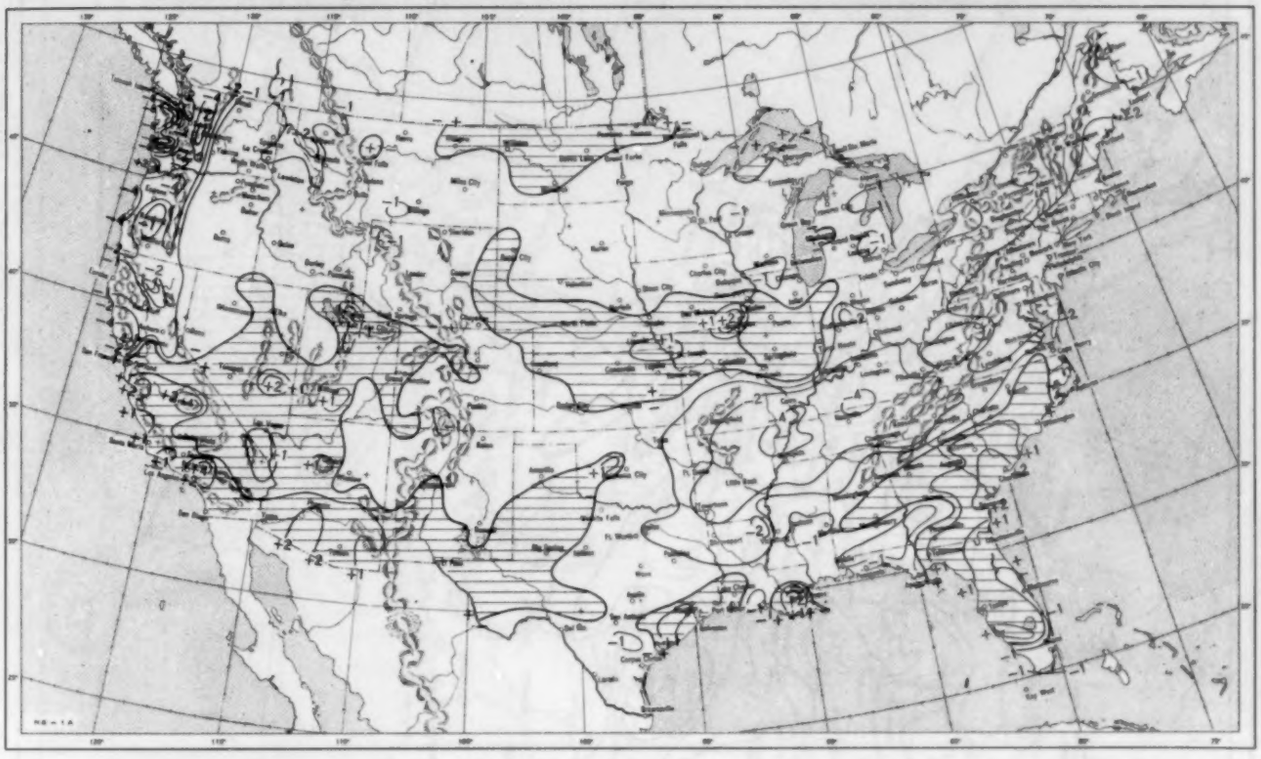

B. Percentage of Normal Precipitation, January 1955.

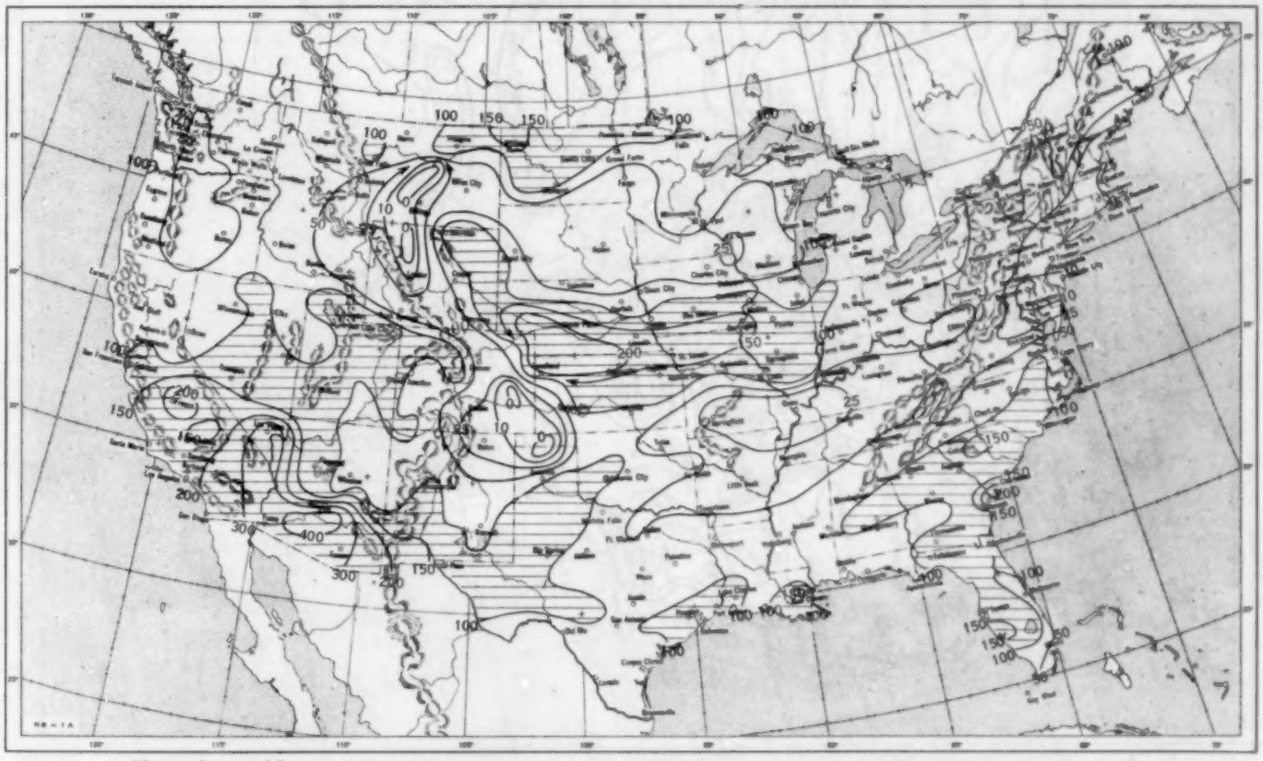

Normal monthly precipitation amounts are computed for stations having at least 10 years of record.

## Chart IV. Total Snowfall (Inches), January 1955.

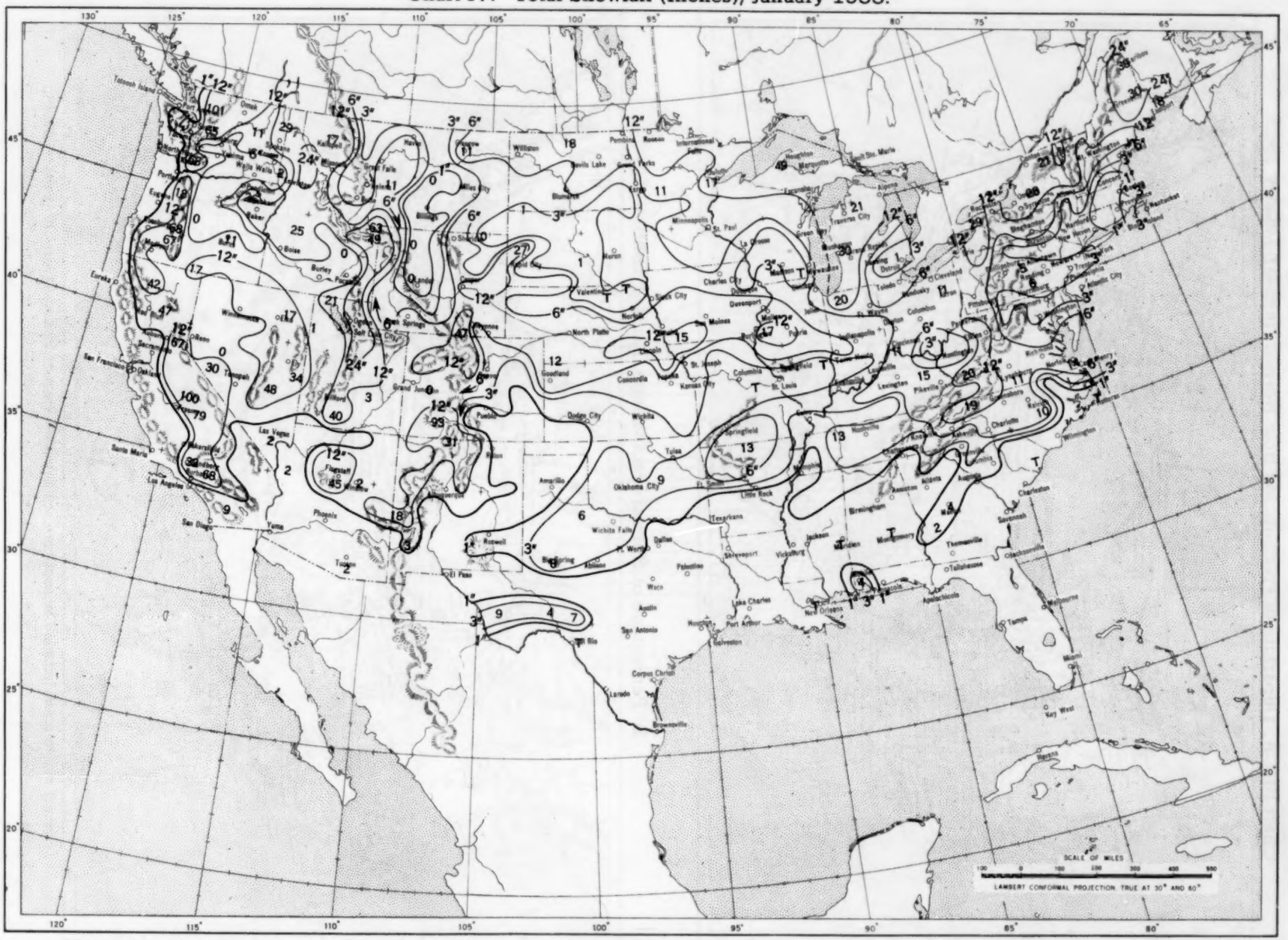


This is the total of unmelted snowfall recorded during the month at Weather Bureau and cooperative stations. This chart and Chart V are published only for the months of November through April although of course there is some snow at higher elevations, particularly in the far West, earlier and later in the year.

## Chart V. A. Percentage of Normal Snowfall, January 1955.

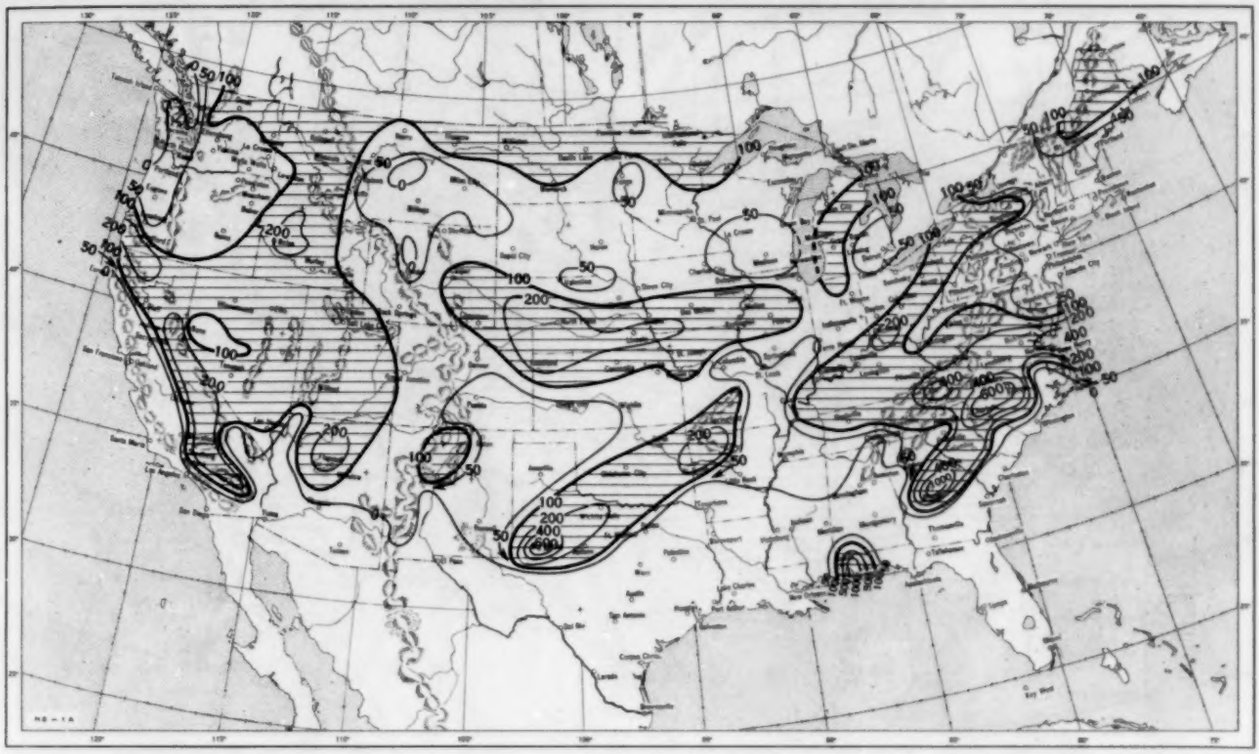

## B. Depth of Snow on Ground (Inches). 7:30 a. m. E. S. T., January 31, 1955.

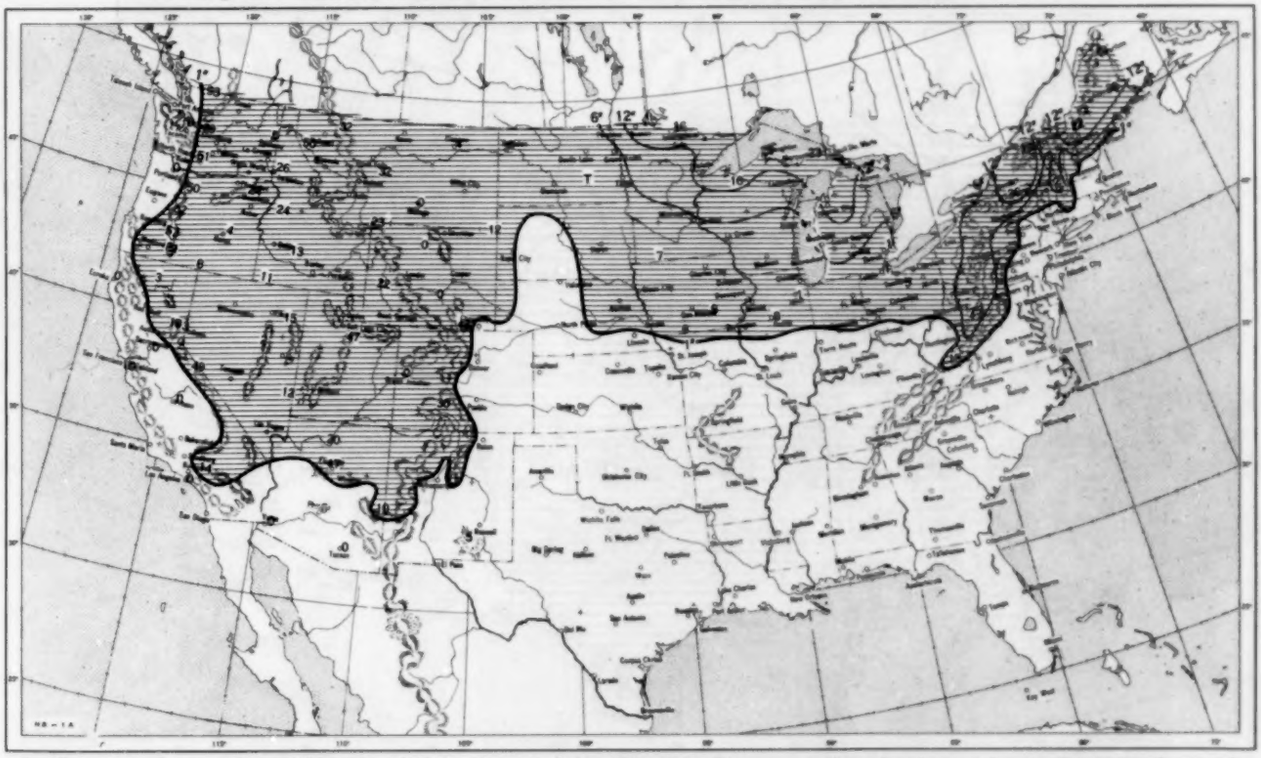

A. Amount of normal monthly snowfall is computed for Weather Bureau stations having at least 10 years of record.
B. Shows depth currently on ground at 7:30 a. m. E. S. T., of the Tuesday nearest the end of the month. It is based on reports from Weather Bureau and cooperative stations. Dashed line shows greatest southern extent of snowcover during month.

Chart VI. A. Percentage of Sky Cover Between Sunrise and Sunset, January 1955.

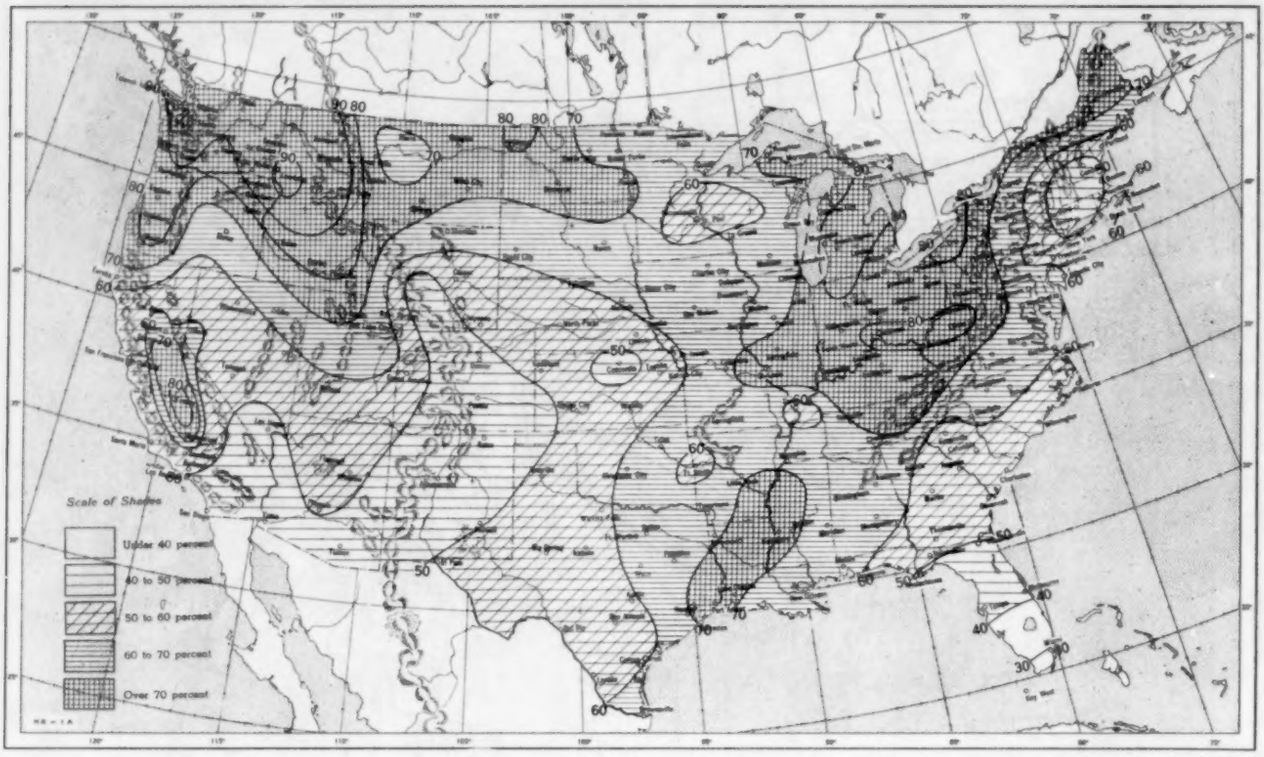


B. Percentage of Normal Sky Cover Between Sunrise and Sunset, January 1955.

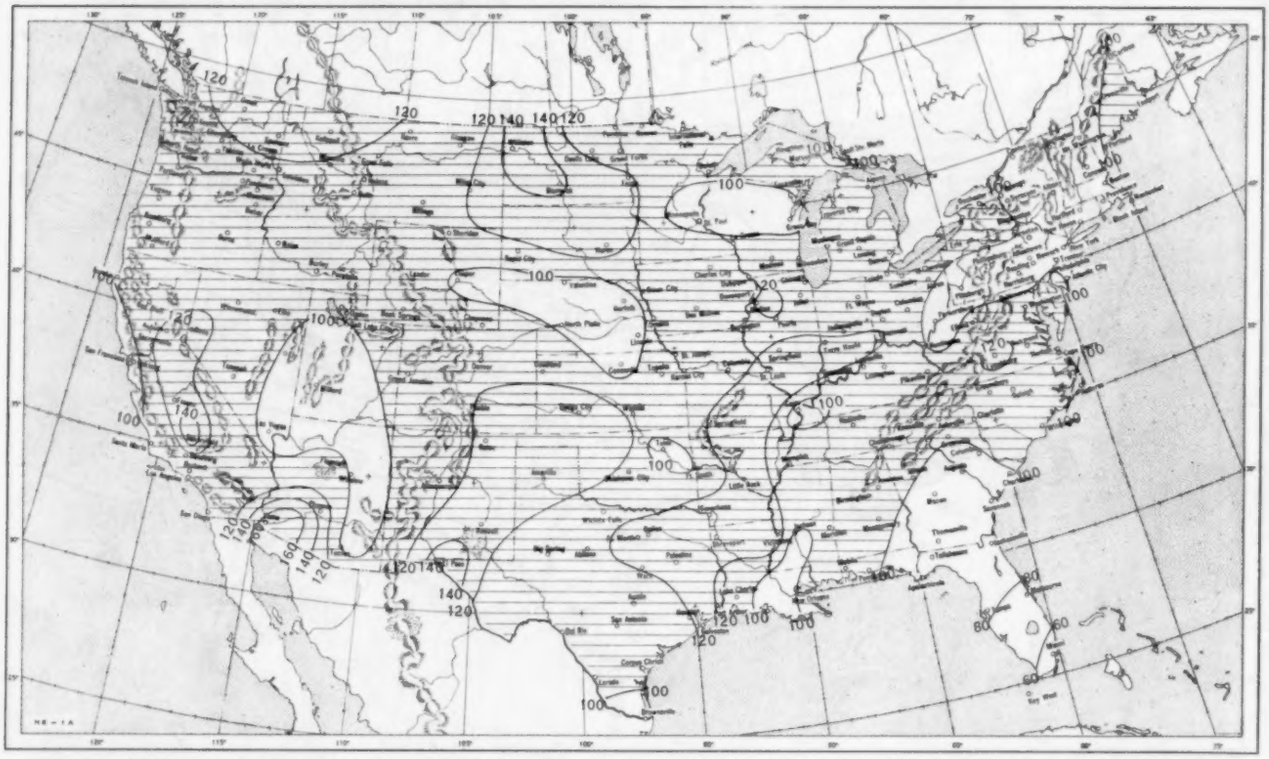

A. In addition to cloudiness, sky cover includes obscuration of the sky by fog, smoke, snow, etc. Chart based on visual observations made hourly at Weather Bureau stations and averaged over the month. B. Computations of normal amount of sky cover are made for stations having at least 10 years of record.

## Chart VII. A. Percentage of Possible Sunshine, January 1955

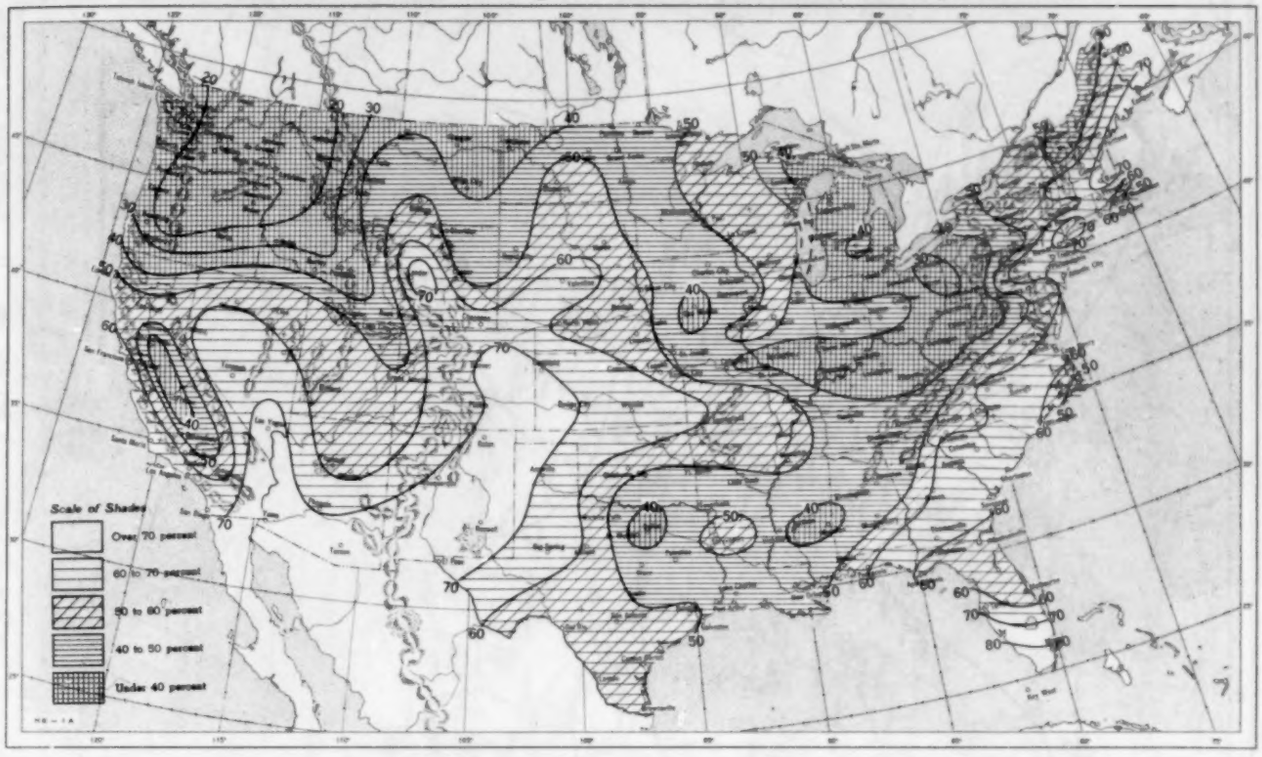


## B. Percentage of Normal Sunshine, January 1955.

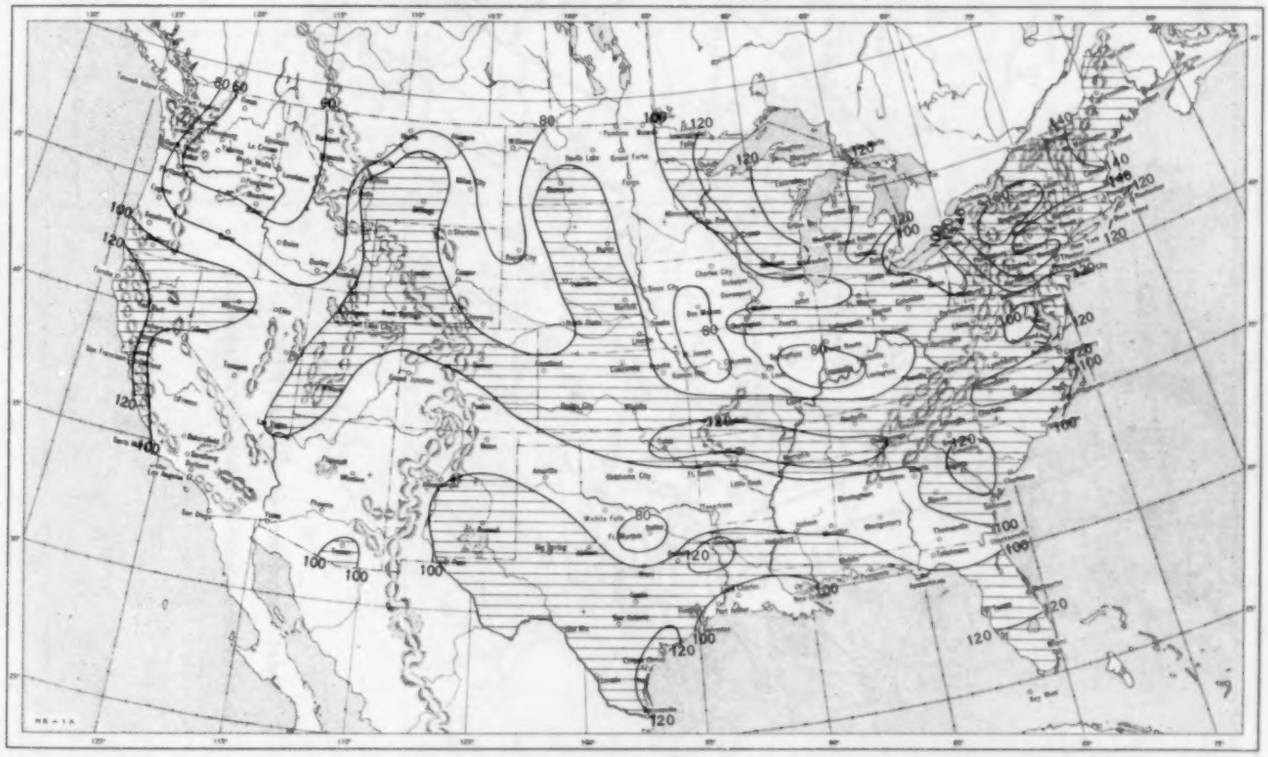

A. Computed from total number of hours of observed sunshine in relation to total number of possible hours of sunshine during month. B. Normals are computed for stations having at least 10 years of record.

Chart VIII. Average Daily Values of Solar Radiation, Direct + Diffuse, January 1955. Inset: Percentage of Normal Average Daily Solar Radiation, January 1955.

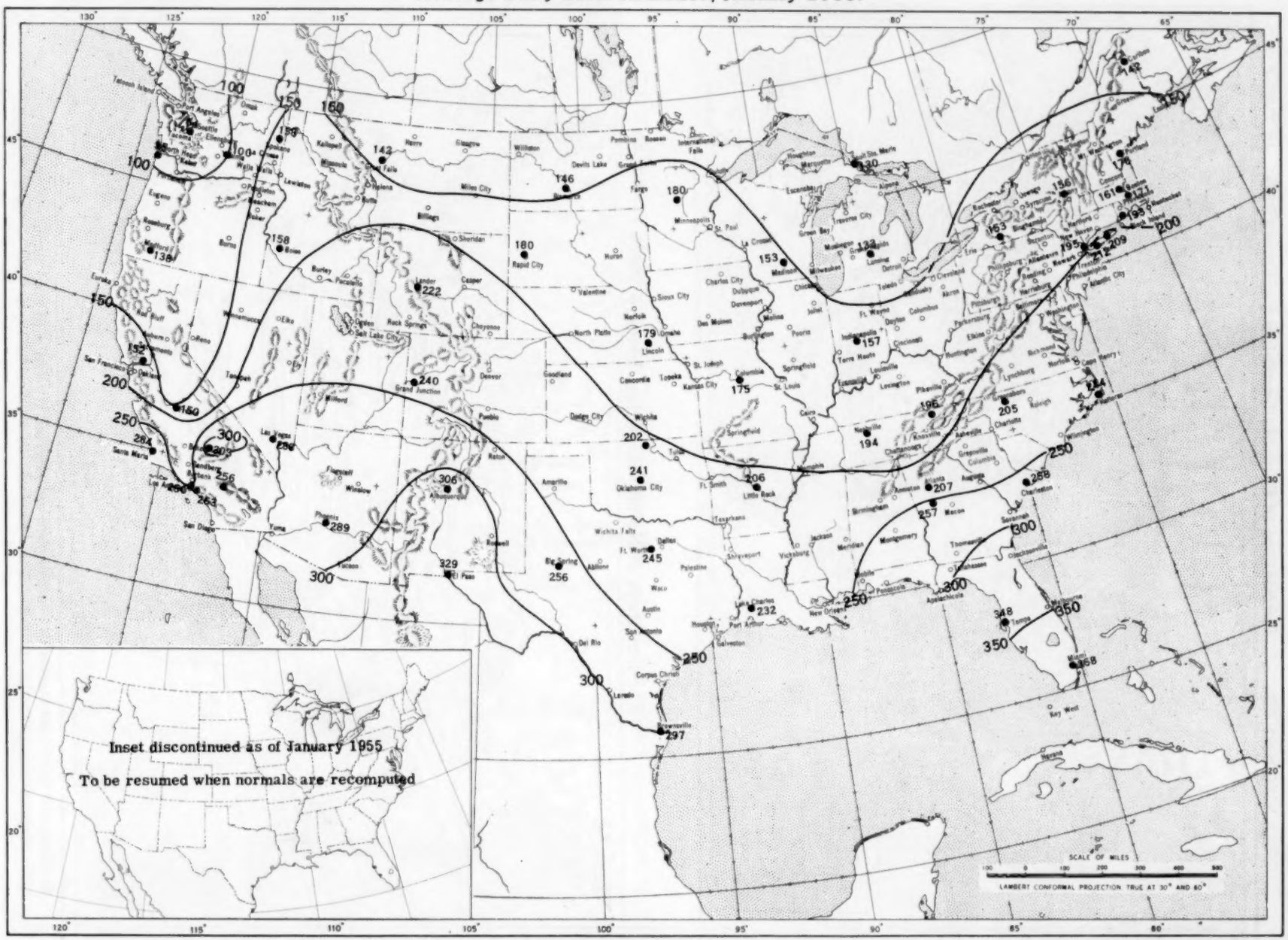


Chart shows mean daily solar radiation, direct + diffuse, received on a horizontal surface in langleys (1 langley = 1 gm. cal. cm. $^{-2}$). Basic data for isolines are shown on chart. Further estimates are obtained from supplementary data for which limits of accuracy are wider than for those data shown. Normals are computed for stations having at least 9 years of record.

## Chart IX. Tracks of Centers of Anticyclones at Sea Level, January 1955.

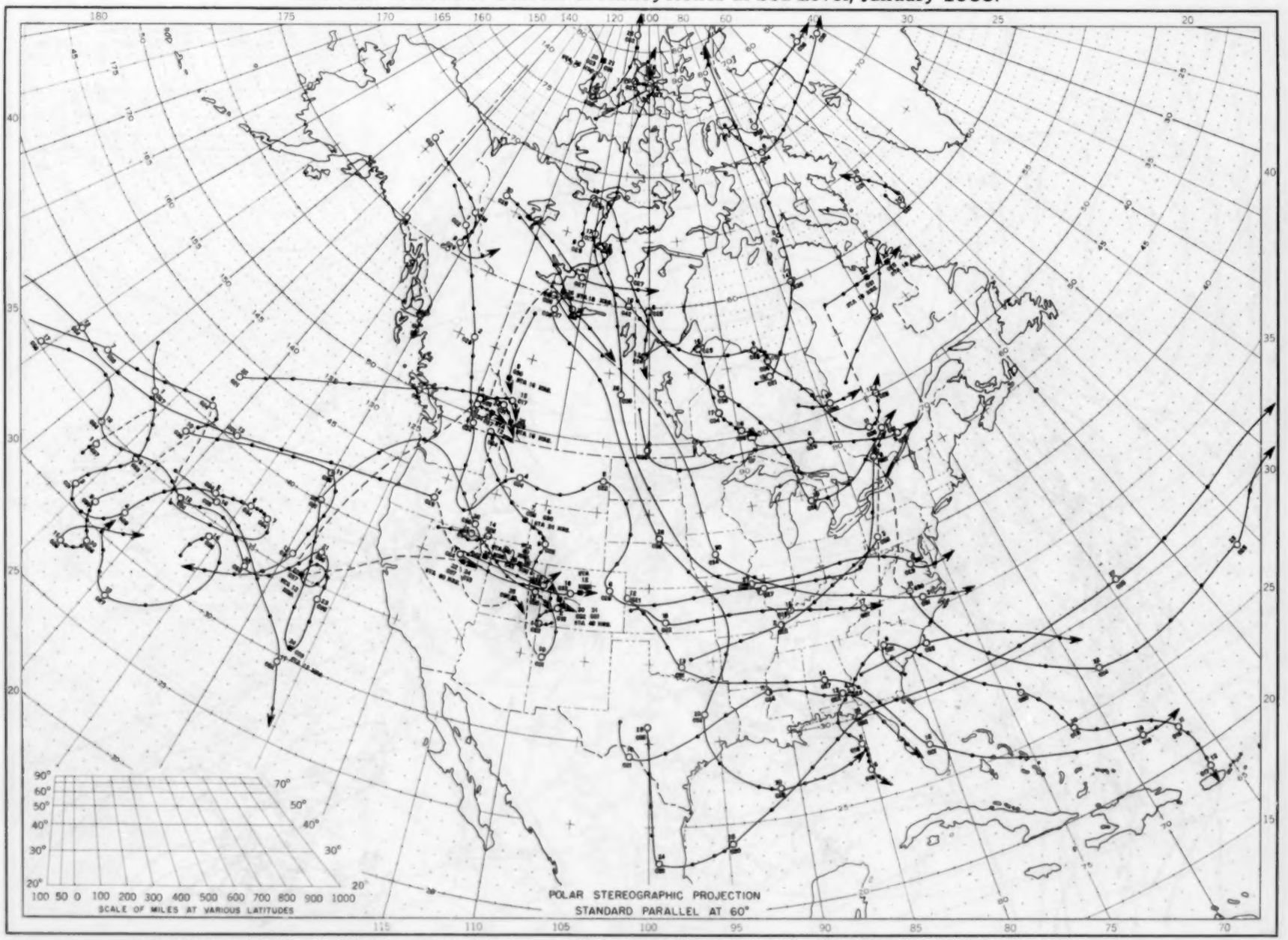


Circle indicates position of center at 7:30 a. m. E. S. T. Figure above circle indicates date, figure below, pressure to nearest millibar. Dots indicate intervening 6-hourly positions. Squares indicate position of stationary center for period shown. Dashed line in track indicates reformation at new position. Only those centers which could be identified for 24 hours or more are included.

## Chart X. Tracks of Centers of Cyclones at Sea Level, January 1955.

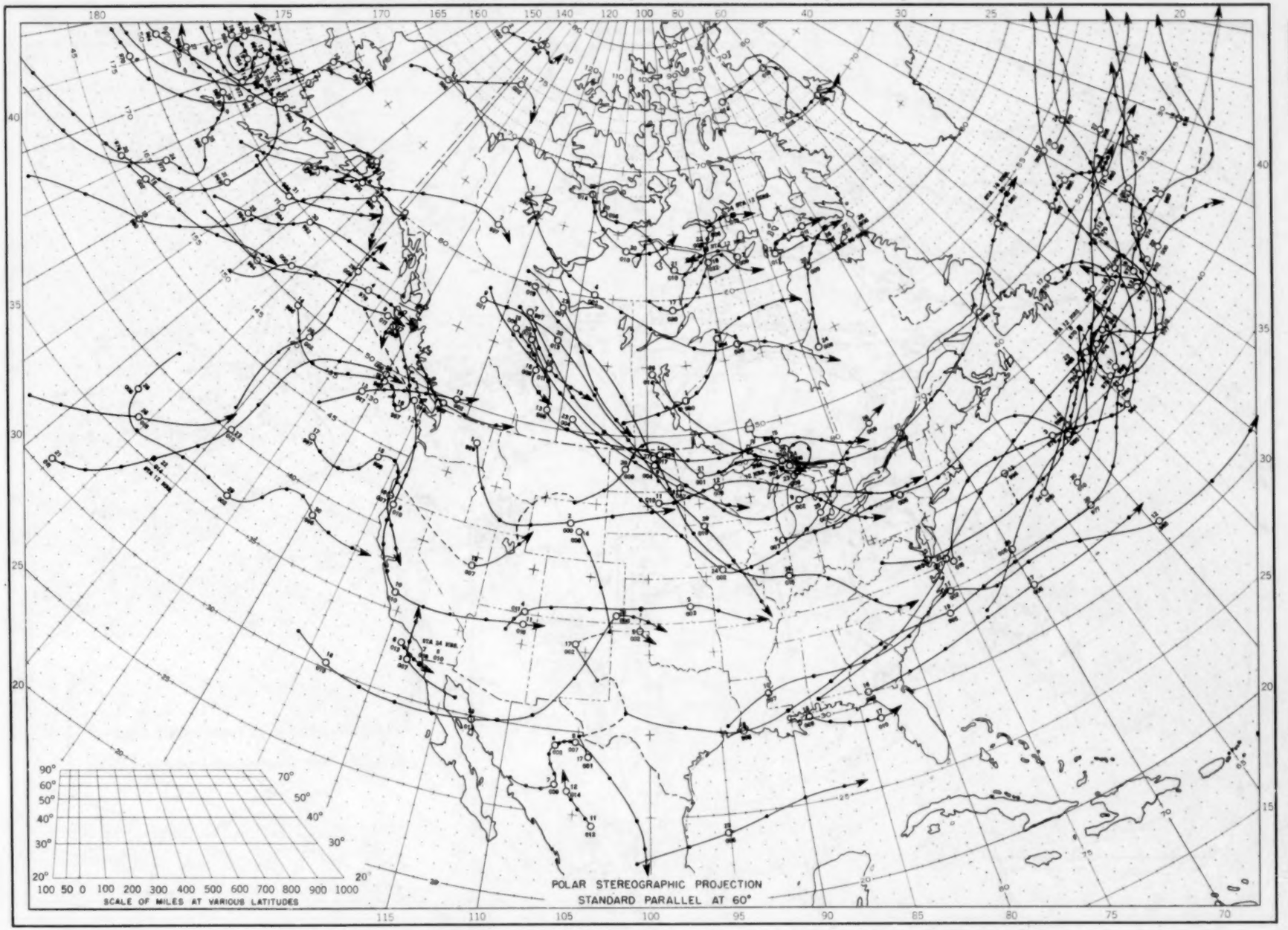


Circle indicates position of center at 7:30 a. m. E. S. T. See Chart IX for explanation of symbols.

Chart XI. Average Sea Level Pressure (mb.) and Surface Windroses, January 1955. Inset: Departure of Average Pressure (mb.) from Normal, January 1955.

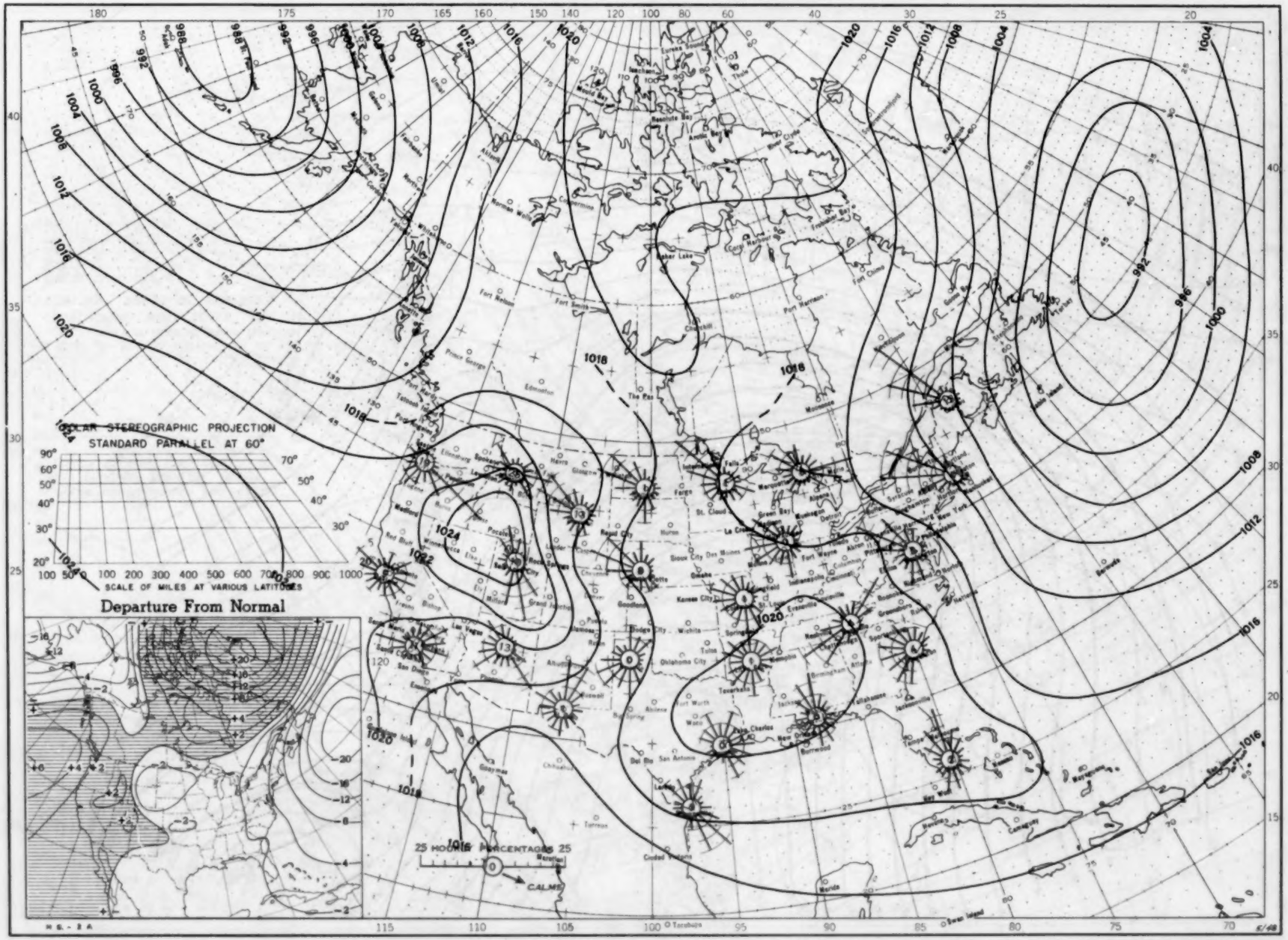


Average sea level pressures are obtained from the averages of the 7:30 a. m. and 7:30 p. m. E. S. T. readings. Windroses show percentage of time wind blew from 16 compass points or was calm during the month. Pressure normals are computed for stations having at least 10 years of record and for 10° intersections in a diamond grid based on readings from the Historical Weather Maps (1899-1939) for the 20 years of most complete data coverage prior to 1940.

Chart XII. Average Dynamic Height in Geopotential Meters (1 g.p.m. = 0.98 dynamic meters) of the 850-mb. Pressure Surface, Average Temperature in °C. at 850 mb., and Resultant Winds at 1500 Meters (m.s.l.), January 1955.

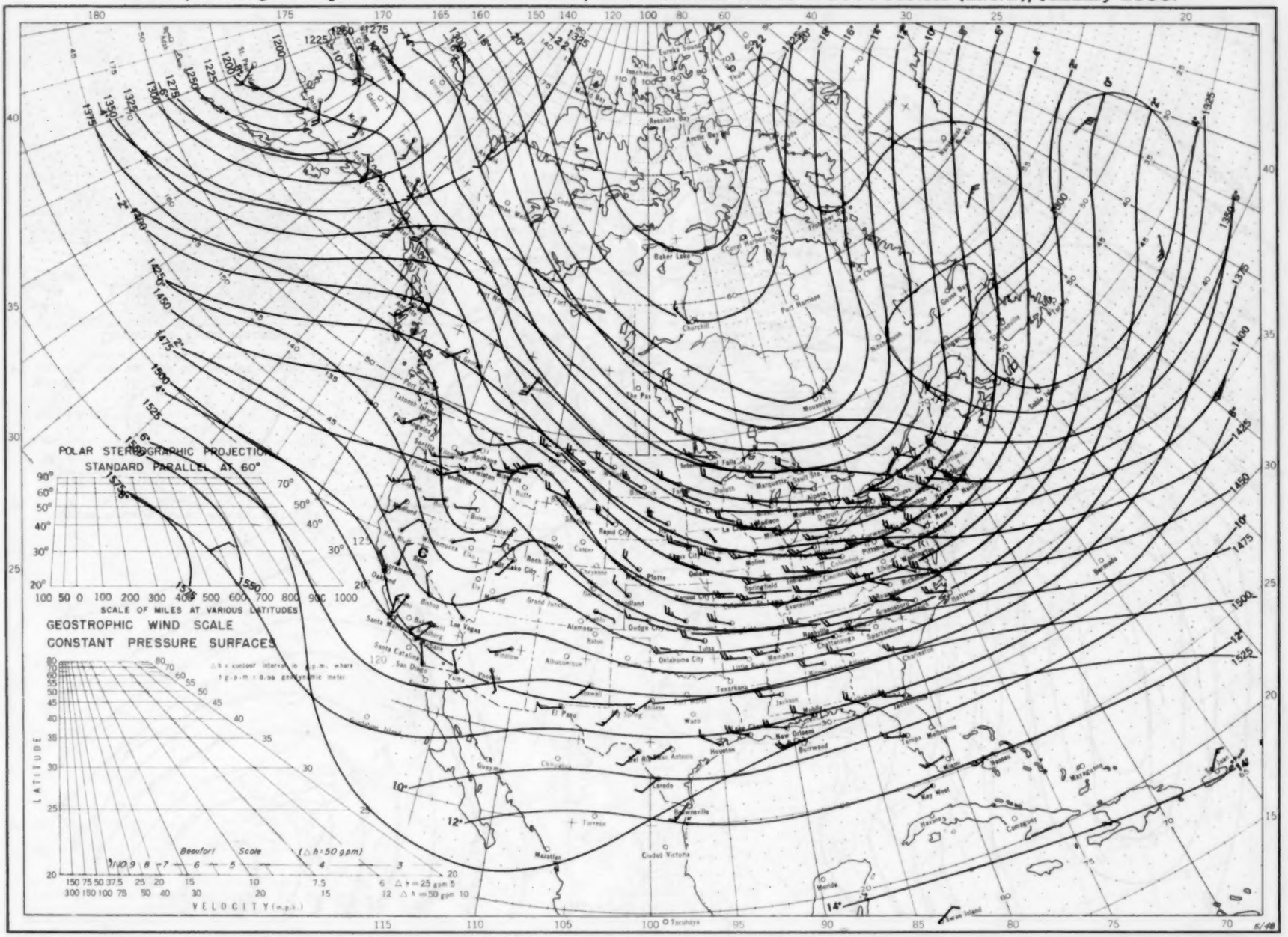


Contour lines and isotherms based on radiosonde observations at 0300 G. M. T. Winds shown in black are based on pilot balloon observations at 2100 G. M. T.; those shown in red are based on rawins taken at 0300 G. M. T. Wind barbs indicate wind speed on the Beaufort scale.

Chart XIII. Average Dynamic Height in Geopotential Meters (1 g.p.m.. = 0.98 dynamic meters) of the 700-mb. Pressure Surface, Average Temperature in °C. at 700 mb., and Resultant Winds at 3000 Meters (m.s.l.), January 1955.

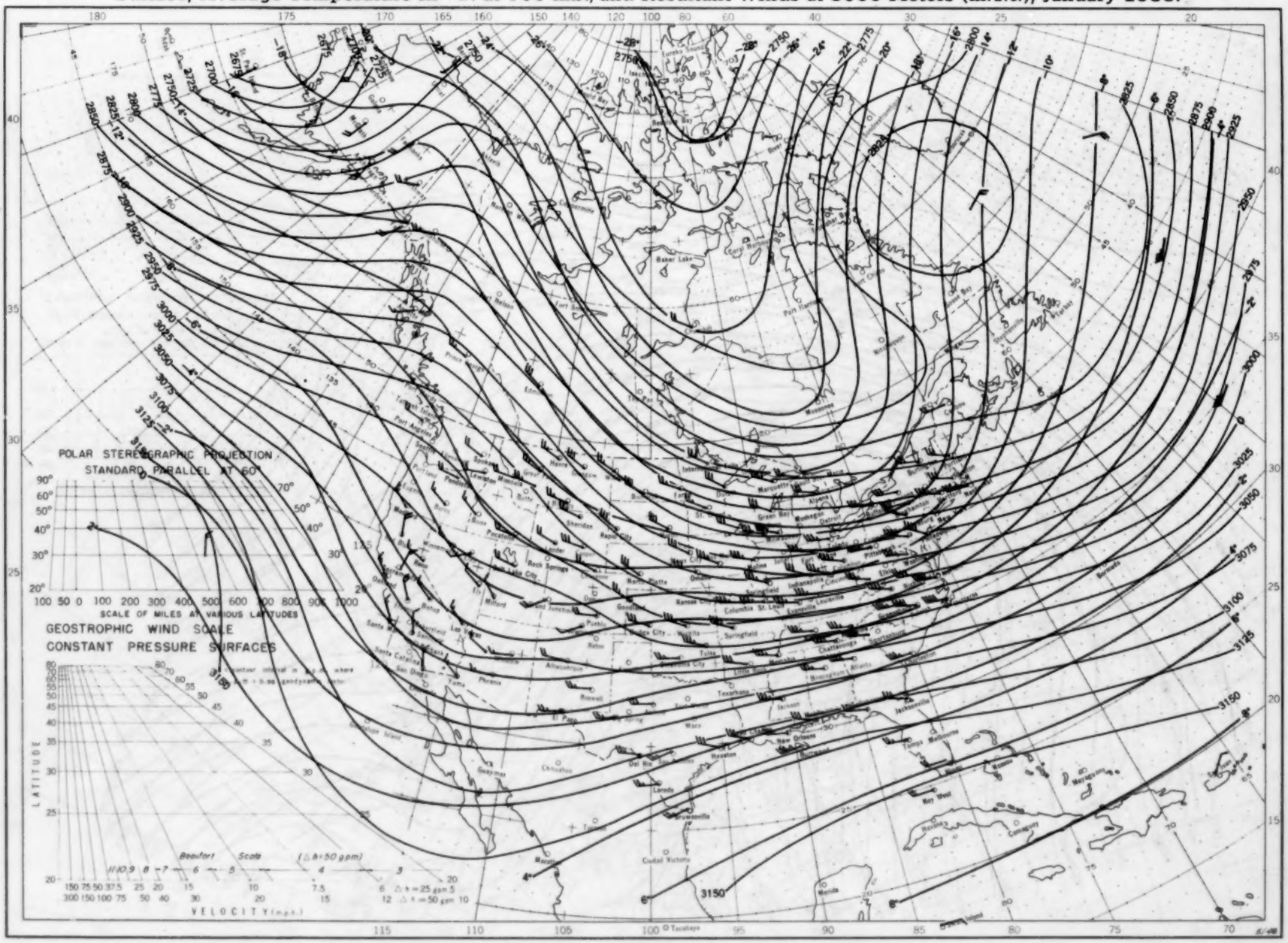


Contour lines and isotherms based on radiosonde observations at 0300 G. M. T. Winds shown in black are based on pilot balloon observations at 2100 G. M. T.; those shown in red are based on rawins taken at 0300 G. M. T. Wind barbs indicate wind speed on the Beaufort scale.

Chart XIV. Average Dynamic Height in Geopotential Meters (1 g.p.m. = 0.98 dynamic meters) of the 500-mb. Pressure Surface, Average Temperature in °C. at 500 mb., and Resultant Winds at 5000 Meters (m.s.l.), January 1955.

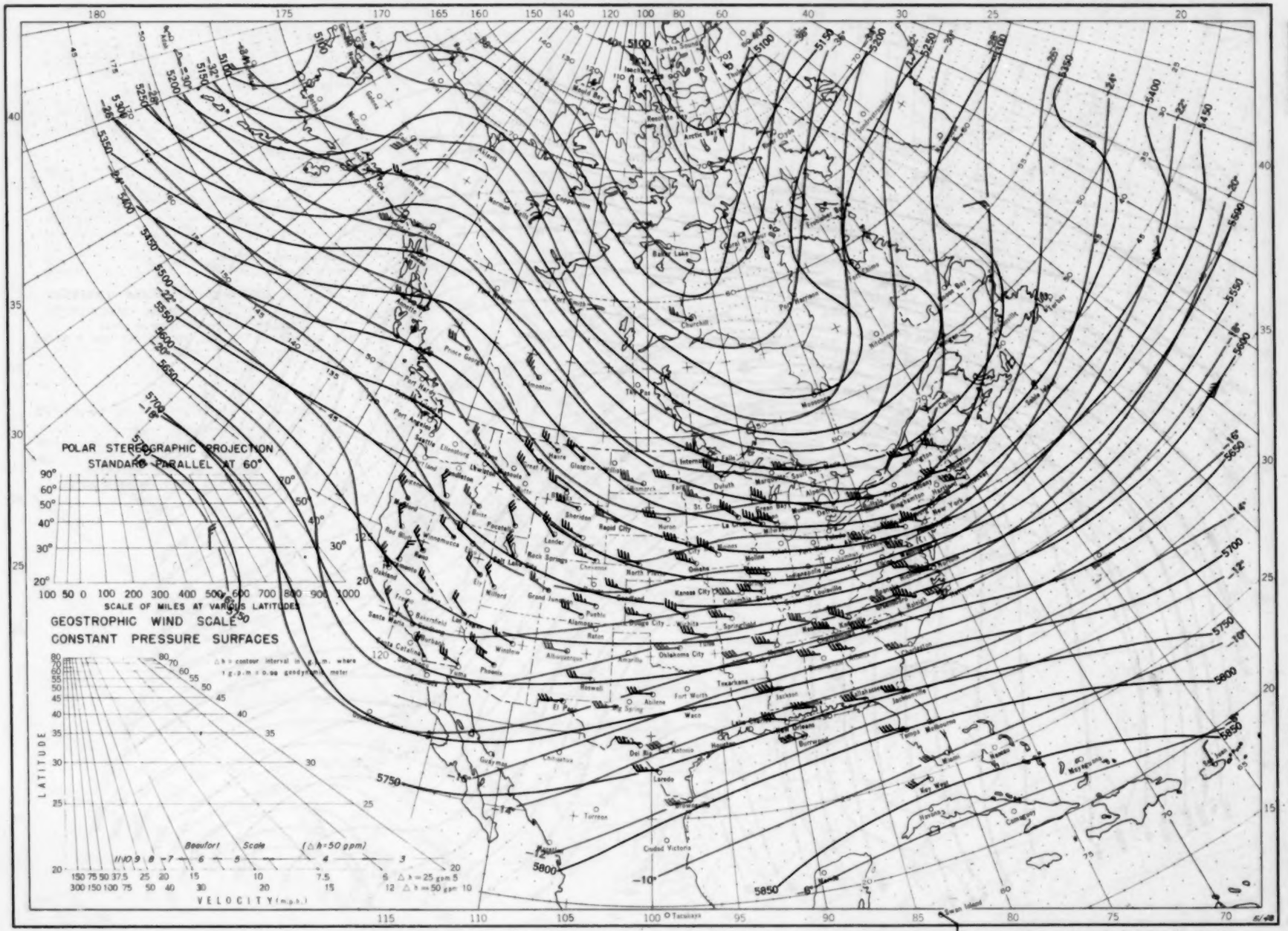


Contour lines and isotherms based on radiosonde observations at 0300 G. M. T. those shown in red are based on rawins at 0300 G. M. T. Winds shown in black are based on pilot balloon observations at 2100 G. M. T.; Wind barbs indicate wind speed on the Beaufort scale.

Chart XV. Average Dynamic Height in Geopotential Meters (1 g.p.m. = 0.98 dynamic meters) of the 300-mb. Pressure Surface, Average Temperature in °C. at 300 mb., and Resultant Winds at 10,000 Meters (m.s.l.), January 1955.

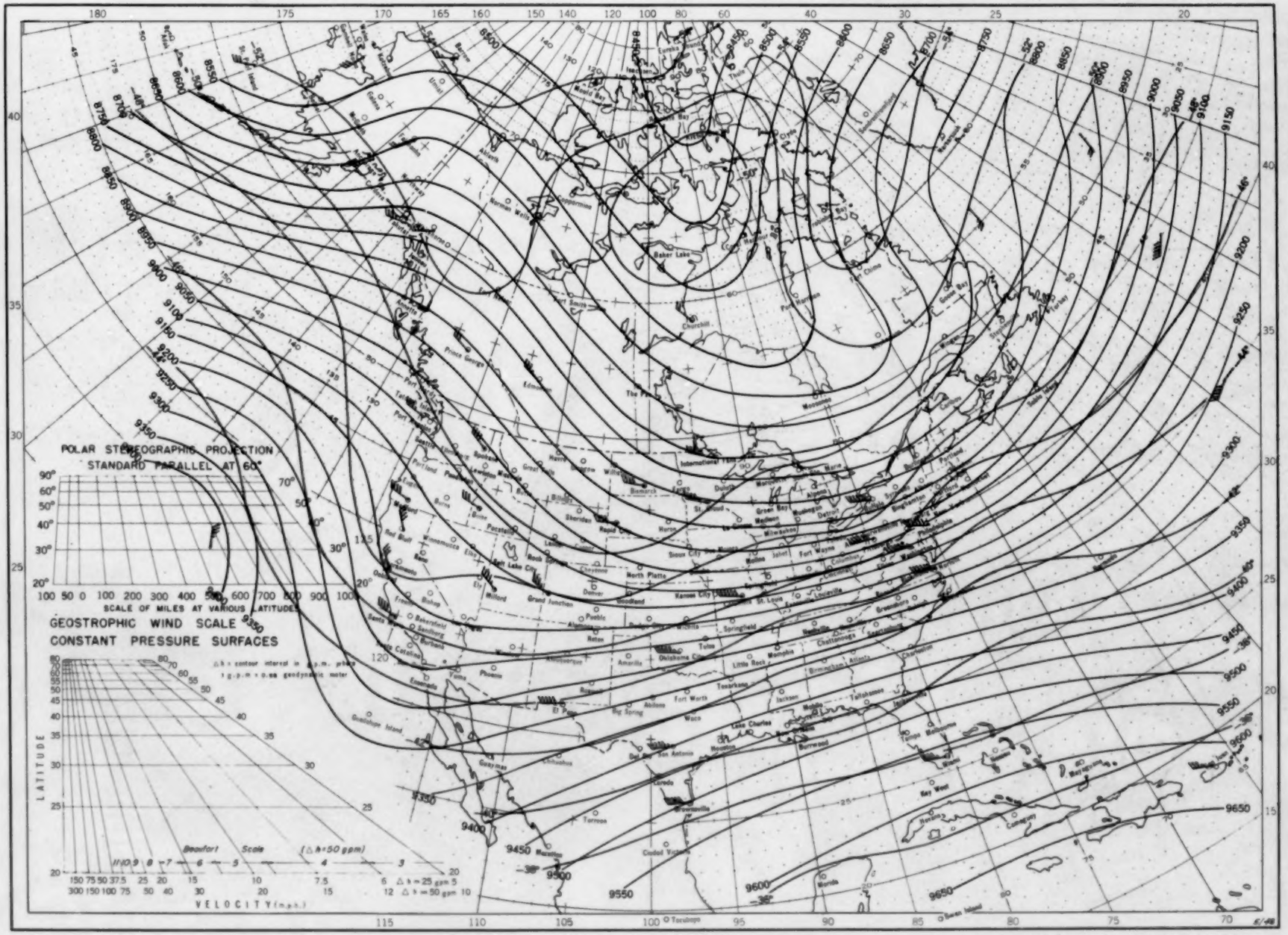


Contour lines and isotherms based on radiosonde observations at 0300 G. M. T. Winds shown in black are based on pilot balloon observations at 2100 G. M. T.; those shown in red are based on rawins at 0300 G. M. T. Wind barbs indicate wind speed on the Beaufort scale.